Development of Cu-Based Metal Matrix Composites Using Silicon Carbide, E-Glass Fiber and Multiwalled Carbon Nanotubes as Reinforcement

A Thesis submitted in partial fulfilment of the requirements for the degree of

Master of Technology (Research)

By

Harshpreet Singh
(Roll Number-612MM3006)

under the supervision of

Dr. S. N. Alam

Department of Metallurgical and Materials Engineering
National Institute of Technology Rourkela
Rourkela, Pin-769008
Odisha, India

2015

Department of Metallurgical and Materials Engineering
National Institute of Technology Rourkela
Rourkela-769008, Odisha, India

CERTIFICATE

This is to certify that the thesis entitled "**Development of Cu-Based Metal Matrix Composites Using Silicon Carbide, E-Glass Fiber and Multiwalled Carbon Nanotubes as Reinforcement**" being submitted by **Mr. Harshpreet Singh** to the National Institute of Technology Rourkela, for the award of the degree of **Masters of Technology (Research)** is a record of bonafide research work carried out under my supervision and guidance. The results presented in this thesis have not been submitted elsewhere for the award of any other degree or diploma. This work in my opinion has reached the standard of fulfilling the requirements for the award of the degree of **Masters of Technology (Research)** in accordance with the regulations of institute.

Date:

Dr. S. N. Alam
(Supervisor)

Acknowledgement

It is a privilege for me to express my profound gratitude and indebtedness to my supervisor Dr. S. N. Alam, Metallurgical & Materials Engineering Department, National Institute of Technology Rourkela. Without his efforts and guidance this work could not have been possible. He has guided me at all stages during this research work. I will cherish all the moments of enlightenment he has shared with me.

I would like to convey my sincere gratitude to Prof. S.C. Mishra, Head of the Department, Metallurgical and Materials Engineering Department, National Institute of Technology Rourkela, for constant guidance and encouragement. I also gratefully acknowledge the support of Prof. B.C. Ray who motivated me and provided valuable suggestions during my research work. I would also like to express my sincere thanks to Prof. B. B. Verma and Prof. S. Sen for constantly encouraging me and helping me understand my research problem. I am very much thankful to Dr. A. Basu for helping me in understanding my research problem and giving valuable suggestions. I would also take the pleasure of thanking all my master scrutiny committee members, Dr. D. Chaira, Dr. S. K. Sahoo and Dr. M. Masanta for assessing my research work and providing me valuable suggestions throughout the work. I would also like to thank Prof. Mushahid Husain, Centre for Nanoscience and Nanotechnology, Jamia Millia Islamia, for helping me in the synthesis of multiwalled carbon nanotubes used in the development of the composites.

I am also thankful to Mr. Rajesh Patnaik, Mr. U. K. Sahoo, Mr. S. Chakraborty, Mr. S. Pradhan, Mr. S. Hembram and Mr.Arindam Pal of NIT Rourkela for their technical guidance in conducting various experimental studies during the research work.

I am also thankful to my friends Lailesh Kumar, Deepanshu Verma and Deepankar Panda for their help and support during my research work.

I am grateful to my brother Mr. Ishpreet Singh for his love, affection and understanding. He has provided constant support thought my period of study. Special thanks to my parents for motivating me and assisting me. Without their help and encouragement it would not have been possible for me to undertake this work. I would like to thank all my friends for making my stay at NIT Rourkela lively and without their help this work would not have been possible.

Harshpreet Singh

Date:

CONTENTS

List of Figures

List of Tables

Abstract

Metal matrix composites (MMCs) combine the ductility of metal and the toughness of the reinforcement which makes it an excellent candidate material for advanced engineering applications. The unique features of MMCs like high strength to weight ratio and high stiffness per unit density results in improvement of the service performance. The decrease in structural weight, increase in creep strength, high fatigue strength, high thermal stability, enhancement in wear resistance and electrical conductivity, further makes it a potential engineering material. Cu has been extensively used as a matrix due to its superior thermal and electrical properties. However Cu has inadequate mechanical properties from the structural application point of view. Incorporation of ceramic particles like oxides or carbides in Cu would strengthen the matrix. Here in our study three reinforcements, SiC particles, E-glass fibers and multiwalled carbon nanotubes (MWCNTs), which are very different in nature and morphology have been used for developing Cu-based MMCs.

Over the last several decades, there has been considerable interest in the use of Cu-based MMCs. However very limited literature is available on Cu-based metal matrix composites. For many applications pure Cu cannot be used because of its low strength and reinforcing Cu with ceramics or fibers is a viable option to overcome this limitation. Here Cu-based metal matrix composites have been developed using SiCp, E-glass fiber and multiwalled carbon nanotube (MWCNT) as reinforcements by powder metallurgy route. A systematic study of the various mechanical properties of the composites developed was done. The hardness and wear properties of the various composites were determined. The fracture surface of the various composites was analyzed and the density of the composites was also determined. Here in our study both the as-received Cu powder and 20 h milled nanostructured Cu powder was used as the matrix for the composites. The as-received Cu powder was milled for 20 h in a high energy planetary ball mill in order to form nanostructured Cu which was later used for

the development of as-milled Cu-based metal matrix composites. The 20 h milled Cu powder doesn't show any contamination during milling from the milling media. The variation of the crystallite size, strain and lattice parameter of Cu were found out from the x-ray analysis of the milled powder after different intervals of milling time. Both x-ray diffraction analysis and HRTEM images of the 20 h milled Cu powder confirmed that the size of the Cu crystallites is less than 25 nm. Cu-E-glass fiber and Cu-SiCp composites with reinforcement contents of 10, 20, 30 and 40 vol. % were developed by powder metallurgy route. Multiwalled carbon nanotubes (MWCNTs) were developed by using low pressure chemical vapour deposition (LPCVD) process. FTIR offers a quantitative and qualitative analysis for organic and inorganic samples which identifies chemical bonds in a molecule by producing an infrared absorption spectrum. FTIR of the functionalized MWCNTs was done in order to determine the different functional groups after acid-modification of the multiwalled carbon nanotubes. The FTIR analysis shows stretching vibrations from carboxyl (C=O) and hydroxyl (-OH) groups. Skeletal vibrations from unoxidized graphitic domains of the carbon nanotube backbone were also observed. MWCNTs were added to the Cu matrix to develop Cu-1, 2 and 5 vol. % MWCNT nanocomposites. The composites were developed by uniaxial cold compaction under a load of 665 MPa followed by sintering at 900^{o}C for 1 h in Ar atmosphere. The microstructure of the composites was analysed using an optical microscope, scanning electron microscope (SEM), field emission scanning electron microscope (FESEM), energy dispersive x-ray spectroscopy (EDX) and high resolution transmission electron microscope (HRTEM). X-ray diffraction of the various composites was done in order to determine the different phases in the sintered composites. Density of the composites was determined using the Archimedes' principle. Hardness was determined using a Vickers microhardness tester. Wear properties of the various composites was analysed using a ball-on-plate tribometer. Fractographic analysis of the various composites fractured in impact test

was done in order to study the fracture behaviour of the samples. The results show that the reinforcement is homogeneously distributed all over the Cu-matrix and the composites prepared show good bonding between the Cu-matrix and the reinforcement. Improvement in hardness and wear properties were observed with increase in the content of reinforcement in the composites.

Keywords: Cu-based MMC, SiC particle, E-glass fiber, MWCNT, microhardness, wear

Chapter 1

Introduction

Introduction

1.1 Motivation and Background

The hunt for finding a material which can perform under adverse environmental conditions is never ending since the birth of mankind. This has encouraged researchers to take up challenges to find new materials having desired properties and applications. This very concept is responsible for the creation of composite materials. Throughout the history of mankind there is evidence of the use of composite type materials. One of the earliest man-made composite material was straw and mud combined to form bricks for constructing houses. A composite material is developed by using two or more materials. In most cases the two materials have very different properties and together they give the composite very unique properties which are not found in the individual components. The mud can easily be dried forming a brick shape to provide a building material. It has high compressive strength but it breaks while bending due to its poor tensile strength. Straw is economic and readily available. The straw is a very strong material but it has poor compressibility and can be crushed easily. However, mixing of mud and straw together can provide the excellent building material that are resistant to both squeezing and tearing. Another ancient composite material is concrete. Concrete is a mixture of small stones, cement and sand. It has very good compressive strength. In current times it has been found that addition of metal rods or wires to the concrete can increase its tensile strength. Concrete containing such rods or wires are called reinforced concrete. There are several such examples of composites which have been used by mankind since early civilization [1-3].

Today composites are used as structural materials for building aircraft and spacecraft. Composite are preferred for many reasons. They are stronger, lighter and less expensive in most cases as compared to the traditional materials. In transportation lighter weight of

vehicles achieved by using composites leads to fuel saving. Although composites are very efficient the raw materials used to develop the composites could be expensive. Composites are manufactured keeping in mind the parameters like shape, durability, stiffness, cost etc. The most widely used composite materials are fiber or particle reinforced composites having a matrix of another material. These composites are often used in structural applications. The matrix of structural composites serves dual purposes. Firstly it binds the reinforcement phase in its place and secondly it distributes the stresses among the reinforcements under an applied stress. The reinforcement withstands maximum load and provides us the desirable properties. In composites a strong bond should exist between the reinforcing materials and the matrix. The interface plays an essential role in manufacturing of composite materials. The interface is the area of contact between the reinforcement and the matrix. The main consideration which should be kept in mind while selection and fabrication of composites is that the constituents should be chemically inert and non-reactive. Composites have their special place in the world of materials. They are capable of giving high strength and toughness and have low density which makes it a useful material for a wide range of application. Fig 1.1(a) shows the strength vs density and Fig 1.1(b) shows the strength vs toughness of various classes of materials like metals and alloys, ceramics, glasses, foams, rubbers, polymers etc.

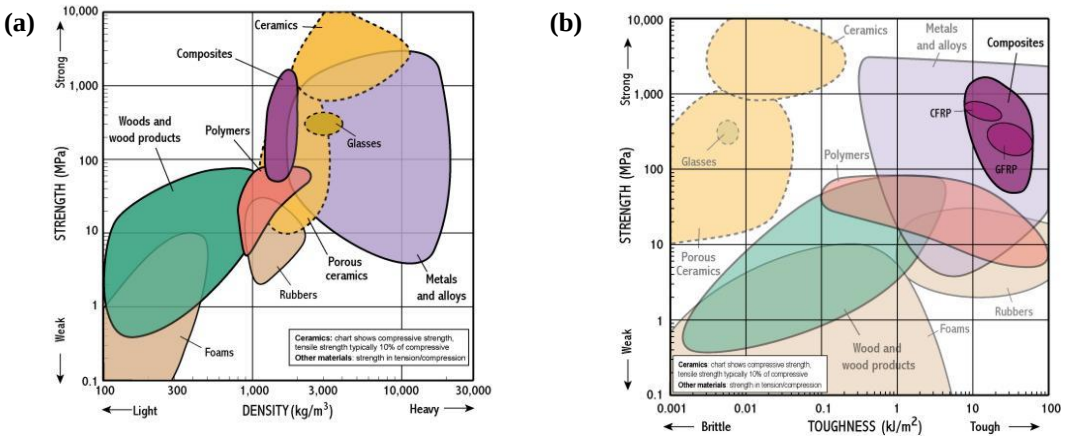

Fig.1.1 (a, b) Profile for various materials

The major advantages of composite materials are their light weight and high toughness. Composites are able to meet various design requirements with important weight savings as well as high strength-to-weight ratio as compared to conventional materials.

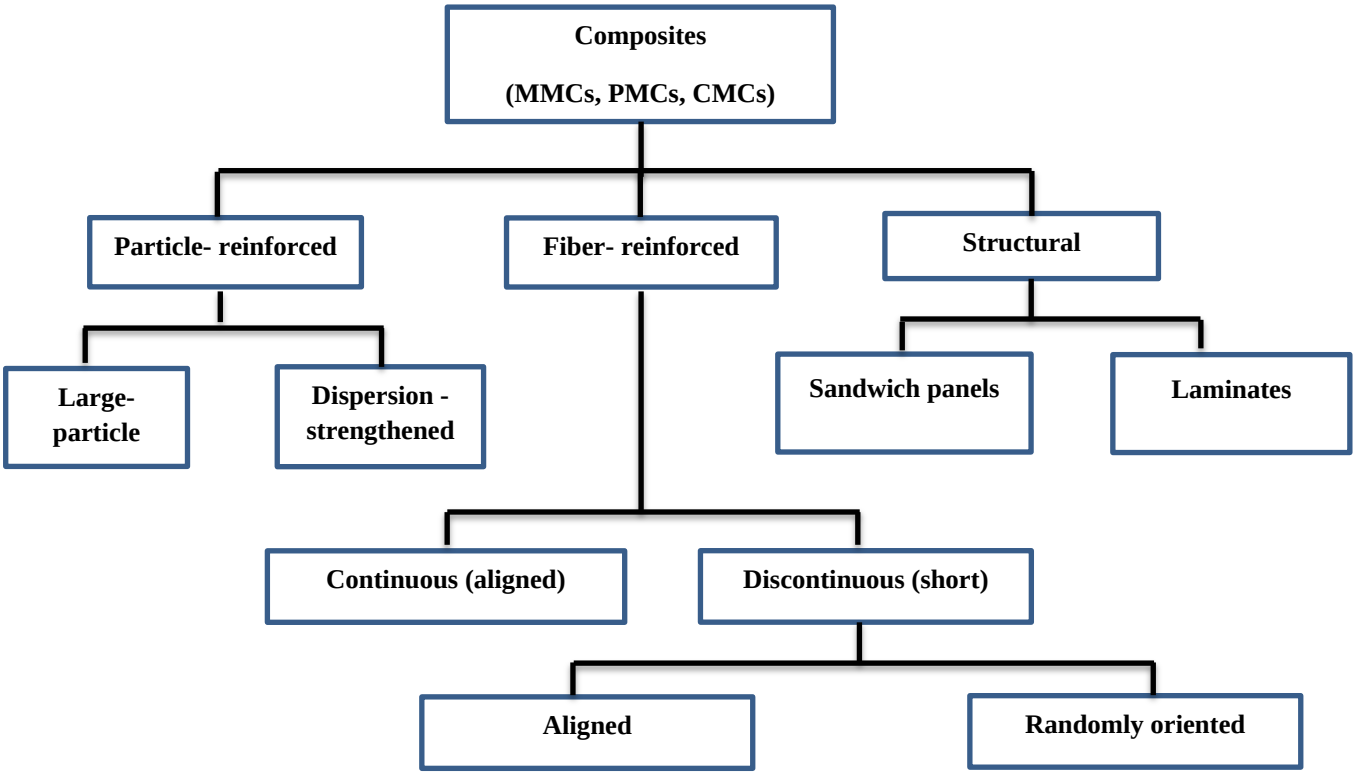

Fig.1.2 Types of composites

Composite materials are usually categorized by the type of reinforcements that are used in the composites. The reinforcements are incorporated into the matrix in order to strengthen the matrix. The different type of reinforcements that are used in composites are particulate reinforcement, flake reinforcement and fibers. Fibers could be of various types like random fiber, short fiber and continuous fiber etc. Fig.1.2 shows various types of composites [4,5].

At present metal matrix composites (MMCs) have generated a wide interest because of its high strength, stiffness and fracture toughness. Beside this they can also resist elevated temperatures in corrosive atmospheres. In MMCs both the metal and alloys used as matrices

and the reinforcement need to be stable over a range of temperature and should be non-reactive. The choice of the reinforcement depends on the matrix material and the application of the MMC. The strength to weight ratios of resulting composites can be higher than most of the metals and alloys. Several factors such as melting point, physical and mechanical properties of the composites at various temperatures determine the service temperature of the composites.

Metal matrix composites have opened up unlimited possibilities for developing innovative materials. MMCs can be used as constructional and functional materials. Powder metallurgy is one of the modern material processing technologies used for the development of MMCs. The major advantage of composites is their low cost and improved performance. The property of MMCs is determined by the property of the reinforcement. The reinforcements can have different objectives as per the desired application of the MMCs. The precondition here is the improvement of the properties of component. The objectives for development of metal matrix composites are to improve properties like yield strength, tensile strength, creep resistance, fatigue strength, thermal shock resistance, Young's modulus and corrosion resistance. The reinforcement not only serves a purely structural part of the MMCs but it also enhances the physical properties of the composites such as wear resistance, friction coefficient and thermal conductivity. The addition of reinforcements like particles, fibers, whiskers and wires in composites show significant improvement in mechanical properties. The reinforcement usually adds rigidity and greatly impedes crack propagation in the composites. Thin fibers as reinforcements can provide high strength to the matrix and can greatly improve the composites overall properties. Composite materials can be useful in several applications and can lead to the evolution curve for modern materials [5,6].The present applications and market prospects for metal matrix composites are primarily in military and aerospace industries. MMC components have been developed for use in jet

engines, missiles and aircrafts. Particulate-reinforced MMCs are used as covers for missile guidance systems. The composite piston is capable of giving better wear resistance and high temperature strength compared to the cast iron piston. Other applications of MMCs include cutting tools and circuit-breaker contacts. Metal matrix composites combine both metallic properties such as toughness and ductility of the matrix and the ceramic properties of the reinforcement such as high melting point and high modulus and strength at elevated temperatures which enables the use of the MMCs at high temperatures. From the study of the consumption of composite materials for several applications it can be concluded that MMCs are not excessively expensive for a cost sensitive application. Metal matrix composites generally consist of metals and alloys of metals like Cu, Al, Mg or Ti reinforced with ceramic particulates, whiskers or fibers. The choice of the reinforcement is very important in determining the cost and mechanical properties of the MMC that is being developed for a suitable application. MMCs provide advantageous mechanical properties due to the presence of reinforcement having high modulus and strength. These properties are very important for any load-bearing structural applications. However, it should be noted that the properties like fracture toughness and ductility of the metal matrix composites deteriorates as compared to the monolithic material as the ductility and toughness of most ceramic reinforcements are very low. Therefore, it is apparent that the matrix alloys having higher ductility and fracture toughness are desirable for MMC applications [7].

1.2 Cu-Based Metal Matrix Composites

Cu shows high formability, high resistance to oxidation and corrosion and has a special place among all metals because of its high electrical (5.96×10^7 S/m) and thermal conductivity (401 W/m.K). So, the most universal application of Cu is where high electrical and thermal conductivity are desired. The modulus of Cu is 130 GPa and its yield strength is117 MPa. Its

ultimate tensile strength is 210 MPa. There has been considerable interest in academics as well as industries in the use of Cu-based metal matrix composites in past few decades. Cu is an outstanding material for electrical applications whose competence can be enhanced by refining its mechanical properties. Pure Cu cannot be used in several applications due to its low strength and high ductility. Therefore it has become essential to improve the properties of pure Cu for its use in cutting-edge technological applications. Cu has high thermal conductivity and is used as a structural material for cooling. In order to increase its high temperature properties different reinforcements are being used. Very limited literature is available on Cu-based metal matrix composites (MMCs). The mechanical strength of copper can be improved either by age hardening or by particle dispersion strengthening. The age-hardenable Cu alloys are prone to precipitate coarsening at high temperatures which results in the degradation of strength. Matrix strengthening can be done by incorporation of reinforcement like continuous or discontinuous fibers, whiskers, wires and particulates. Cu-based metal matrix composites are used for manufacturing hybrid modules, electronic relays, electrically conducting springs and other electrical and electronic components [8,9].

Cu-based composites developed by powder metallurgy route have vast applications in manufacturing of tribological engineering parts such as bearings and bushes. Cu-based MMCs have applications in the area where good wear resistance without loss of electrical and thermal conductivity of the matrix is needed. Many applications depend on the surface property of the product so it is essential to modify the surface of the product by reinforcing with ceramic particles to achieve desired properties.

1.3 Scope and Objective of the Present Work

Cu-based metal matrix composites by the addition of different reinforcement such as E-glass fiber, SiC particle and multiwalled carbon nanotubes were developed by powder metallurgy route. The objectives of the present investigation are:

i. To develop Cu-based metal matrix composites using E-glass fiber, SiC particle and multiwalled carbon nanotubes by powder metallurgy route. Here in our study both as - received Cu and 20 h milled nanostructured Cu as have been used as matrix for the development of Cu-based metal matrix composites in order to study the effect of nanostructured Cu on sinterability and densification.

ii. Synthesis and characterization of multiwalled carbon nanotubes (MWCNTs) using low pressure chemical vapour deposition (LPCVD) method for use as reinforcement in Cu-based composites.

iii. To develop Cu-SiCp, Cu-E-glass fiberand Cu-MWCNTs composites and to study their microstructure and properties. The various properties like hardness, density and wear were studied for all the composites developed. Fracture surfaces of the various composites were also analyzed.

1.4 Thesis Outline

The thesis contains five chapters. The **1st Chapter, 'Introduction',** attempts to provide an insight to the work carried out and highlights the background and motivation for the present work. The **2nd Chapter, 'Literature Review',** is dedicated to an extensive study of the work carried out by other investigators in the field. The work carried out by them has been referred wherever necessary to explain and support the experimental findings. The **3rd Chapter, 'Experimental Details',** explains the various experimental procedures adopted in the present investigation. The various instruments and the prescribed experimental norms have been explained in detail in this chapter. The **4th Chapter, 'Results & Discussions',** shows the various results in the form of tables, graphs, optical, SEM and HRTEM images, fractography etc. The results have been analysed and explained in the present chapter. Finally, on the basis

of the experimental findings useful conclusions have been drawn which are listed in the **5th Chapter, 'Conclusions'**.

……

Chapter 2
Literature Review

Literature Review

2.1 Composites

A composite can be well-defined as a combination of two or more materials that results in improved properties as compared to those of the individual components. The two constituents in a composite are matrix and reinforcement. In contrast to metallic alloys, each material holds its separate mechanical, chemical and physical properties. The reinforcement is usually harder, stronger and stiffer than the matrix. The reinforcement phase provides the strength and stiffness. The main advantages of the composite materials are their high strength and stiffness, combined with low density. Composites are today used in several industries in order to develop high-performance products economically.

During 20^{th} century, arrival of the composites as a distinct classification came into existence. The major advantage of modern composite materials is their strength and light weight. Selection of appropriate combination of matrix and reinforcement is necessary to develop a new material that meets the requirement for a specific application. In matrix-based structural composites, the matrix serves dual purposes. It binds the reinforcement phase in place and also distributes the stresses between the constituent reinforcement materials under an applied force. Composite materials comprise some of the most advanced engineering materials today. Fig.2.1 shows the relation between the classes of materials showing the evolution of composites. Fig.2.2 shows the different types of reinforcements that can be incorporated inside the matrix. The reinforcements can be a particulate, short fibers or continuous fibers. The type of reinforcement and its orientation can alter the properties of the developed composite [1-4, 10, 11].

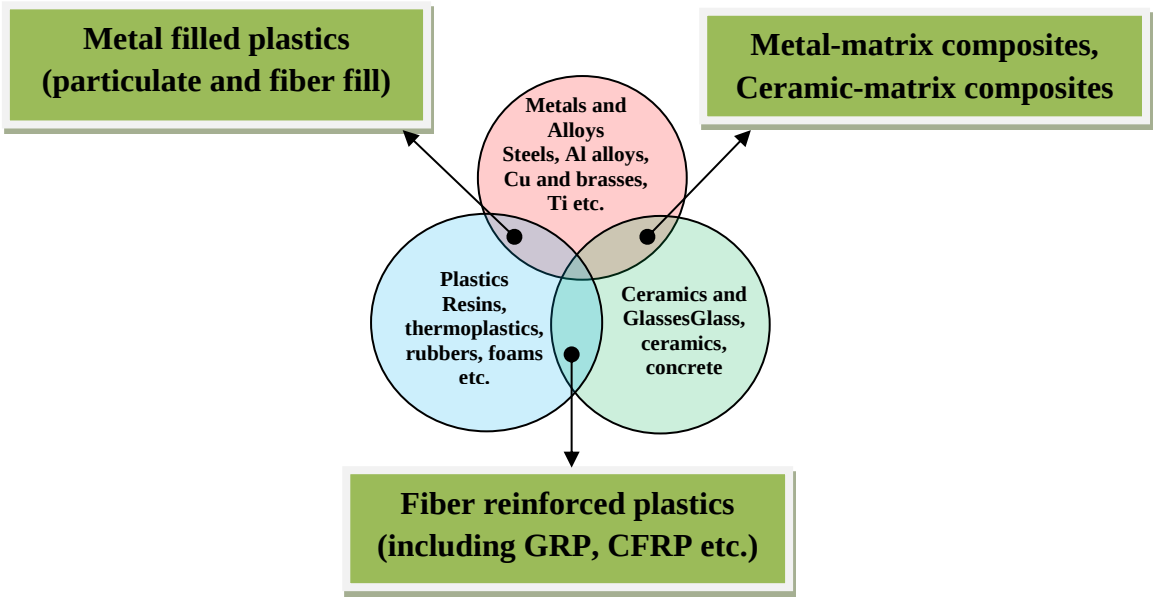

Fig.2.1 Relationship between the classes of materials showing the evolution of composites

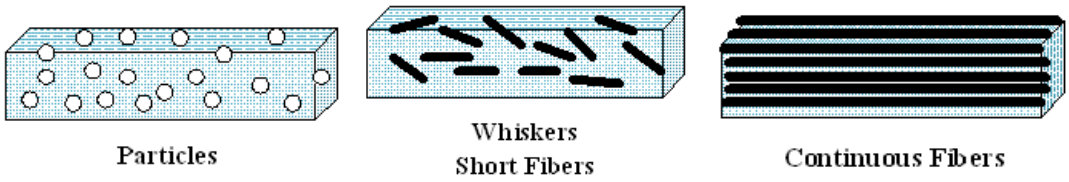

Fig. 2.2 Different type of reinforcements in matrix

2.2 Metal Matrix Composites

Metal matrix composite (MMC) are materials comprised of two different constituents one being a metal acting as a continuing matrix and the other material being an organic compound or a ceramic material contributing as reinforcement. Metal matrix composites are excellent materials for structural applications in automotive and aerospace industries owing to their high strength and thermal stability. In recent years MMCs have found improved application due to their excellent properties. The major advantages of the MMCs include greater strength, low density, improved high temperature properties, low coefficient of thermal expansion, and resistance to thermal softening, improved abrasion and wear resistance. When fine ceramic or other hard particles are embedded in the soft metal matrix to

form MMCs the properties of the metal matrix can be substantially improved or strengthened. The variation in reinforcement particle size and shape alters the overall chemistry and character of the microstructure and mechanical performance of the composite. The significant shift in metal matrix composite knowledge began in the middle of 1980's with replacement of continuous reinforcement. The low cost composites offers high strength, stiffness and fatigue resistance with a minimal increase in density over the base alloy. Most metals and alloys could be used as matrices and they require reinforcement materials which should be stable over a range of temperature and non-reactive with the matrix. In case of composites reinforced with hard particles, interfacial bonding between the matrix and particle should be strong. If the reinforcement is not well bonded to the matrix, the reinforcement elements cannot contribute to the properties like strength and wear resistance. Since the matrix phases are generally softer than the reinforcement phases, the extent of debonding of the reinforcement phase can play a critical role in wear behaviour of the composite. So the choice of reinforcement must be made judiciously in order to develop composites for a particular application [12,13]. At present MMCs have found application in many areas of our daily life. MMCs are being used to replace the conventional materials in numerous applications. They are used in a wide range of applications like automobiles to sport equipment. MMCs with high stiffness and strength could be used in applications in which weight reduction is a dynamic factor. MMCs are used to develop high-speed machineries and high-speed rotating shafts. Good wear resistance, with high specific strength, favours the use of MMCs in automotive engine and brake parts. Tailorable coefficient of thermal expansion and thermal conductivity make them favourable candidates for precision machinery, and electronic packaging [14].

2.3 Cu-Based Metal Matrix Composites

Cu and its alloys are one of the main groups of profitable metals. Cu is one of the most significant materials for thermal and electronic applications. They are extensively used because of their excellent electrical (5.96×10^7 S/m) and thermal conductivities (401 $W\cdot m^{-1}\cdot K^{-1}$) , exceptional resistance to corrosion, ease of fabrication and low cost. The coefficient of linear thermal expansion (CTE) of Cu (16.6×10^{-6} K^{-1}) is lower than that of Al (22.2×10^{-6} K^{-1}). Cu-matrix composites are promising applicants for applications in electrical sliding contacts. Cu-based metal matrix composites are also promising candidates for magnet design and robotics because of their excellent combination of strength and electrical conductivity. Cu-based MMCs can also be used to create high performance substrates for microelectronics packaging. However, it has several other good properties like good corrosion resistance, high ductility, high toughness etc. All these properties make Cu-based MMCs a very significant material which has a wide range of applications. Cu has a melting point of 1083.4°C and its density is 8.96 gm/cc. It's Young's modulus is 130 GPa. It's yield strength is 117MPa while its tensile strength is 210MPa. It's Poisson's ratio is 0.36. The mechanical strength of Cu can be enhanced either by age-hardening or by particle dispersion strengthening. The age-hardenable Cu alloys are subjected to precipitate coarsening at high temperatures which results in deterioration of its strength. The most general application of Cu is where high electrical and thermal conductivity are needed. Therefore it has become essential to improve the properties of pure Cu for its use in cutting-edge technological applications. There has been substantial interest in academics as well as industries in the use of Cu-based metal matrix composites in past few decades. Cu has high thermal conductivity and is used as a structural material for cooling. In order to increase its high temperature properties diverse reinforcements are used. Cu-matrix composites have a superior combination of thermal and electrical conductivity as well as high strength. They display

significantly improved mechanical and tribological properties. These exceptional properties make these composites suitable for sliding electrical contact applications in which high electrical and thermal conductivity as well as increased wear resistance are necessary [15,16]. Cu composites produced by powder metallurgy route are widely used in tribological parts like bearing and bushes. Composites based on Cu-Sn alloys can behave as self-lubricating materials under various conditions such as excessive temperature and load. Cu-based composites are used in the area where improved wear resistance is required with minimal loss of thermal and electrical conductivity. The durability of the component in various applications depends on surface properties. Therefore, it is appropriate to modify the surface of the component by reinforcing with ceramic particles while the inner matrix remains ductile and tough. Pure Cu is not used as a bearing material due to its poor mechanical and hardness pproperties. Today self-lubricated sintered bearings and plastic materials are being used where continuous lubricating is impossible. Cu-based composites prepared by powder metallurgy route from Cu, Sn and solid lubricant MoS_2 powders are being used for this purpose [17].Like other metals or alloys Cu and its alloys also soften at high temperature. This is why reinforcing Cu with ceramic particles or carbon fibers is one of the finest solutions to overcome this problem. Although Cu has very good thermal and electrical properties. Very limited literature is available on Cu-based MMCs. Here in this work a very systematic investigation on Cu-based MMCs using SiCp, E-glass fiber and multiwalled carbon nanotubes (MWCNTs) as reinforcement was carried out in order to find out the effect of addition of three different types of reinforcement in the Cu matrix.

2.3.1 Cu-SiCp Composites

Cu shows high formability, high resistance to corrosion and oxidation and is a very good thermal and electrical conductor. These properties make Cu an excellent candidate for applications where high thermal and electrical conductivity are desired. The major limitations

of Cu are its low strength and poor wear resistance. In order to improve these properties discontinuous reinforcements can be incorporated in the Cu matrix. SiCp could be used as a reinforcement to achieve the desired properties. Cu-SiCp composites combine together the high ductility and toughness of Cu and the high strength and modulus of SiC reinforcements. SiC has a melting point of 2730°C and its density is 3.20gm/cc. It's specific heat is 0.66 J/g.K. It's elastic modulus is 450 GPa. The hardness of SiC is 20.5 GPa which is comparable to that of corundum and diamond. SiC has high chemical resistance. It's coefficient of thermal expansion is 4.0×10^{-6}/K N and its thermal conductivity is 250 W/mK. It has a fracture toughness of 2.94 MPa.$m^{1/2}$. Particulates like SiC behave as an outstanding inclusion because of their expectable isotropic behaviour in composites. These properties make SiC particulates a desired reinforcement that can be incorporated in the Cu matrix. With the incorporation of SiC particulates as reinforcement in the Cu matrix the high-temperature mechanical properties can be enhanced. The wear resistance of pure Cu can also be improved with the addition of SiC particulates in the Cu matrix. Particulate-reinforced Cu matrix composites may have many evident advantages compared to Cu alloys. These kinds of materials are considered to be favourable candidates for applications where properties like high conductivity, high mechanical property and good wear resistance are required [18].

Several researchers have reported on Cu-SiCp composites. Yih and Chung [19]have fabricated Cu composites containing 33-54 vol.% SiC whiskers by hot pressing. The whiskers were coated with Cu prior to pressing. They reported that the resulting composites display several good properties such as low porosity, high hardness, low electrical resistivity and high thermal conductivity. Tjong et al.[20]reported that dry sliding wear of a Cu composite with 20 vol.% of SiC produced by hot isostatic pressing technique shows better wear resistance than pure Cu. They have indicated that the SiC particle is the major load bearing component and also established that delamination is the leading wear mechanism in this

composite. Schubert et al.[21] studied materials that could dissipate the heat generated in electronic packages and according to their study Cu-SiC composites could be used successfully for this application. They developed the Cu-SiC composites by powder metallurgy route. These composites were prepared by pressure-assisted sintering using a hot press. The authors investigated that enhancement in bonding strength and thermophysical properties of the composites could be achieved by vapour deposition of Mo on SiC powder. Dhokey and Paretkar [22] studied the wear mechanism in Cu-20 vol. % SiCp reinforced composite. They studied the wear behaviour of Cu-SiCp composites in terms of its thermal and mechanical characteristics. Dimensional equation between the collaborative variables is stated in their study to relate their effect on the wear parameters of the material. The composites were fabricated by powder metallurgy route and were sintered in N_2 atmosphere. They have reported results of mechanical, physical and microstructural characterization of the developed composites. It was found from the tribological studies conducted by them that there was a reduction in wear rate with increase in sliding speed. Efe et al. [23] studied the effect of sintering temperature on the properties of developed Cu-SiCp composites. Cu-based metal matrix composites were developed with different wt. % of SiC particles by powder metallurgy method. Their study shows that that SiC particles are distributed uniformly in the Cu matrix. It has been concluded from their study that with the increase in the content of SiCp the hardness of the composite increases but the relative density of the composite decreases. The highest electrical conductivity was achieved with the lower percentage of SiCp at a sintering temperature of 900^{o}C. Akramifard et al. [24] developed composites using pure Cu sheets reinforced with 25 μm SiC particles by friction stir processing (FSP). For achieving the uniform distribution of reinforcing SiC particles in the Cu matrix, a net of holes were drilled on the surface of the pure Cu sheets. From their study it was concluded that the

SiC particles improved the wear resistance of the composites and there was a rise in the average friction coefficient of pure Cu.

2.3.2 Cu-E-Glass Fiber Composites

Glass fibers are one of the most versatile and useful industrial materials known. They are easily produced from the raw materials which are obtainable in abundant supply. E-glass fibers show excellent mechanical properties. They have a tensile strength of 3500 MPa and a hardness of 6000MPa. It's Young's modulus is 85 GPa and it's compressive strength is 5000 MPa. Typically glass fibers belong to two different categories, the low cost general purpose fibers and the premium special purpose fibers. E-glass fibers come in the class of general purpose fibers. The general purpose glass fibers are less costly as compared to the premium category fibers. Fig.2.3 below shows the cost band for different fibers.

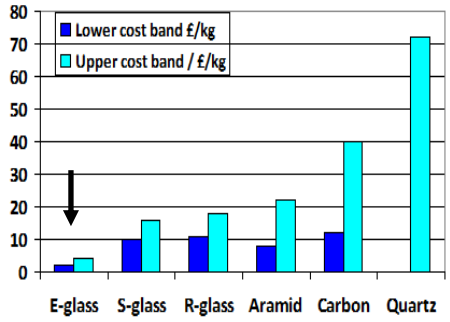

Fig. 2.3 Cost band for different fibers

Table 2.1 Properties of different type of glass fibers

Properties	E-glass	C-glass	S-glass
Density, ρ(mg/m^3)	2.58	2.49	2.48
Thermal conductivity, K(W/m.K)	13	13	13
Coefficient of Thermal Expansion, α(10^{-6}/K)	4.9	7.2	5.6
Tensile strength, σ,(GPa)	3.5	3.30	4.6
Young's Modulus, E(GPa)	76.0	69	85.5

E-glass fibers are found to be one of the most suitable materials for the development of composites due to its low cost and high strength. Glass fibers are used ina wide range of applications. Glass fibers offer excellent properties from high strength to fire resistance. Glass fiber is a dimensionally stable engineering material. It does not stretch or shrink after exposure to extremely high or low temperatures. The maximum elongation of E-glass fiber at break is 4.8 % with a 100 % elastic recovery when stressed close to its point of rupture. The density of E-glass fiber is 2.58 gm/cc. It's coefficient of thermal expansion is 5.3× 10^{-6}/^{o}C [25].

E-glass fiber has been used extensively as reinforcement in polymer based composites. However, report on use of E-glass fiber as reinforcement in metal matrix composites is limited. Zak et al. [26] studied a rapid engineering process for the development of polymer-based composite parts using short discontinuous fibers as reinforcements. The mechanical testing of these composite specimens showed up to 60% improvement in the modulus values compared to unreinforced layered specimens. In their paper author has reported the use of a UV-laser-based system for the selective solidification of the composite liquid. Schutte [27] investigated the durability of glass-fiber/polymer composites. It was reported that environmental attack by moisture can degrade the strength of the glass fibers and the fibers can plasticize, swell, or produce microcracks in the matrix and degrade the fiber/matrix interface by either chemical or mechanical attack.

2.3.3 Cu-Multiwalled Carbon Nanotubes Composites

Carbon nanotubes have emerged as promising reinforcement for a variety of nanocomposites because of their sharp geometry, mechanical strength, chemical stability and electrical conductivity since their discovery in the early 1990s. It is a tube-shaped material made of carbon with diameter in nanometric scale. Single walled carbon nanotubes (SWCNTs) consist of a single layer graphene sheet wrapped to form a tube structure having diameters at nanoscale. Several experiments and simulations reported that CNTs have surprising mechanical properties. They have elastic modulus of 0.3-1TPa, tensile strength of the order of 10-60 GPa and thermal conductivity of up to 3000 W/mK. The strength of carbon nanotubes is approximately 100 times superior to that of steel of the same diameter. Carbon nanotubes come in two principal forms, single walled carbon nanotubes (SWCNT) and multiwalled carbon nanotubes (MWCNT).The density of multiwalled carbon nanotubes (MWCNTs) is 2.60 gm/cc and their specific surface area is about 200-400 m^2/g.

Cu-based metal matrix composites having carbon nanotubes as reinforcement are used for structural applications and functional materials because of their high strength and excellent electrical and thermal conductivity. CNTs are promising candidates that could be used as nanoscale reinforcement in Cu-based metal matrix composites. It has been reported in literature that with the addition of carbon nanotubes the bulk properties of Cu could be improved. The Cu-based MMCs reinforced with CNTs have superior mechanical properties and are more thermally stable compared to pure Cu. Carbon nanotubes act as a filler material which reduces the thermal expansion coefficient of the Cu matrix. With the addition of CNTs the bulk electrical conductivity of the Cu composites can also be modified. The two main types of CNTs are single-walled carbon nanotubes (SWCNTs) and multiwalled carbon nanotubes (MWCNTs). SWCNTs are an allotrope of sp^2 hybridized carbon similar to fullerenes. The structure of SWCNTs is that of a cylindrical tube comprising six-membered carbon rings which are similar to graphite. On the other hand MWCNTs have several concentric tubes. Here we have used MWCNTs as a reinforcement for developing Cu-MWCNT composites[28,29].Fig.2.4 shows the number of publications for the past few years on CNT reinforced composites. It can be seen from the figure that the bulk of the research has been done on polymer-based composites reinforced by CNTs. In past few years there is a significant increase in the publications on metal matrix composites reinforced by CNTs. Fig.2.5 shows the number of publications in the area of for various CNT reinforced metal matrix composites using CNTs as reinforcement between 1997 to 2007. The figure shows that the number of publications in this area has increased several times since 2003 making the topic for current research [30].

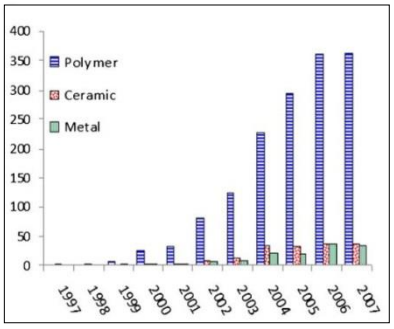

Fig.2.4 Graph showing number of publications in different years of CNT reinforced composites

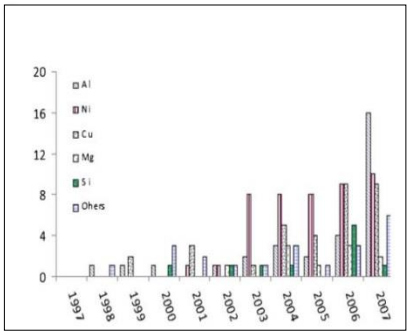

Fig.2.5 Graph showing number of publications in different years of CNT reinforced MMCs

Several researches have reported that with the addition of carbon nanotubes the strength and toughness of the material can be enhanced. Li et al. [31] studied the properties of Cu-CNTs composites. They have reported that the composites developed shows high strength and good ductility. It was investigated from the pillar testing that the strength and plastic strain of the composites could be as large as 1700 MPa and 29 % respectively. From the results it is evident that addition of 1wt. % CNTs could lead to an increase in the strength, stiffness and toughness of the material. Microstructural analysis discloses that in the composites, CNTs could be either distributed at the grain boundaries or inside the Cu grains. Trinh et al. [32] studied the calculation of friction coefficient of Cu-CNT composite. They developed the composites by powder metallurgy route and the friction coefficients were evaluated. From their study it was concluded that the coefficient of friction of the developed composites decreases with the increase in the mass fraction of CNTs in the composites. Lal et al.[33] investigated an alternative method for the dispersion of CNTs in the Cu matrix. In their work they used the molecular level mixing technique coupled with high energy ball milling followed by powder metallurgy to synthesize the Cu-CNTs composites. It is observed that there has been an increase in the mechanical properties over pure Cu and the method used shows a distinct advantage for the synthesis of Cu-CNTs composites.

It could be concluded form the above research papers that the most important factors in developing Cu-MWCNTs composites is the homogeneous dispersion of the CNTs in the Cu matrix, interfacial bonding between the CNTs and the Cu matrix and the retention of structural integrity.

2.4 Processing Techniques for Metal Matrix Composites

Manufacturing is a very comprehensive area and include numerous processes such as machining, fabrication and joining. The fabrication approach of a composite part depends mainly on three factors: (i) the nature of the matrices and reinforcements, (ii) the shape and sizes of products and (iii) their end use. There are numerous kinds of composite materials which cover a wide spectrum of applications ranging from an engine valve to an aircraft wing. The fabrication technique varies from one product to the other.

There are mainly two types of processing techniques. They are,

i. Liquid State Processing Techniques
ii. Solid State Processing Techniques

2.4.1. Liquid State Processing Techniques

The liquid state processing technique includes the ease of handling liquid metal related to the powder. There is lesser cost involvement for obtaining liquid metals as compared to metal powder and this technique also gives us the possibility of creating various shapes by using several methods available in casting industry. Liquid state processing also suffers from a number of limitations like incomplete control of the processing parameters and unwanted chemical reactions at the boundary of the liquid metal and the reinforcement [34].

A brief description of the various liquid state processing techniques is given below:

2.4.1.1 Infiltration Process

The liquid infiltration process comprises infiltration of a particulate or fibrous reinforcement by a liquid metal. In this process the molten matrix is infiltrated in a pile of continuous or discontinuous reinforcements. It is then allowed to solidify between the inter-reinforcement spaces. This process of developing MMCs is not straight forward because of the difficulty of wetting the reinforcement by the molten metal. The reinforcement can be pre-mixed with the matrices prior to casting in the case of discontinuous reinforcement. The several techniques available for pre-mixing the metal and the reinforcement are injection gun, dispersion of reinforcements in a mildly agitated melt, mechanical agitation and centrifugal dispersion. To improve wettability and to control the interfacial reactions a fiber coating is applied prior to the process to achieve better results. However, it could be disadvantageous if the fiber coating is exposed to air leading to surface oxidation.

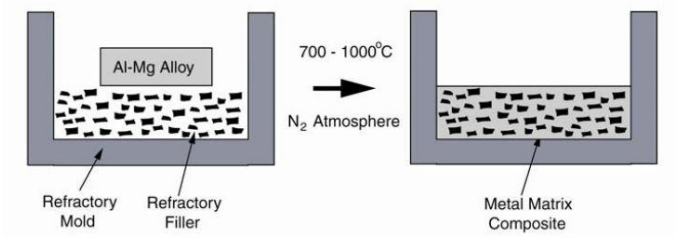

Fig.2.6 Schematic diagram showing the setup of the pressure less liquid metal infiltration technique

Fig.2.6 shows the schematic diagram of pressure less liquid metal infiltration technique for developing MMCs. It can be used with reactive metal alloys such as Al-Mg to infiltrate ceramic preforms. For Al-Mg alloys, the process takes place between 850 -1000°C in a N_2-rich atmosphere and typical infiltration rates are less than 25 cm/h.

2.4.1.2 Dispersion Process

Dispersion process is a liquid state processing technique in which the reinforcement is incorporated in loose form into the metal matrix. To combine the two phases a mechanical force is required and this can be achieved by stirring as most systems have poor wettability.

The major advantage of this process is its low cost. In addition this process can be adopted during both casting and extrusion. The simplest type of dispersion process is the vortex method in which the liquid is stirred and the reinforcement particles are added during stirring. The main disadvantage of this process is the presence of porosity resulting from gas penetration during the process. The other drawbacks are the reaction between the matrix and the reinforcement that takes place due to long interaction time and clustering that can occur during mixing.

2.4.1.3 Spray Process

Monolithic alloys were produced initially by spray forming techniques. However, with the advancement in technology particle reinforced MMCs are also being developed by this process. One of the examples of this process is the co-spray process in which the heated SiC particles are injected inside the molten Al alloy using a spray gun. SiC particles upto 20 vol. fraction with aspect ratio 3-4 are incorporated in the Al alloy by this method. An optimum particle size is needed for the process to be efficient as very fine particles and whiskers are very difficult to transfer. The co-sprayed MMCs are subjected to scalping, consolidation and several secondary finishing processes to form the wrought composite material. It is a liquid metallurgy process and it is fast and automated. As the time of flight is very short there is no possibility of formation of any toxic materials. The major advantage of this process is its flexibility and the ease with which different types of composites can be developed. However, this process is quite expensive because of the high cost of the equipment.

2.4.1.4 In-Situ Process

In-situ process is one of the widely used liquid state processing technique in which the reinforcement is formed in-situ. Composites in this process are developed in a single step from the starting alloy thus minimizing the efforts to form composites by combining different constituents as generally done in the development of typical composites. One of the examples

of in-situ processing is unidirectional solidification of eutectic alloys. Unidirectional solidification of a eutectic alloy typically results in one phase being distributed in the form of fibers or ribbon in the matrix phase. Several parameters such as spacing and relative size of the reinforcement can be precisely controlled by controlling the solidification rate. In this process the volume fraction of the reinforcement remains constant throughout the process. The solidification rate in practice, however, is limited to a range of 1-5 cm/h because of the need to maintain a stable growth front which requires a high temperature gradient.

2.4.2 Solid State Processing Techniques

Solid state processing techniques are one of the most preferred techniques to develop metal matrix composites. In these techniques the MMCs are developed as a result of bonding between the matrix metal and the dispersed reinforcement phase due to mutual diffusion occurring between them at elevated temperatures and pressure. In solid state sintering there is a reduction of undesirable reactions at the interface of the matrix and the reinforcement phase as compared to liquid state fabrication techniques as the processing temperature is below the melting point of both the metal matrix and the reinforcement. Metal matrix composites formed by this process can further be deformed by rolling and extrusion [34].

Brief description of the various solid state processing techniques are given below:

2.4.2.1 Diffusion Bonding

Diffusion bonding is a common solid state processing technique for joining similar and dissimilar metals. It is generally carried out at a higher temperature where the inter diffusion of atoms between the metals takes place easily leading to bonding of the atoms. There are several advantages of this method, one being the capability to develop a wide range of metal matrices and other being the control of fiber fraction and their orientation. High temperature and pressure is used during the diffusion process. Vacuum hot pressing is one of the important steps in the diffusion bonding process for the development of metal matrix

composites. Hot isostatic pressing (HIP) is preferred for diffusion bonding. Using HIP it will be relatively easy to apply high pressures at elevated temperatures. It also enables the development of products having variable geometries. Diffusion bonding also has several disadvantages such as long processing time, requirement of high processing pressure and temperature. Due to need of high processing temperature and pressure the process becomes costly.

2.4.2.2 Powder Metallurgy

Powder metallurgy is one of the preferred methods of solid state processing technique for the development of metal matrix composites. It is a process for producing useful products using metal powders. It is one of the most important techniques through which particulate materials are consolidated to finished products. Nowadays powder technology is used to develop components providing exceptional properties that are desired in highly advanced aerospace and nuclear energy industries. Automobile industries are also one of the major consumers of powder metallurgy products. There are several significant reasons for using powder metallurgy as the processing technique by the industries such as the creation of complex components like tungsten filament, porous self-lubricating bearings etc. This process minimizes or eliminates the scrap and machining losses leading to high volume production of components. This process is economical, saves energy and raw materials. It also enables mass production of quality precision components. Fig.2.7 shows the flowchart of the sequence of operations in the powder metallurgy process. This process involves the combination of blending the metal powders and other constituents followed by compaction to produce the desired shape. The green compacts developed are then sintered at higher temperatures usually below the melting point of the major constituent to develop a product of desired structure, density and properties.

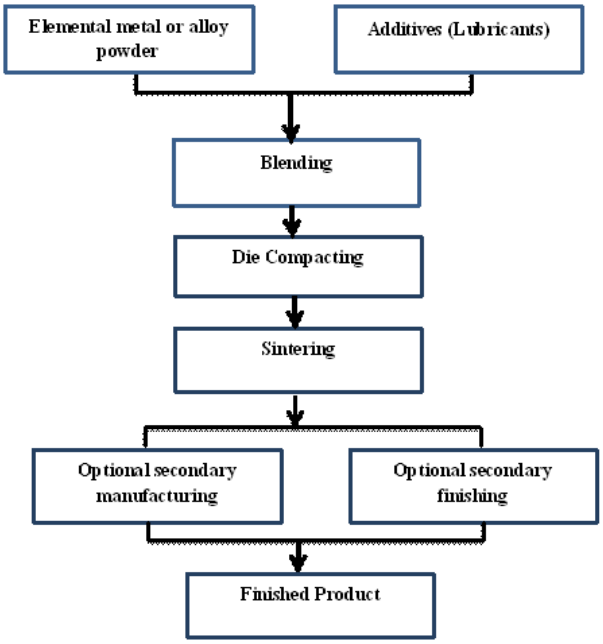

Fig.2.7 Simplified flowchart showing the sequence of operations in powder metallurgy

For solid state sintering the sintering temperature is kept below the melting point of all the constituents. Wherever, for liquid state sintering the sintering temperature is kept above the melting point of any of the constituents. In hot pressing the two stages of compaction and sintering are combined into one single step. Powders can also be rolled continuously and sintered to produce strips and other flat products. Powder metallurgy process enables the manufactures to develop products that are very consistent and predictable in behaviour. Powder metallurgy products have a wide range of applications [35-37].

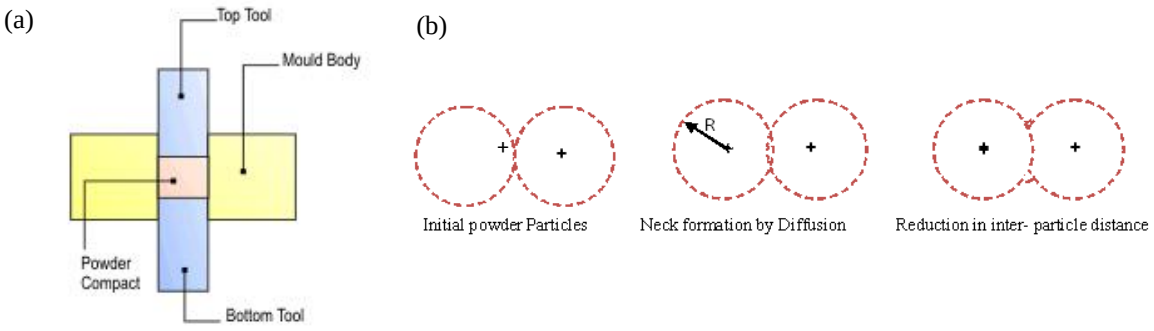

Fig.2.8 (a) Schematic of uniaxial cold compaction (b) Schematic diagram showing the sintering mechanism using solid state diffusion process

Fig. 2.8(a) shows the schematic diagram of a uniaxial cold compaction machine. Uniaxial cold compaction involves the compaction of powder in a die by applying pressure in a single axial direction through the punch. Fig. 2.8(b) shows the sintering mechanism using solid state diffusion process. In solid state sintering the densification is attained through changes in particle shape, deprived of particle rearrangement.

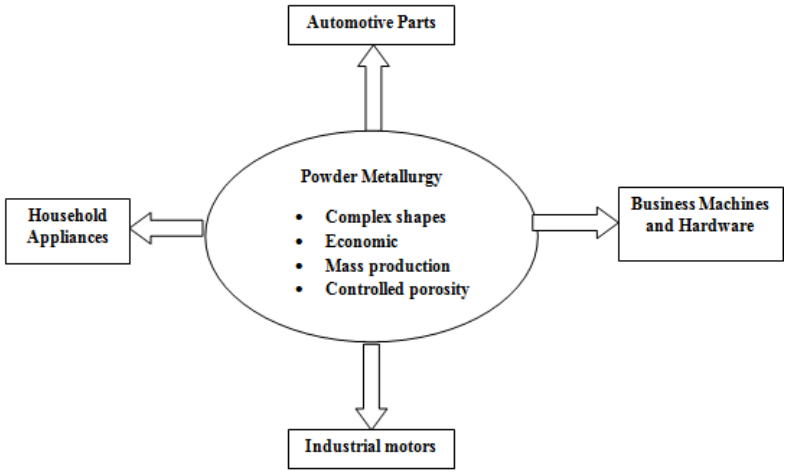

Fig.2.9 Applications and Advantages of Powder metallurgy

Fig.2.9 Applications and Advantages of Powder metallurgy

There has been an increasing interest in powder metallurgy with the expansion of various industries since 1950. Several advantages and application of this technique are shown in Fig.2.9. Nearly 90% of powder metallurgy products are used in transportation markets. Several technologies are being developed for reducing fuel consumption. The automotive industry is in the trend of developing lightweight technology and engine downsizing for environmentally friendly vehicles. To achieve this reduction, powder metallurgy products, which are components of the latest systems, are also required to have higher performance[38].

2.4.2.3 Mechanical Alloying

Mechanical alloying (MA) is used as one of the preferred method for powder processing. In this technique production of homogenous materials is done starting from blended elemental

powder. John Benjamin and his colleagues at the Paul D. Merica Research Laboratory of the International Nickel Company (INCO) developed the process around 1966. This technique was the result of an extended search to develop nickel-base super alloy for gas turbine applications. MA is one of the solid state processing techniques which comprises repeated welding and fracturing of powder particles in a high-energy mill. However, in earlier days this process had been used to develop oxide-dispersion strengthened (ODS) nickel and iron base super alloys for applications in aerospace industry. It is a complex process and hence involves optimization of a number of variables to achieve the desired product. Mechanical Alloying (MA) is described as a high energy milling process in which powder particles are exposed to repeated cold welding, fracturing, and rewelding. Due to the high energy of the impacts a large amount of strain is introduced in the powder particles. As a result a large number of dislocation and other defects are generated which act as fast diffusion paths. The initial process of mechanical alloying starts with the mixing of powders in the desired proportion. Then this powder is loaded in the mill with the grinding medium. Several grinding media like tungsten carbide (WC), hardened chrome steel, stainless steel, zirconia etc. are available. The powders are then grinded for the desired time until a steady state is reached. Process control agents (PCA) like toluene could be used during milling. The powder obtained after milling is then consolidated into a bulk sample and sintered at a desired temperature to obtain the desired microstructure and properties [39-49].

Some of the important parameters of mechanical alloying that have an effect on the final constitution of the powder are:

1. The yield or the amount of powder obtained from milling is determined by factors like the milling speed, milling time and the amount of process control agent used. The process control agent has a lubricating effect that minimizes the cold welding effect. Without the use of the PCA, the powder being milled welds on the milling chamber vessel walls,

resulting in a lesser fraction of the charge being recovered. However, a large amount of PCA could also affect the kinetics of the mechanical alloying process. Therefore, an optimum amount of PCA should be used during milling in order to ensure a higher yield and shorter downtime.

2. type of mill (High energy planetary ball mill, spex mill, cryogenic mill etc.)
3. milling media (Zirconia, tungsten carbide, hardened chrome steel, stainless steel etc.)
4. milling speed (can be varied)
5. milling time (can be varied)
6. size of the balls used for milling (Various sizes of ball are available. If the balls are too large then the number of breaking contacts will be low and as result the grinding capacity will also be lower. Whereas, if the balls are too small, the grinding efficiency could be decreased as the contacts may be too weak to break the particles.)
7. ball-to-powder weight ratio (1:10 , 1:20 , etc.)
8. milling atmosphere (Dry or wet milling. For wet milling toluene could be used as the process control agent. Argon inert gas atmosphere can also be used.)

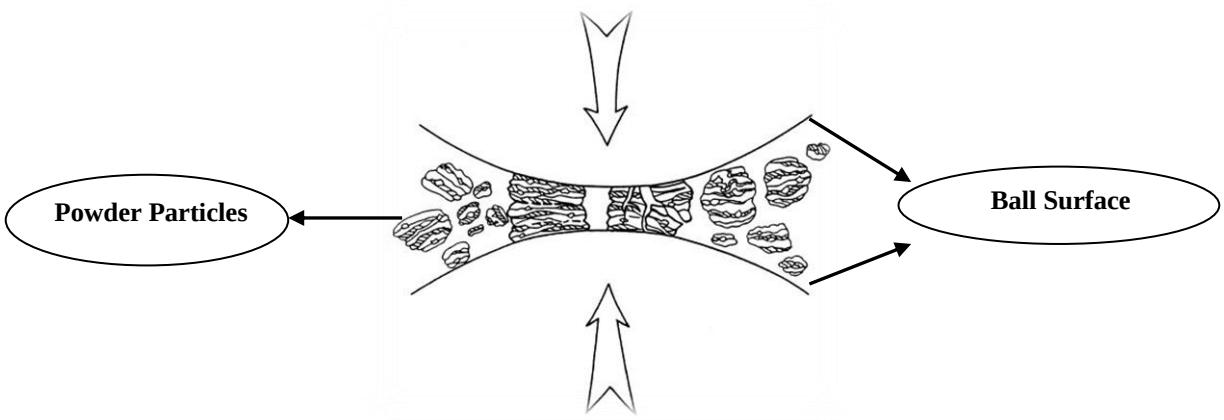

Fig.2.10 Ball-powder-ball collision during high energy ball milling

Fig.2.10 shows the collision of ball-powder-ball during high-energy ball milling. The powder particles during the process are repeatedly flattened, cold welded, fractured and rewelded.

Whenever the balls collide there is always some amount of powder particles that get trapped in between the balls. Typically around 1000 particles with an approximate weight of 0.2 mg could be trapped during every collision of balls. Fig.2.11 shows the motion of the balls and the powder. As the rotation directions of the bowl and the turn disc are opposite in nature, the centrifugal forces are alternately synchronized.

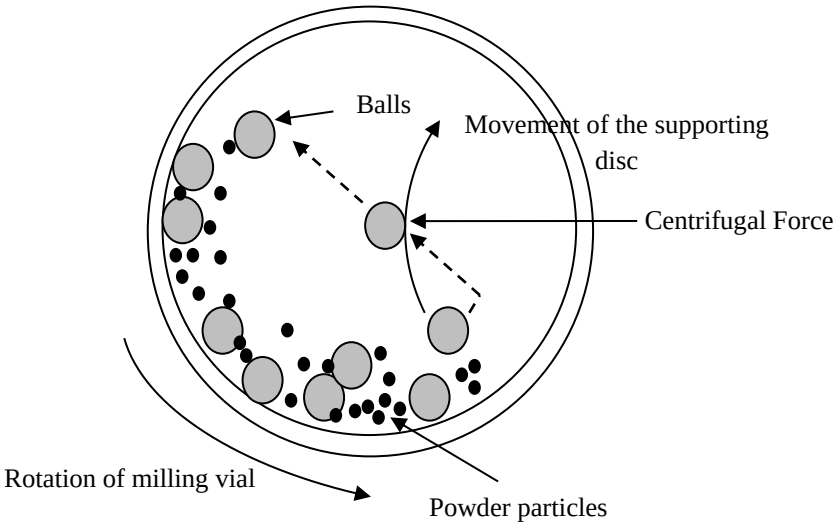

Fig. 2.11 Schematic view of motion of the ball and powder mixture

The powder particles get work hardened and fractured during the continuous collision of balls. The powder particles get deformed during the process. Initially the particles have strong affinity to weld together due to their soft nature resulting in the formation of larger particle. With continued deformation, the particles get work hardened and fracture by a fatigue failure mechanism. Fragments generated by this mechanism may continue to reduce in size in the absence of strong agglomerating forces [50].

…….

Chapter 3

Experimental Details

Experimental Details

Introduction

This chapter describes the experimental procedure as adopted in the present investigation. The equipment/instruments used to carry out the experiments are listed below indicating their specific use in the project along with their specifications and particulars in details. A detailed report is also provided on the raw materials procured and synthesized that have been used for the fabrication of the Cu-based metal matrix composites. This chapter provides the detailed step-wise methods adopted for the fabrication of the composites. The following work plan has been adopted:

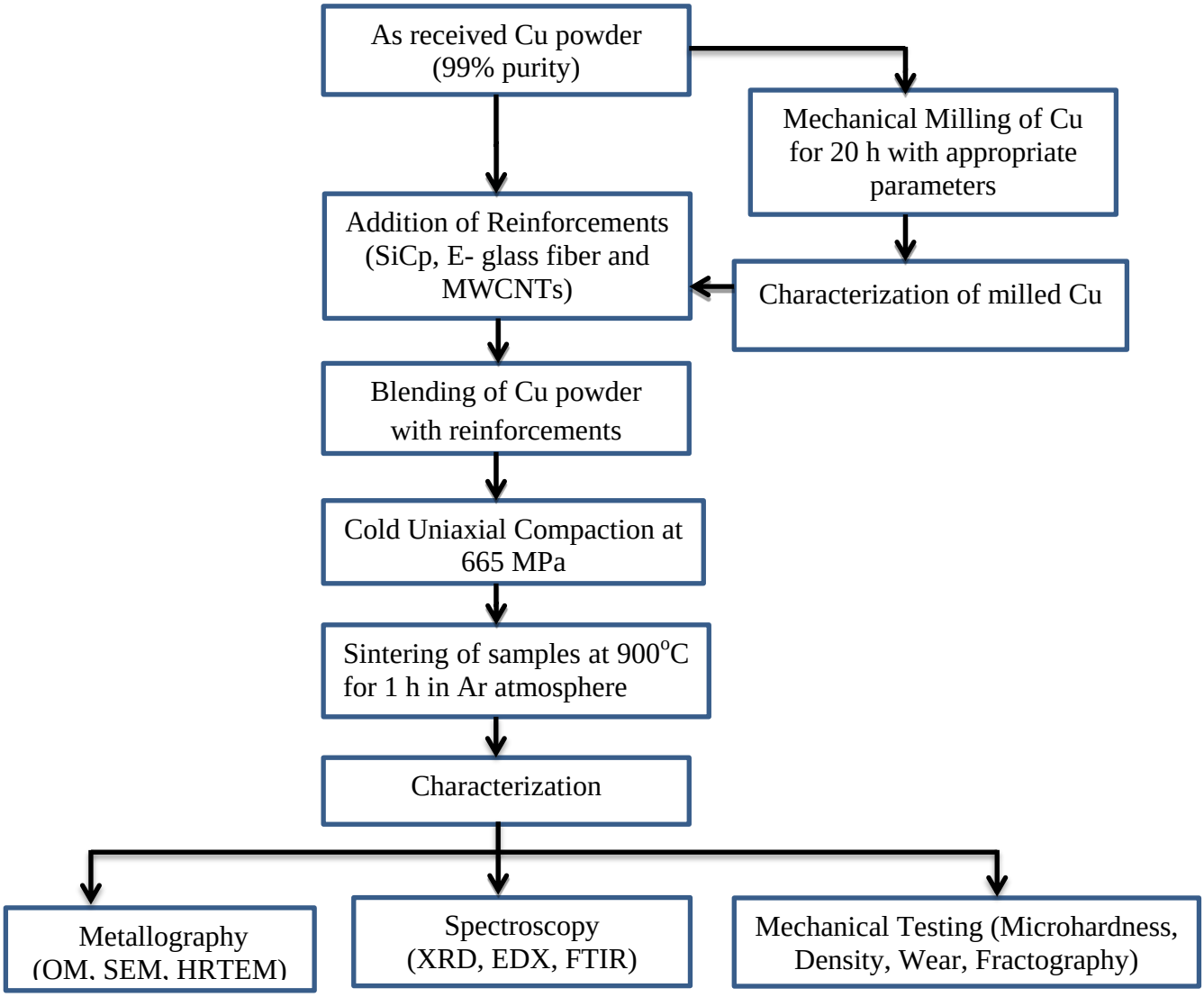

Fig.3.1 Work plan for present investigation

3.1 Equipment used in the Present Investigation

1. Planetary Ball Mill

Here a high energy ball mill is used for the milling of elemental Cu to reduce its crystallite size to nanometer scale. The as-milled nanocrystalline Cu is later used for the development of Cu-based metal matrix composites. The powder particles during the process are repeatedly flattened, cold welded, fractured and rewelded. Whenever the balls collide some amount of powder particles get trapped in between the balls. The powder particles get work hardened and fractured during the continuous collision of balls throughout the process. The powder particles get deformed during the process. Initially the particles have strong affinity to weld together due to their soft nature resulting in the formation of larger particles. With continued deformation, the particles get work hardened and fractured by a fatigue failure mechanism. Fragments generated by this mechanism may continue to reduce in size in the absence of strong agglomerating forces.

There are several advantages of ball milling such as:

i. Low installation cost
ii. Low powder cost
iii. Low grinding medium cost

The milling conditions used in the present investigation are:

Milling Conditions:

- Ball Mill: Fritsch P5
- Milling Medium: Wet (Toluene)
- Vials and Balls: Hardened chrome steel
- Milling Speed: 300 rpm
- Diameter of Balls: 10mm
- Ball to powder weight ratio = 10:1

(a) 

(b) 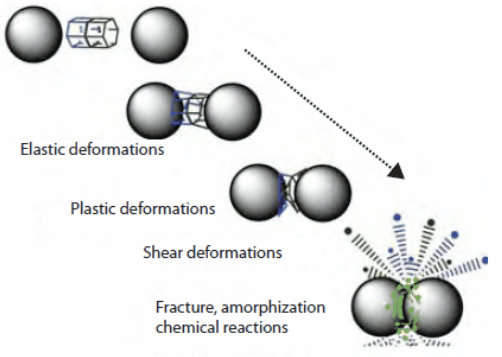

Fig.3.2 (a) Planetary Ball Mill (b) Schematic diagram showing the mechanism of ball milling

Fig. 3.2(a) above shows the Fritsch planetary ball mill. Fig. 3.2(b) shows the schematic diagram of the milling process and the behaviour of powder particles during milling. The speed used for the current investigation is 300 rpm with ball to powder ratio of 10:1. Planetary ball mill (pulverisette-5) manufactured by Fritsch Germany is used for the above purpose.

2. Cold Uniaxial Hydraulic Press

Uniaxial die pressing is one of the ideal methods which is commonly used to manufacture near net shaped components. It is used for making the green samples which were later sintered in the tubular furnace. Uniaxial pressing includes the compaction of powder in a die by applying pressure in a single axial direction through the punch or piston. The presses used are generally mechanical or hydraulic and the pressing cycle repeats at 6 to 100 times/min.

(a) 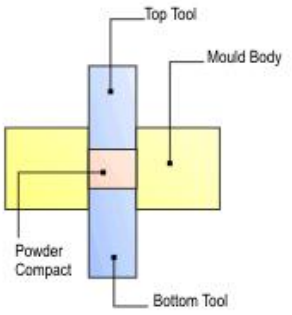

(b) 

Fig.3.3 (a) Schematic Diagram of Uniaxial Pressing (b) Uniaxial Hydraulic Press

In the present study a die with 15mm diameter is used and the applied stress is 665 MPa for all the samples. The press used was designed by Soil lab with maximum capacity of 1130 MPa.

3. X-Ray Diffraction

A diffractometer is a measuring instrument for analyzing the structure of a material from the scattering pattern created when a beam of radiation or particles (such as x-rays or neutrons) interact with it. X-ray diffraction of the milled Cu powder after several intervals of milling has been carried out to study the different phases formed during milling. The variation of crystallite size, r.m.s. strain and lattice parameter with milling time was also calculated. A Philip's X'pert Pro high-resolution x-ray diffractometer has been used for the purpose. The maximum scanning range (2θ) for the instrument is 0 to 160^{o}.The radiation used in x-ray diffraction was Cu-Kα having wavelength of 1.5409 Å. Ni was used as filter.

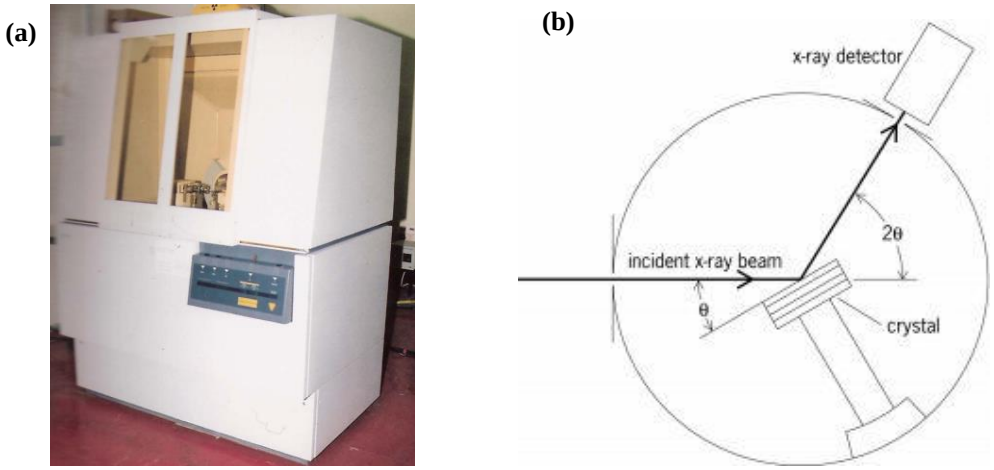

Fig.3.4 (a)Philip's X'pert Pro high resolution x-ray diffractometer (b) Schematic diagram of the diffractometer

4. High Temperature Horizontal Tubular Furnace

A high temperature tubular furnace is used for sintering the green samples. The sintering of the samples was done in an inert atmosphere of Ar gas. A tubular furnace is an electric heating device used to conduct synthesis and purification of inorganic compounds. The design comprises of a cylindrical cavity surrounded by heating coils that are rooted in a

thermally insulating matrix. Temperature can be controlled via response from a thermocouple. The samples were heated in a crucible in a tubular furnace in the presence of inert argon gas atmosphere. The casting temperature in the furnace was maintained at 900^{o}C with the holding time of 1 h for all the samples. A vacuum and control atmosphere furnace manufactured by Naskar & Company with maximum attainable temperature of 1750^{o}C is used for the above investigation.

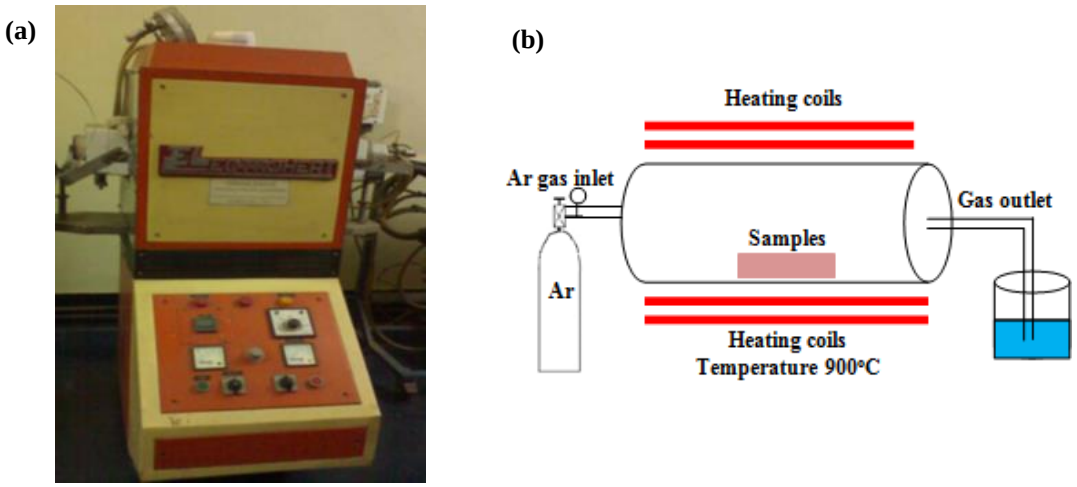

Fig.3.5 (a) Tubular furnace (b) Schematic diagram of the tubular furnace

5. Instron-1195

A universal testing machine (UTM) is used to determine the tensile stress and compressive strength of the materials. It is used to perform several standard compressive and tensile tests on components, structures and materials. TheInstron-1195 (Universal Testing Machine) machines is used to calculate the mechanical properties of the components by carrying different tests such as tension, impact, compression and torsion tests. Here it has been used for carrying out the tensile test of E-Glass fiber to determine its mechanical properties. During the test the control system and software records the values of load applied, displacement and other parameters. The Instron 1195 manufactured by Instron Ltd. with load carrying capacity between 0.1 kN to 100 kN is used for the present investigation.

Fig.3.6 Instron 1195

.

6. Scanning Electron Microscopy (SEM) and Field Emission Scanning Electron Microscopy (FESEM)

Scanning Electron Microscope (SEM) uses high energy beam of electrons that are directed at the specimen to produce a two dimensional image of a specimen. The electrons which are produced from the hot filament are accelerated by magnetic and electric fields. The signals produced provide the information about the surface topography composition and other properties. In the present investigation pure Cu and the composites developed were characterized and studied. The electron beam is concentrated to a fine probe to produce the images. The electron beam is scanned in a raster scan pattern and the beam's position is combined with the detected signal to produce an image. A resolution of less than 1 nm is achievable in a SEM. Every point on the sample emits signals in the form of electromagnetic radiations. Selected portions of this radiation, usually secondary electron (SE) and backscattered electron (BSE) are collected by a detector. The signals are amplified and displayed on a monitor. The subsequent image is generally straight forward to interpret, at least for topographic imaging of objects at low magnifications.

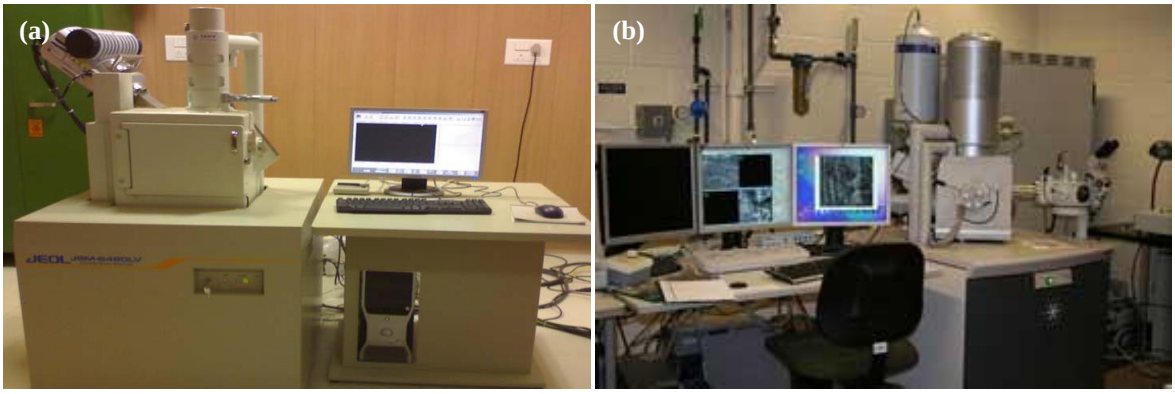

Fig.3.7 (a) Scanning electron microscopy (b) Field emission scanning electron microscopy

A JEOL-JSM-6480LV has been used in the present investigation. For energy dispersive x-ray spectroscopy (EDX) analysis, an INCAPentaFET-x3 x-ray microanalysis system with a high-angle ultra-thin window detector and a 30 mm^2 Si (Li) crystal was used.

The composites developed were also analyzed using a FEI Nova Nano FEG-SEM *450* FESEM. FESEM produces clearer, less electrostatically distorted images with spatial resolution down to 1.5 nm which is 3 to 6 times better than the conventional SEM. FESEM uses field-emission cathode in the electron gun of a SEM. A field-emission cathode in the electron gun provides narrower probing beams at low as well as high electron energy, resulting in both improved spatial resolution and minimized sample charging and damage. High quality images are obtained with negligible electrical charging of the samples using an accelerating voltage in the range of 0.5 to 30 kV. Also in FESEM the need for conducting coatings on insulating materials is virtually eliminated.

7. High Resolution Transmission Electron Microscopy (HRTEM)

High resolution transmission electron microscopy (HRTEM) is a technique that uses a beam of electrons which are transmitted through thin specimens and it interrelates with the specimen as it passes through it. From the interactions of electrons transmitted through the specimen an image is formed. This image is then magnified and focussed with the help of imaging device. The magnified image is focussed on a fluorescent screen on a layer of

photographic film. This is then detected by the CCD camera. In our study the 20 h milled nanostructured Cu powder and MWCNTs were observed under a HRTEM. The samples were dispersed by ultrasonication in acetone solution. The dispersed powder is then taken out using a pipette and drops of powder dispersed in acetone is put on a carbon coated copper grid for seeing the samples in the HRTEM. Selected area diffraction (SAD) pattern of all the samples have also been taken using the HRTEM. A Philips CM12 TEM has been used for analysing the samples and the accelerating voltage of 120 kV has been employed.

Fig.3.8 High resolution transmission electron microscopy

8. Density Measurement

Archimedes' principle was used for the measurement of density of samples. Precise measurement of the density of sintered samples was carried out. There are several errors in density measurement of the sintered samples usually due to the interconnected pores and the disconnected pores present in the samples. Liquid gets into the interconnected pore and affects the density measurement. To remove this error three different weight measurements were taken, namely weight in air, weight of the sample dipped in liquid and weight of the sample in air after soaking in liquid for a long time. The liquid used is distilled water (ρ =1.0 gm/cc). The density of the sample was calculated using the following formula.

$$\text{Density of the composite} = W_{air} / (W_{soaked} - W_{liquid}) / \rho_{liquid} \ldots (1)$$

- Weight of the sample in air $W_1 = W_{air}$
- Weight of the sample in liquid $W_2 = W_{liquid}$
- Weight of the sample soaked in liquid for a long time $W_3 = W_{soaked}$

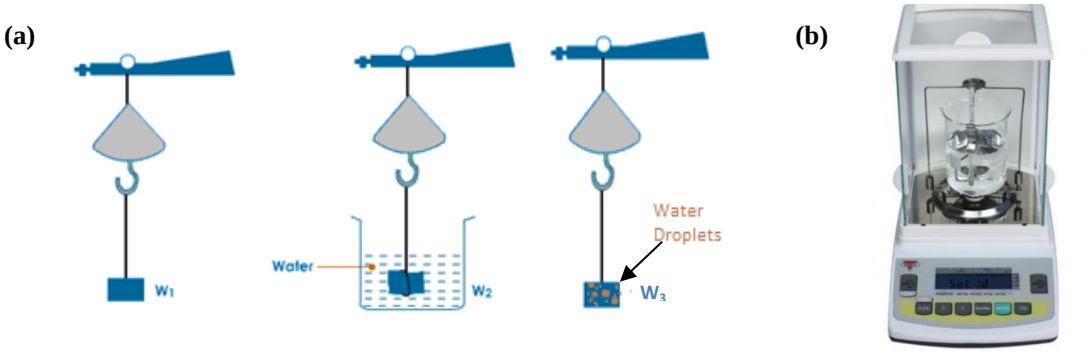

Fig.3.9 (a) Experimental setup for density measurement (b) Density measurement kit

9. Vickers Microhardness

A Vickers microhardness tester uses a diamond indenter in the form of right pyramid with a square base. The angle is supposed to be 136^o between the opposite faces. Generally the results are reported in kg/cm^2 which is proportional to the load divided by the square of the diagonal of the indentation calculated from the test. The load on the Vickers microhardness indenter can be taken usually from a few grams to kilograms. The resulting indentation is measured and converted to a hardness value using a mathematical formula. The test samples were polished before measuring the hardness.

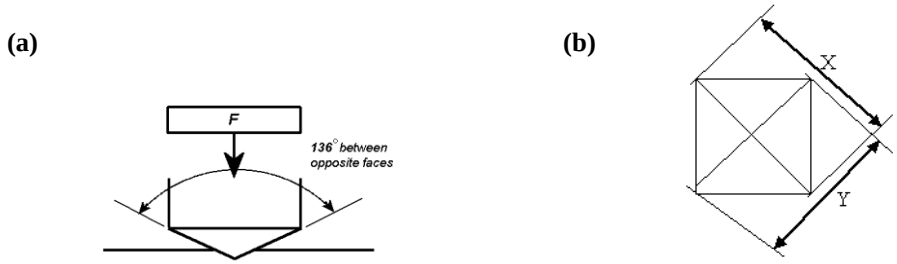

Fig. 3.10 (a, b) Schematic figure of the Vickers pyramid diamond indentation

The lengths of the two diagonals X and Y of the indentation left on the surface of the material after removal of the load are measured and their arithmetic mean L is calculated. In the present study, a load of 100 gf was considered (F = 0.98 N) and the Vickers hardness number is calculated using the following equations:

$$H_V = \frac{0.1889F}{L^2} \ldots (1)$$

$$L = \frac{X+Y}{2} \ldots . (2)$$

Where F is the applied load (N), L is the diagonal of square impression (mm), X is the horizontal length (mm) of the indentation and Y is the vertical length (mm) of the indentation.

(a) **(b)**

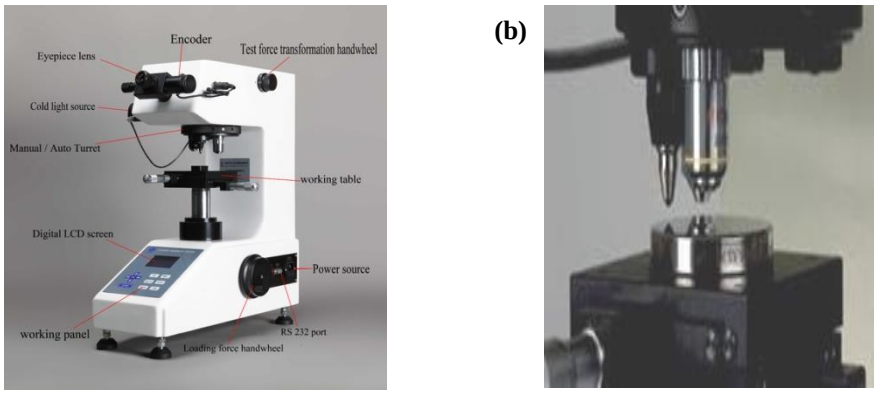

Fig. 3.11 (a, b) Vickers microhardness tester

The micro-hardness measurements were done using Lecco Vickers microhardness (LV 700) with a diamond indenter in the present investigation.

10. Wear Test

Wear is the progressive loss of materials from contacting surfaces which are relative in motion. It is basically the erosion of material from its base position on a solid surface. Wear is linked to the interactions between two surfaces. Specifically it is the removal and deformation of material on a surface due to the mechanical action of the opposite surfaces. The relative motion between the two surfaces and the initial mechanical contact between

asperities are one of the important factors in wear. Wear test is carried out to find the wear characteristic of the composites developed and to understand the wear mechanism.

Fig. 3.12 Ball-on-plate wear tester

A computerized ball on plate wear tester (TR-208-M1, DUCOM) equipped with a diamond indenter is used in the present investigation. The samples were polished with emery before doing the wear test. The load given was 20 N for a period of 10 minutes for all the wear tests conducted.

11. Fourier Transform Infrared Spectroscopy (FTIR)

The Fourier transform infrared spectroscopy (FTIR) is one of the most important infrared spectroscopy methods. In this process an infrared (IR) radiation is passed through a sample. Some of the radiations are absorbed by the sample and some of them are transmitted by it. The spectrum indicates the molecular absorption and transmission which is a distinctive molecular fingerprint of the sample. The infrared spectroscopy is useful for numerous types of analysis. Molecular spectroscopy involves the interaction of the electromagnetic radiation with the molecules in the material. Molecular spectroscopy involves the absorption of electromagnetic radiation by the material whose molecular structure we are attempting to determine. The absorption spectra of the atoms and molecules can be related to its physical properties such as electronic structure, atomic or molecular mass and molecular geometry. There are several factors like length and strength of the bonds, mass of atom which governs the frequency of these vibrations. Molecular vibrations are stimulated by bonds absorbing radiation of the same frequency as their natural vibrational frequency. Fourier transform

infrared spectroscopy (FTIR) is one of the most versatile, fast, inexpensive, and conclusive techniques for surface and bulk characterization.

Fig. 3.13 FTIR spectrophotometer

Here the spectra were collected in the 4000cm^{-1} to 400 cm^{-1} region with 8 cm^{-1} resolution, 60 scans and beam spot size of 10µm-100µm.The FTIR imaging was performed in AIM-800 Automatic Infrared Microscope (SHIMADZU).

3.2. Selection Synthesis and Characterization of Raw Materials

Cu powder, SiC particles, E-glass fiber and multiwalled carbon nanotubes (MWCNTs) were used as the raw materials to carry out the present investigation. Research grade Cu powder, SiC particulates and E-glass fiber were procured directly from the manufacturers. MWCNTs were synthesized by us using low pressure chemical vapour deposition (LPCVD) process. The raw materials procured and synthesized by us were analysed using various techniques. The detailed specification of the chemicals procured and the synthesis process used to develop them are given below.

i. Cu Powder

Copper (Cu) is a ductile metal having high thermal and electrical conductivity. Pure Cu is soft and malleable and its surface has a reddish-orange colour when exposed to atmosphere. Cu has a melting point of 1083.4°C and its density is 8.96 gm/cc. It is mainly used as a conductor of heat and electricity, building material, and a constituent of various metal alloys. Cu has high electrical conductivity (5.96×10^6 S/m) and also high thermal conductivity (401 W/m.K).The yield strength of Cu is117 MPa while its tensile strength is 210 MPa .The Young's modulus of Cu is 130 GPa. Cu is an integral part of several industries. It is the third

most extensively used metal in industries. It's resistance to corrosion; high thermal and electrical conductivity and malleability guarantee that it will continue to be used for a long time. Here for our experimental work Cu was procured from Loba Chemie India. The Cu powder had a purity of above 99% and an average particle size of 27.61 μm.

ii. Silicon Carbide (SiC) Particles

Silicon carbide is a compound of silicon and carbon having chemical formula SiC. SiCp is formed of tetrahedral structure of carbon and silicon atoms having strong bonds in the crystal lattice. This makes silicon carbide a very hard and strong material. SiC shows strong resistance to chemicals and corrosion up to 800^{o}C. In air, it forms a protective oxide layer composed of silicon oxide at 1200^{o}C and can it maintains it strength upto a temperature of 1600^{o}C with no loss in strength. Significantly grains of silicon carbide (SiC) can be bonded together at elevated temperatures to form a hard ceramic material that are efficiently used in several applications like car brakes, clutches, ceramic plates and bullet proof vests possessing high durability. SiC does not show melting at any known pressure. It is also highly chemically inert in nature. SiC also has a very low coefficient of thermal expansion (4.0×10^{-6}/K) and experiences no phase transitions which prevent discontinuities in thermal expansion. SiC has a melting point of 2730°C and its density is 3.20gm/cc. The elastic modulus of SiC is 450 GPa and it has a hardness of 20.5 GPa. SiC was procured from Search Chem for our experimental work. It had a purity of above 98% and its average particle size was 220 mesh.

iii. E-Glass Fiber

Glass fibers are among the best multipurpose industrial materials known today. They are easily produced from raw materials, which are available in almost unlimited supply. They have very useful bulk properties such as hardness, transparency, resistance to chemical attack, stability, and inertness, as well as desirable fiber properties such as strength,

flexibility, and stiffness. The major constituents of E-glass fiber are SiO_2 (52-56 wt. %), CaO (16-25 wt. %), Al_2O_3 (12-16 wt. %) and B_2O_3 (5-10 wt. %). Apart from this it also contains oxides of Na and K (0-2 wt. %), MgO (0-5 wt. %), oxides of Fe and Ti and fluorides. E-glass (electrical) fibers have lower alkali content and are stronger than A-glass (alkali) fibers. E-glass fibers were initially used for electrical applications which why they were called E-glass fibers. E-glass fiber is alkali free and was the first glass formulation that was used for continuous filament formation. It is the largest type of glass fiber produced in the world. It high stiffness and possesses good tensile and compressive strength. It also has good electrical properties and has a relatively low cost [25].

Table 3.1 Properties of E-glass fiber

Property	Minimum Value	Maximum Value
Bulk Modulus	43 GPa	50GPa
Compressive Strength	4000 MPa	5000MPa
Hardness	3000 MPa	6000MPa
Tensile Strength	1950 MPa	3500MPa
Young's Modulus	72 GPa	85GPa

The fiber used in the present investigation has been manufactured by Saint Gobain.

iv. Synthesis of Multiwalled Carbon Nanotubes (MWCNTs)

The Chemical Vapour Deposition (CVD) method is one of the preferred and suitable methods to synthesize carbon nanotubes (CNT). The synthesized carbon nanotubes from CVD method possess high purity and can be used for large scale production. The CVD method involves the catalytic decomposition of the hydrocarbon with the aid of supported transition metal catalysts (Fe, Co, Ni, etc.). It is a versatile process in which the gas phases are decomposed to form reactive species. These species leads to particle or film growth. The CVD process can be used to deposit a wide range of conducting, semiconducting and insulating materials [51].

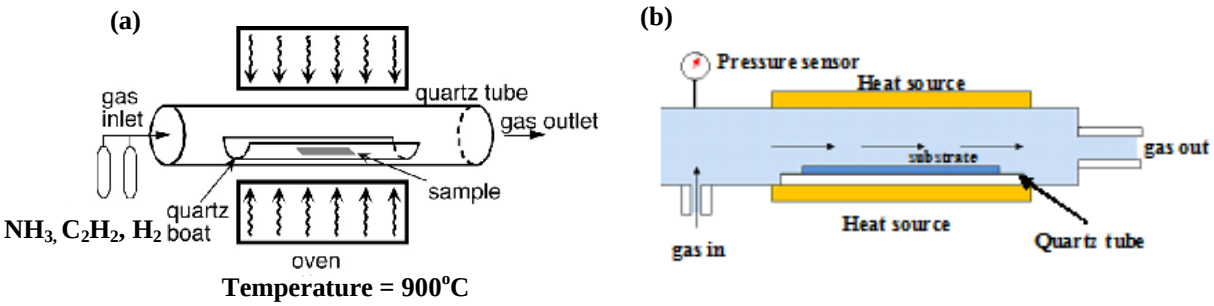

Fig.3.14 (a, b) Schematic of a typical CVD furnace setup used for the synthesis of MWCNTs

A conventional horizontal quartz tube with dimensions approximately 1 m long and 50 mm in diameter was used. The temperature was maintained at 900°C with holding time of 40 mins. Subsequently, the synthesis was initiated by introducing a flow of 20 sccm acetylene (C_2H_2), 50 sccm ammonia (NH_3) and 40 sccm hydrogen (H_2) for 40 mins. Acetylene (C_2H_2) was used as the carbon source and was fed into the tube furnace at a controlled rate. To prevent oxidation and removal of gaseous by products argon (Ar) gas was fed at a controlled rate of 600 sccm during the whole heating-up, growth and cooling down periods. Fig. 3.14 (a, b)shows the schematic of a typical CVD furnace setup used for the synthesis of MWCNTs. Carbon nanotubes are the strongest and stiffest materials discovered in terms of tensile strength and elastic modulus respectively. Single walled carbon nanotubes (SWCNTs) are known to have a Young's modulus value of ~1 TPa and a tensile strength of 13-53GPa.Multiwalled carbon nanotubes (MWCNTs) was tested to have a tensile strength of 63 GPa. Standard single-walled carbon nanotubes can withstand a pressure up to 25 GPa without deformation [52-55].

Table 3.2 Properties of MWCNTs

Properties	**Values**
Specific Gravity	1.8 g/cm^3
Elastic Modulus	0.3-1TPa
Strength	10-60GPa
Thermal Conductivity	3000 W m^{-1}K^{-1}
Thermal Stability	2800°C
Specific Surface Area	200-400 m^2/g

The current uses and applications of carbon nanotubes have been limited to be used as bulk nanotubes. These bulk nanotubes are referred as the mass of unorganized carbon fragments. Bulk nanotube materials may never achieve a tensile strength similar to that of individual tubes, but such composites may, nevertheless, yield strengths sufficient for many applications. The superior mechanical properties of CNTs are applicable for the development of many products ranging from daily use items like sports gear to combat jackets and space elevators. We have used the acid functionalization route for dispersion of MWCNTs. Multiwalled carbon nanotubes were stirred using magnetic stirrer for 8 h in an acidic solution containing H_2SO_4 and HNO_3 in 3:1 ratio having 50 % acid concentration. CNTs were then filtered and washed repeatedly with distilled water till the pH value of 7 is reached. Drying of CNTs was carried out in a vacuum oven at 80^{o}C for 5 h. The Van der Waal's forces between the CNTs are overcome by the presence of carboxyl and hydroxyl groups which were introduced during functionalization of the carbon nanotubes preventing agglomeration of the CNTs [56,57].

3.3. Synthesis and Characterization of Cu-Based Metal Matrix Composites

It is known that matrix strengthening can be done by incorporation of reinforcements like continuous or discontinuous fibers, whiskers, wires and particulates. Here in our work three different types of reinforcements, SiCp, E-glass fibers and MWCNTs have been used to develop Cu-based MMCs. Cu-10, 20, 30 and 40 vol. % SiCp, Cu-10, 20, 30 and 40 vol. % E-glass fiber and Cu-1, 2 and 5 vol. % MWCNTs composites were developed by powder metallurgy route. Green compacts of the composites were developed by blending the constituents followed by uniaxial cold compaction under a load of 665 MPa. The green compacts were then sintered at 900^{o}C for a period of 1 h in Ar atmosphere. The microstructure, composition, fractography and mechanical properties like hardness and wear

resistance of the various Cu-based MMCs were then determined. X-ray diffraction of the various composites was done in order to determine the different phases in the sintered composites. The microstructure of the composites was analyzed using an optical microscope, scanning electron microscope (SEM) and field emission scanning electron microscope (FESEM). Hardness of the composites was determined using a Vickers microhardness tester. Wear properties of the various composites was analysed using a ball-on-plate tribometer. The density of all the composites was determined using the Archimedes' principle.

…….

Chapter 4
Results and Discussion

Results and Discussion

Introduction

Cu powder has been used in numerous industrial applications since many years. The most popular application known till date is the development of self-lubricating bearings which was the first major application and still accounts for about 70 % of the granular copper powder used. The above application of Cu shows the ability to produce a component with controlled surface-connected porosity. Pure Cu is generally used in electronics and electrical industries because of their outstanding electrical conductivity (5.96×10^7 S/m) and thermal conductivity (401 W/m K).The melting point of Cu is 1083.4°C and its density is 8.96 gm/cc. Cu is widely used as an alloying element in several components to improve its mechanical properties and control its dimensional changes during sintering. In order to increase high temperature properties of Cu different reinforcements are being used. The mechanical properties of pure Cu can only be improved by two processes either age hardening or particle dispersion strengthening. Cu matrix can be strengthened by the incorporation of several reinforcements like particulates, fibers, whiskers and wires. Cu matrix composites are used for manufacturing hybrid modules, electronic relays, electrically conducting springs and other electrical and electronic components.

4.1 Mechanical Milling of Cu

Elemental Cu powder was milled in a high-energy planetary ball mill in order to synthesize nanocrystalline Cu. Mechanical milling is a convenient and promising process to produce nanostructured powders. It is a very effective processing technique for the preparation of nanocrystalline metallic and ceramic powders.

It is a solid-state powder processing technique which involves repeated welding, fracturing, and rewelding of powder particles in a high-energy ball mill. Heavy deformation of particles takes place during milling and increase in lattice strain can be depicted by the presence of peak broadening.

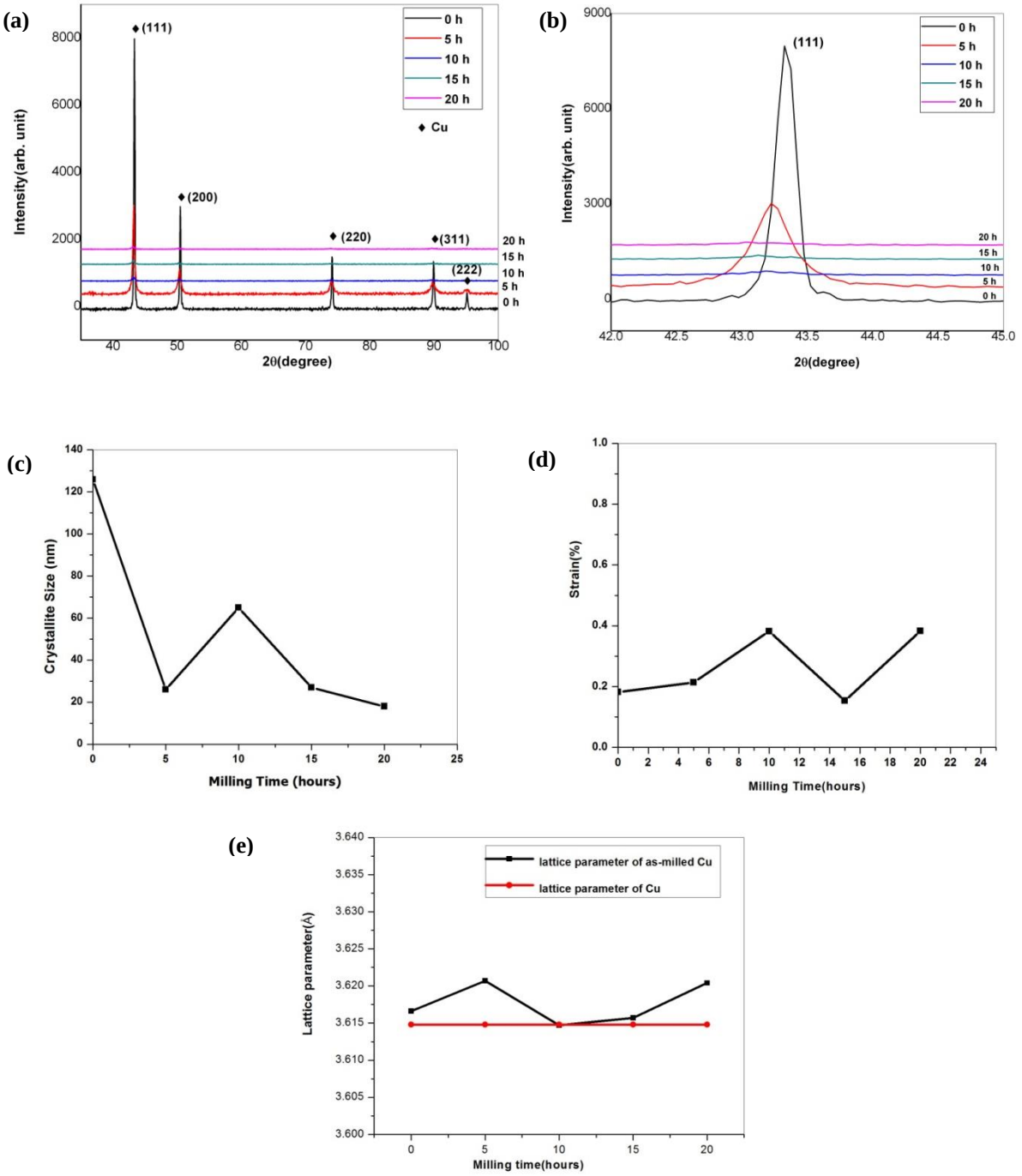

Fig.4.1 (a, b) X -ray diffraction plots of Cu milled for various periods of time and variation of (c) crystallite size (d) r.m.s. strain and (e) lattice parameter of Cu with milling time

The x-ray diffraction of Cu powder milled for various durations of time are shown in Fig.4.1 (a). The various peaks in the x-ray diffraction pattern could be indexed to the different crystallographic planes of Cu. Fig. 4.1(b) shows the (111) peak of the as-milled and unmilled Cu samples. This plot shows shift of the (111) peak with milling time. The (111) peak of Cu at 5 h of milling shows shift towards the lower 2θ angle. The shift of the peak towards the lower 2θ angle is possibly due to the increase in lattice parameter of Cu upto 5 h of milling. Beyond 5 h of milling the (111) peak of Cu shows significant broadening. No other peaks could be detected in the x-ray pattern suggesting that there is no contamination from the milling media. Voigt's method was used for calculating the crystallite size of the milled Cu powder.

In the Voigt'sapproach the crystallite size and lattice strain comprises both the Lorentzian and Gaussian component convolutions varying in 2θ as a function of 1/cosθ and tanθ respectively. It is expected that both the crystallite size and strain effects are considered by the Voigt's function. According to Balzar [58], integral breadths of the size and strain components of Cauchy and Gaussian parts can be expressed as,

$$\beta_C = \beta_{SC} + \beta_{DC} \ldots (1)$$

$$\beta_G^2 = \beta_{SG}^2 + \beta_{DG}^2 \ldots (2)$$

where β_C and β_G are the Cauchy and Gaussian components of the total integral breadths β respectively. The term β_{SC} and β_{DC} represents the Cauchy components of size and strain integral breadth, respectively and β_{SG} and β_{DG} are the corresponding Gaussian components. After the components are calculated by the above equations, the maximum lattice strain (e) and volume weighted crystallite size (D_V) , can also be determined using equations (3) and (4) [59].

$$e = \beta_D / 4\tan(\theta) \ldots (3)$$

$$D_V = \lambda / \beta_S \cos(\theta) \ldots (4)$$

Here, β_D and β_S are the integral breadths of a Voigt's function comprising the Gaussian and the Lorentzian components respectively. λ is the wavelength and θ is the diffraction angle.

After 20 h of milling the crystallite size of Cu was found to be 18 nm (Fig. 4.1(c)). There is a gradual drop in the crystallite size with milling time. From Fig. 4.1(c) it is evident that Cu could be reduced to nanometric dimension within 5 h of milling. Cold welding was also evident between 5 to 10 h of milling which led to the increase in crystallite size. There is a gradual increase in the lattice strain due to severe deformation of the milled powder and strain reaches a maximum value after 20 h of milling when the crystallite size is smallest (Fig.4.1 (d)). Precise lattice parameter of milled Cu was also determined using the Nelson-Riley function. Fig. 4.1(e) shows the variation of lattice parameter of Cu with milling time. The lattice parameter of Cu shows a slight increase with milling time [60-64].

The lattice strain measured from the x-ray diffraction line broadening increased continuously upto 10 h of milling due to the increase in dislocation density in the grains. The dislocation density is very high within the heavily strained regions. With further milling upto 15 h, the lattice strain decreases as the crystal disintegrates into subgrains that are separated by low-angle grain boundaries. The dislocations annihilate and recombine to form small angle grain boundaries separating the individual grains. This results in a decrease of the lattice strain. During further processing, deformation occurs in shear bands located in previously unstrained parts of the material. The grain size decreases steadily and the shear bands coalesce. The small angle boundaries are replaced by higher angle grain boundaries, implying grain rotation and random orientation of the grains. As a result dislocation-free nanocrystalline grains are formed. The minimum grain size obtainable by milling has been attributed to a balance between the defect and dislocation structure introduced by the plastic deformation of milling and its recovery by thermal processes.The variation of lattice strain is also reflected in the lattice parameter of Cu calculated from the x-ray diffraction plots using Nelson-Riley

function in Fig. 4.1(e). The lattice parameter shows an initial increase upto 5 h of milling. This increase of lattice parameter is probably caused by the grain expansion due to the increase in the density of dislocations. As a result of the increase in the dislocation density the dislocations are closer to each other resulting in repulsion between them as the potential energy increases when the dislocations are closer. Between 5 to 10 h of milling the lattice parameter of Cu was found to decrease which is possibly because of the grain compression due to the presence of compressive stress fields within the nonequilibrium grain boundaries in the nanocrystallites. This results in the shrinkage of the lattice parameter. In addition the decrease in the lattice parameter could also be due to the oxidation of the nanocrystalline Cu. Oxidation of the nanocrystalline Cu accelerates their fracture. Beyond 15 h of milling both the strain and the lattice parameter of Cu shows an increase. This is possibly due to the strain hardening of the Cu powder that takes place when milling is done for a longer period of time. [65-74].

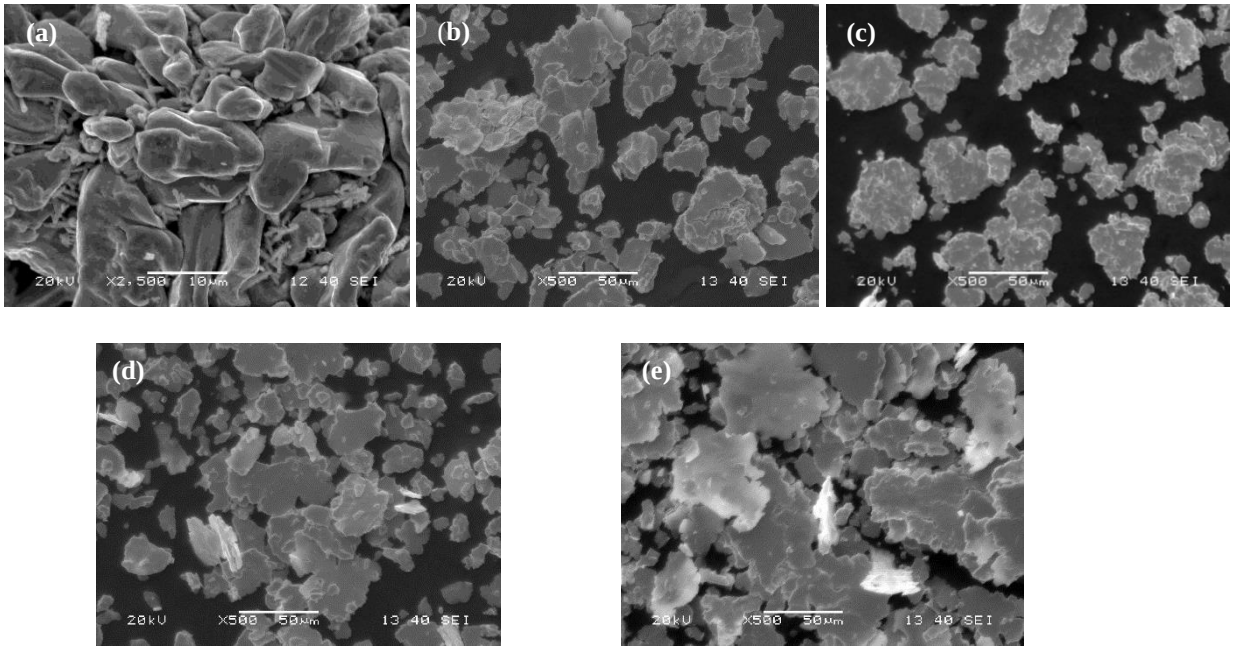

Fig. 4.2 SEM images of (a) unmilled Cu and Cu milled for (b) 5h (c) 10 h (d) 15h (e) 20 h

Figs. 4.2 (a-e) show the SEM images of milled Cu powder at different intervals. Due to the ductile nature of Cu it was possible to flatten Cu particles to flat flakes within 5 h of milling. 20 h of milling leads to thickening of the plates due to cold welding.

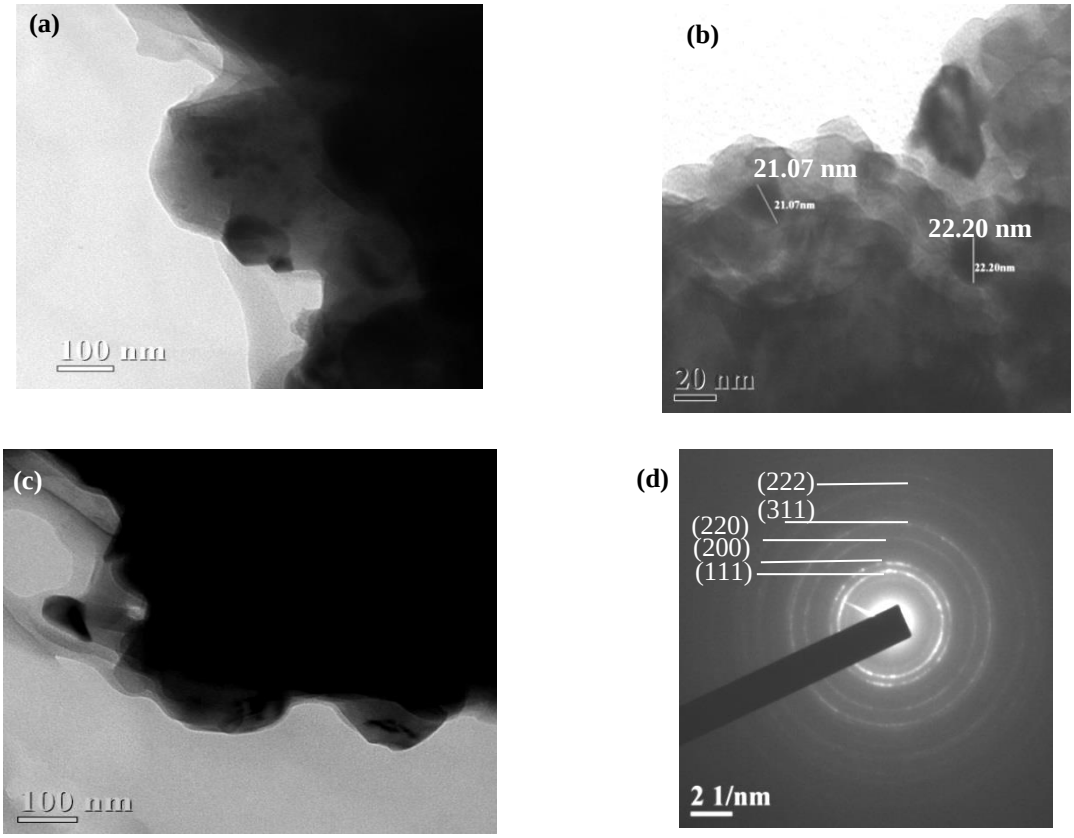

Fig. 4.3(a-c) HRTEM images and (d) SAD pattern of 20 h milled Cu

The results for HRTEM analysis of 20 h milled powder is shown in Figs. 4.3(a-c), which indicates that the powder has been reduced to nanometric dimension after high-energy milling for 20 h. The SAD pattern in Fig. 4.3 (d) shows complete ring patterns which suggest that the 20 h milled Cu powder has nanometric dimension. The ring patterns could be indexed to the various crystallographic planes of Cu. The most important physical property of particulate samples is its particle size. Particle size measurement is routinely carried out across a wide range of industries and is often a critical parameter in the manufacture of many products. The particle size analysis was done using a particle size analyser [75].

(a)

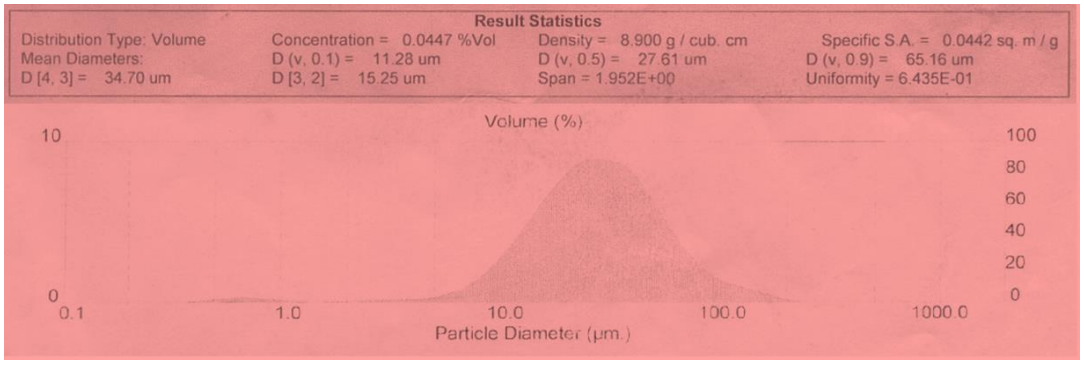

(b)

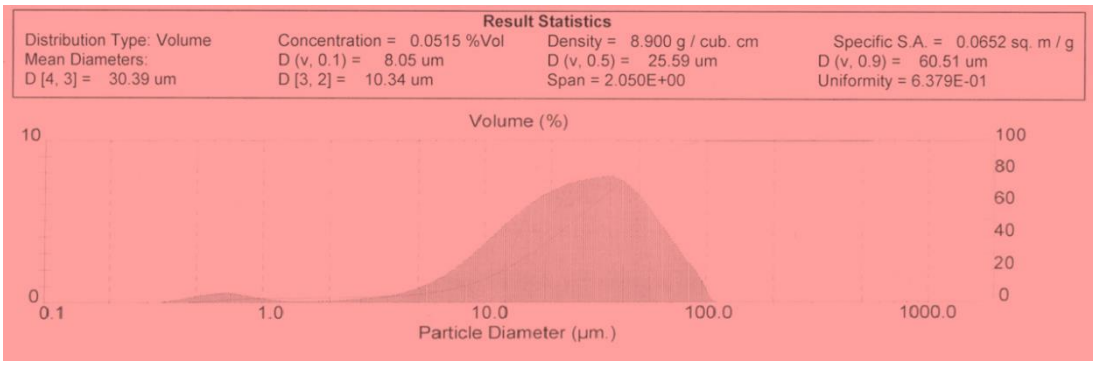

Fig.4.4 Particle size analysis for (a) unmilled Cu and (b) 20 h milled Cu powder

Figs.4.4 (a, b) show the particle size analysis for unmilled Cu and 20 h milled Cu powder. The average size of the particles was found to be 25.59 µm after 20 h of milling. Table 4.1 shows the particle size analysis of pure elemental Cu at different milling time. The results show that there is a sudden increase in particle size at the initial stage of milling. This is due to the cold welding effect in Cu as Cu is soft and ductile. At later stage the size of the particles get reduced due to the fracture of the particles. The lowest particle size of 25.59 µm is attained after 20 h of milling [76].

Table 4.1 Particle size analysis of pure Cu at different milling time

Milling Time (hours)	Average Particle Size, D(v,0.5) (µm)
0	**27.61**
5	**57.36**
10	**35.72**
15	**25.91**
20	**25.59**

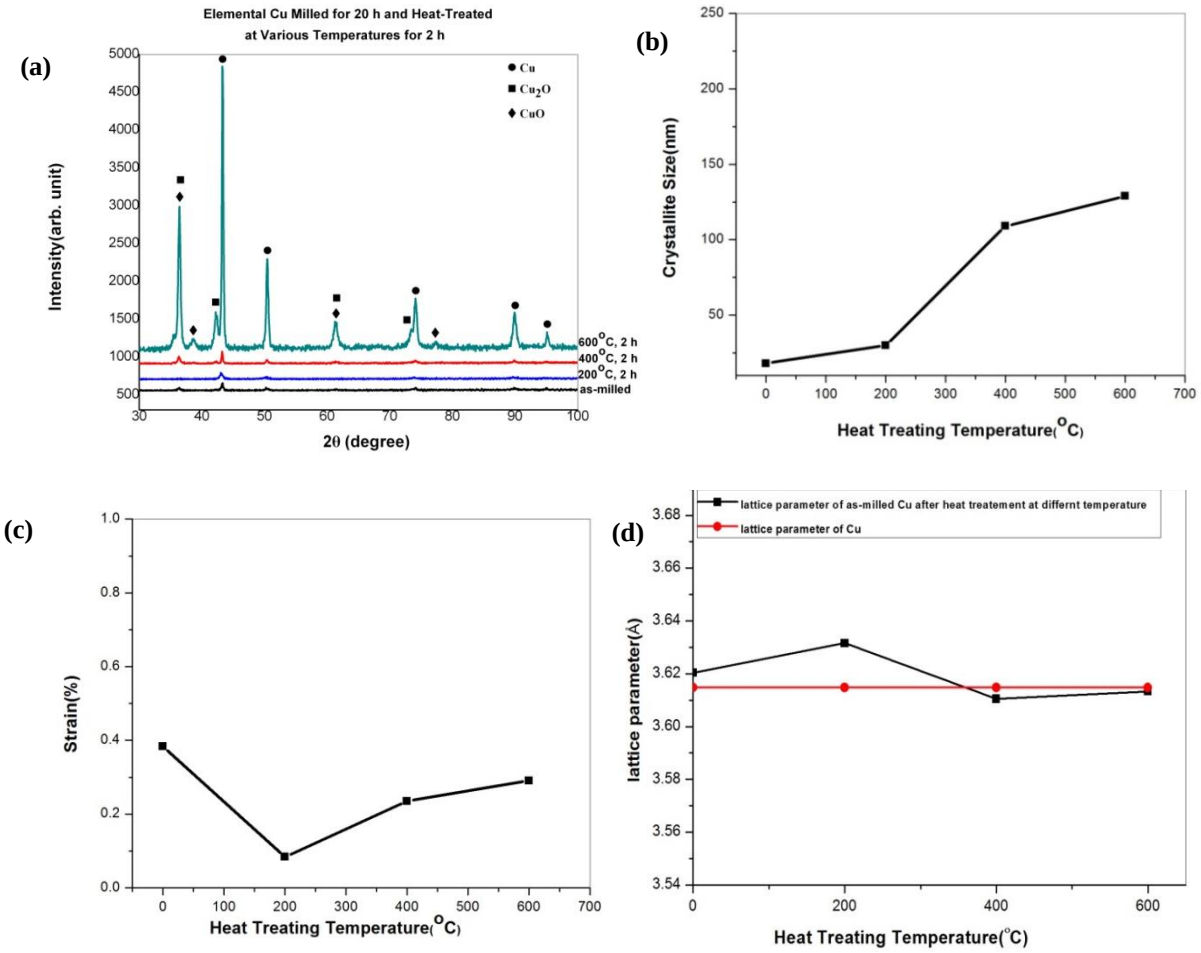

Fig. 4.5 (a) X-ray analysis of 20 h milled Cu at different heat treating temperatures(b) Variation of crystallite size with variation in heat treating temperature (c) Variation of strain with variation in heat treating temperature (d) Lattice parameter at different heat treating temperatures.

Fig.4.5 (a) shows the x-ray diffraction plots of 20 h milled Cu heat treated at 200, 400, 600^{o}C for 2 h in Ar atmosphere. Apart from the peaks of Cu few peaks of CuO and Cu_2O are also visible in the x-ray diffraction patterns of the 20 h milled samples heat treated at 200, 400, 600^{o}C. This is possibly due to the oxidation of Cu during heat treatment. There is an increase in crystallite size with the increase in heat treating temperature due to the grain growth of Cu during heat treatment as can be seen in Fig (4.5(b)). The lattice strain in Cu decreases after heat treatment as can be seen in Fig.4.5(c). There is a contraction in lattice parameter with the increase in the heat treatment temperature as shown in Fig.4.5 (d). This is possibly due to the

presence of a high concentration of oxygen in the Cu powder as the presence of oxygen leads to the contraction of the lattice.

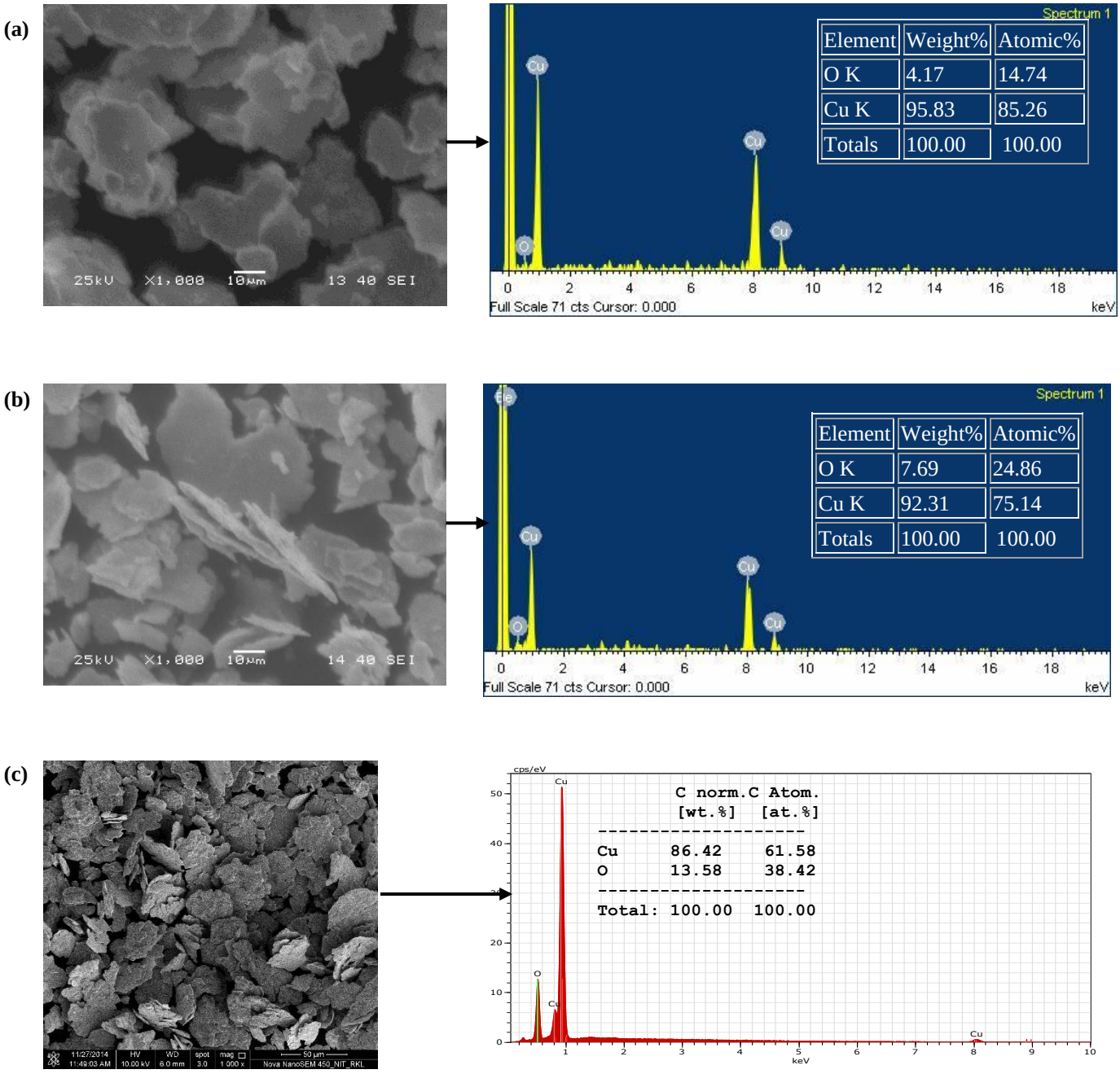

Fig. 4.6 SEM and EDX analysis of 20h Cu (a) heat treated at 200^{o}C for 2 h (b) heat treated at 400^{o}C for 2 h (c) heat treated at 600^{o}C for 2 h

Figs. 4.6 (a-c) show the SEM image and EDX analysis after heat treatment of the 20 h milled Cu powder at 200^{o}C, 400^{o}C and 600^{o}C respectively. EDX analysis confirms the presence of

oxygen in the heat treated samples. This was also seen in the x-ray diffraction plots of the heat treated samples in Fig.4.5 (a).

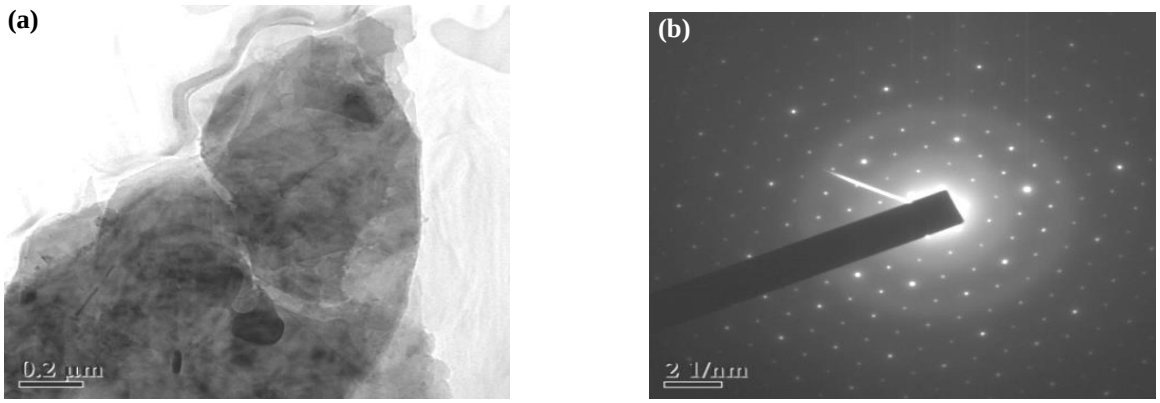

Fig. 4.7(a) HRTEM image (b) SAD pattern of 20 h milled Cu powder heat treated at 200^{o}C

The HRTEM image in Fig.4.7 (a) suggest that the 20 h milled Cu powder still has nanomteric dimension even after heat treatment for 2 h at 200^{o}C. The SAD pattern inFig.4.7 (b) also indicates the nanometric nature of 20 h milled Cu powder heat treated at 200^{o}C for 2 h.

4.2 Cu-SiCp Composites

Cu is commonly used in electronics and thermal applications dueto its high electrical (5.96×10^{7} S/m) and thermal (401 W/m K) conductivity. It also shows good corrosion resistance and high melting point (1083.4^{o}C). However, the low mechanical strength of Cu limits its application in several fields. Metal matrix composites reinforced with discontinuous particles exhibits enhanced properties.Particle reinforced metal matrix composites have significant improved properties due to the high strength and modulus of the reinforcement particles like TiC, Al_2O_3, SiC, TiB_2 etc. In the present study, the focus was towards the development of Cu-based metal matrix composites using SiCp as reinforcement by powder metallurgy route. Silicon carbide (SiC) is widely used as reinforcement because of its very high thermal stability. Its coefficient of thermal expansion is 4.0×10^{-6}/K. SiC also has high thermal conductivity (16.7 W/m.K) and high hardness (20.5 GPa). Its melting point is above

2600°C and it is also highly chemically inert in nature. The above properties mentioned makes SiC particles a potential additive to Cu-based metal matrix composites. The Cu-SiCp composites were prepared by powder metallurgy route. Cu containing different volume fractions of SiC particles (10, 20, 30 and 40 vol. %) were developed by blending the constituents followed by cold compaction of the samples in a uniaxial compaction machine under a load of 665 MPa. Sintering of the samples was done at 900^{o}C for 1 h in Ar atmosphere. The optical micrographs of the various Cu-SiCp composites in Figs.4.8 (a-d) show that the SiCp are homogeneously dispersed in the Cu matrix. The SiCp are found to be less than 100 µm in size. Figs. 4.9 (a-d) are the SEM images of the various Cu-SiCp composites developed using different vol. % of SiCp reinforcement in the Cu matrix. From the microstructure it is clear that the SiC particulates are irregularly shaped and are homogenously distributed in the Cu matrix [77-79].

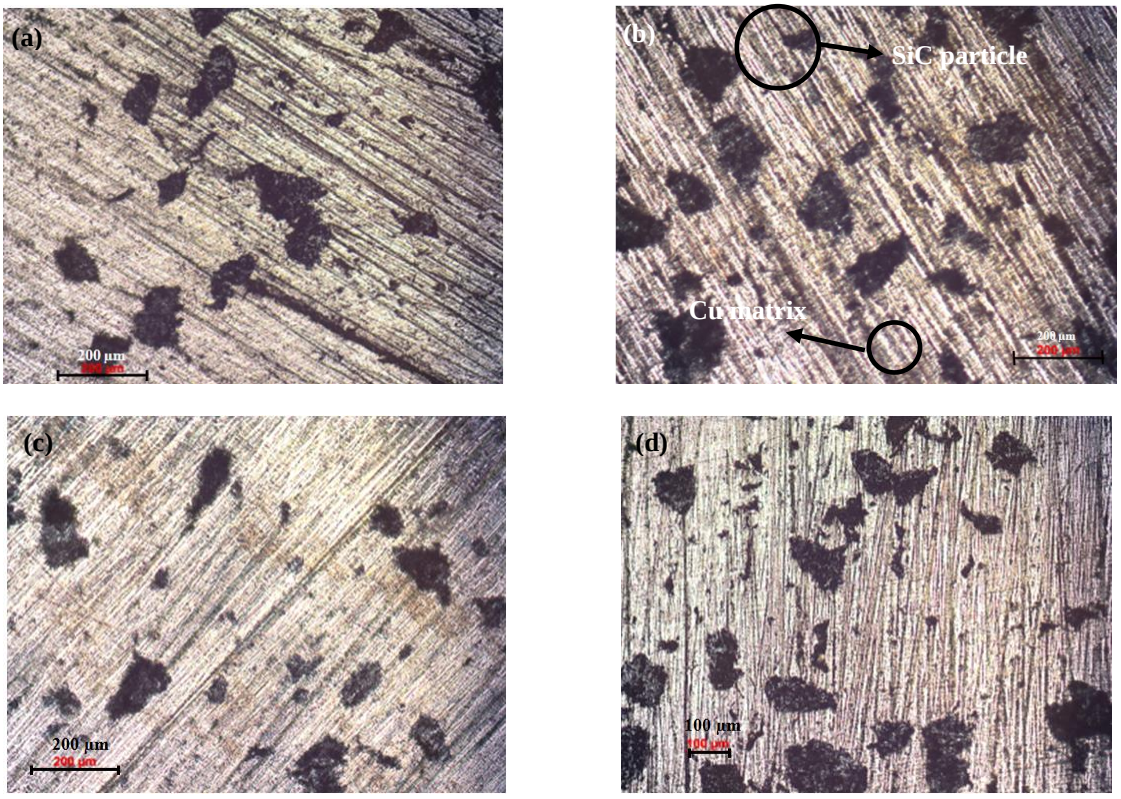

Fig.4.8 Optical micrographs of (a) unmilled Cu- 10 vol. % SiCp composite (b) unmilled Cu- 20 vol.% SiCp composite (c) unmilled Cu- 30 vol. % SiCp composite (d) unmilled Cu-40 vol. % SiCp composite

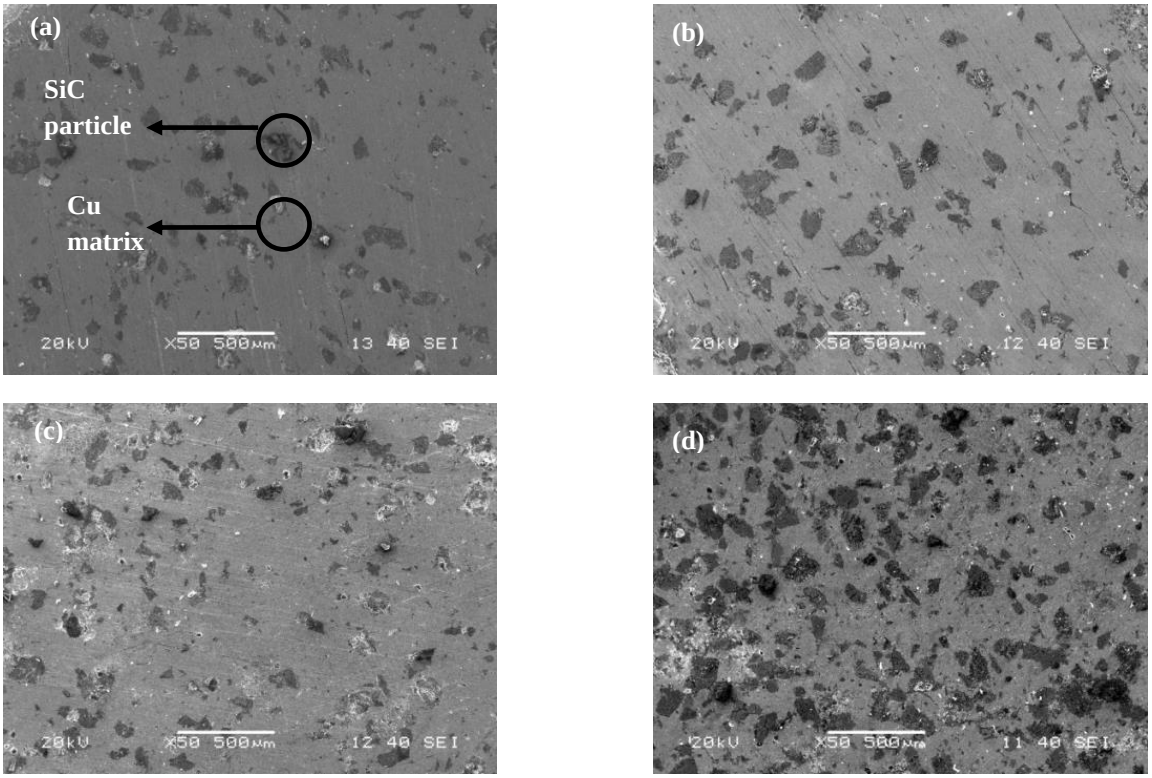

Fig. 4.9 SEM imagesof (a) unmilled Cu- 10 vol. % SiCp composite (b) unmilled Cu- 20 vol. % SiCp composite (c) unmilled Cu- 30 vol. % SiCp composite (d) unmilled Cu- 40 vol. % SiCp composite

(a)

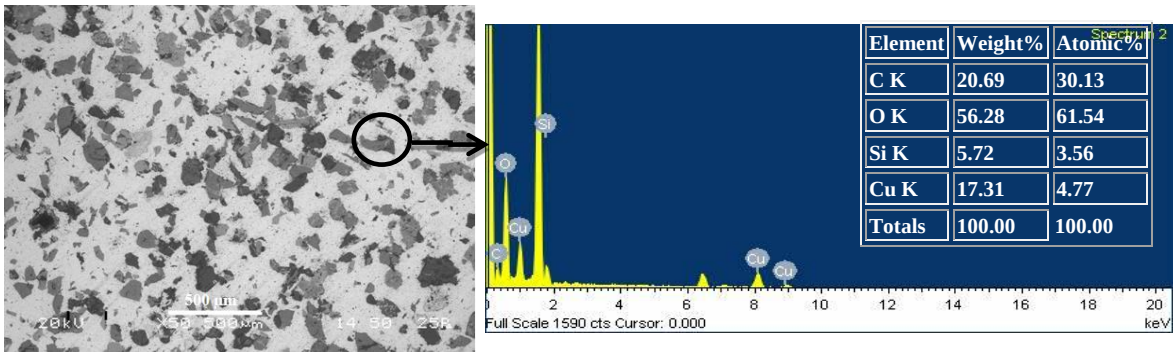

(b)

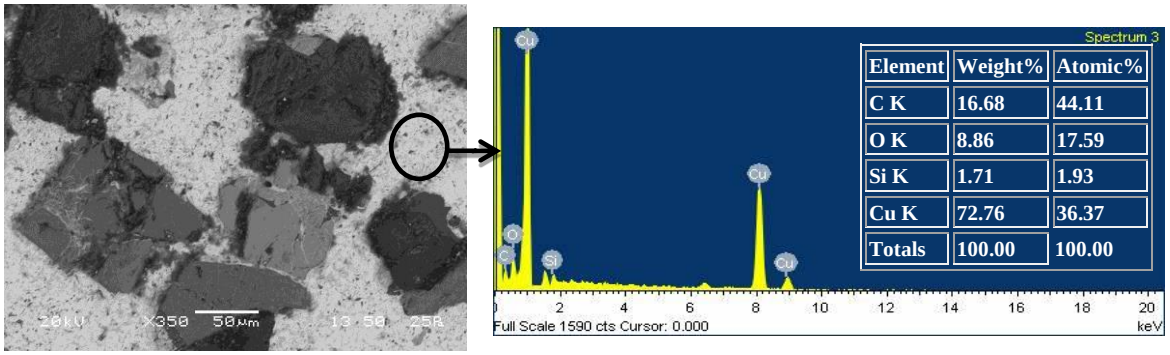

Fig. 4.10 EDX analysis of (a) unmilled Cu-40 vol. % SiCp composite at SiCp rich region (b) unmilled Cu-40 vol. % SiCp composite at Cu rich region

The EDX analysis in Fig. 4.10 suggests that the dark region in the SEM image corresponds to the SiC particles and the light coloured region corresponds to the Cu matrix. The dark coloured SiC particles are surrounded by the light coloured Cu rich regions. EDX analysis shows the presence of oxygen in the sintered sample. This is due to the undesirable oxygen present during sintering in the Ar atmosphere. The x-ray diffraction analysis of the various unmilled Cu-SiCp composites in Fig.4.11 also show peaks corresponding to Cu_2Owhich confirms the oxidation of Cu by unavoidable oxygen present during sintering. Fig.4.11 shows the x-ray diffraction plots of various unmilled Cu-SiCp composites having different vol. % of SiCp. The x-ray diffraction plots show peaks corresponding to Cu and SiC. The higher content of SiCp in the composites leads to more intense peaks corresponding to SiC. Peaks corresponding to copper oxide (Cu_2O) were also found in the composites.

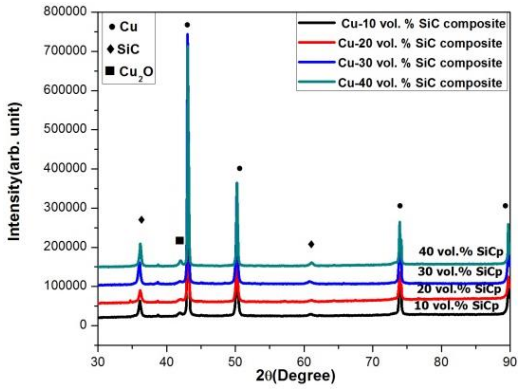

Fig. 4.11 XRD plots of various unmilled Cu-SiCp composites

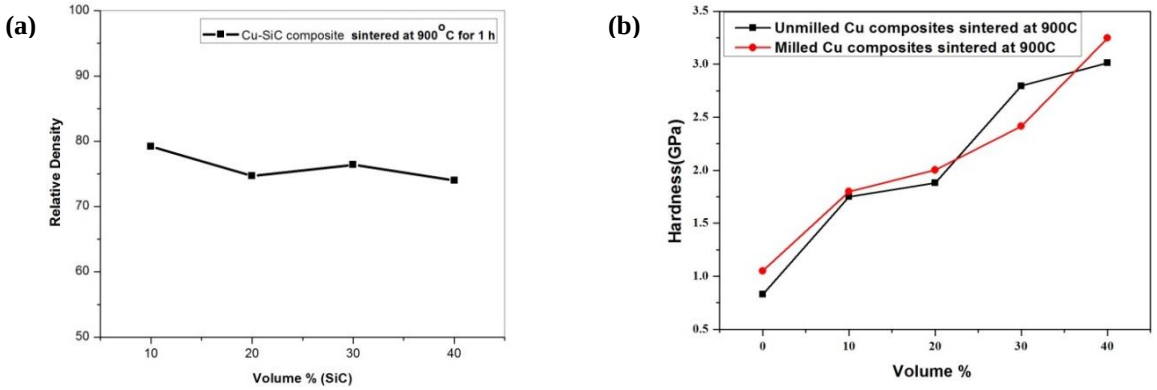

Fig. 4.12 (a) Variation of relative density of various unmilled Cu-SiCp composites
(b) Variation of microhardness of various as-milled and unmilled Cu-SiCp composites

Fig. 4.12(a) shows the variation of relative density of the various unmilled Cu-SiCp composites. There is a gradual decrease in the relative density with the increase in vol. % of SiCp reinforcement in the Cu matrix. This is possibly due to the increase in the content of brittle SiC particles in the soft Cu matrix. The variation of hardness in as-milled Cu-SiCp composites and unmilled Cu-SiCp composites in Fig. 4.12(b) shows that the hardness of both the unmilled Cu-SiCp composites and the as-milled Cu-SiCp composites increases with the increase in the vol. % of SiCp reinforcement. However it can be seen from the Fig.4.12 (b) that the as-milled Cu-SiCp composites show better hardness than the unmilled Cu-SiCp composites. Milled Cu due to its smaller particle size leads to better sinterability and densification resulting in higher hardness of the composites.

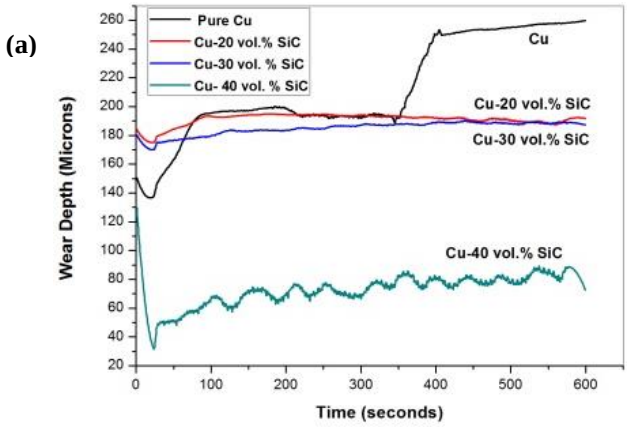

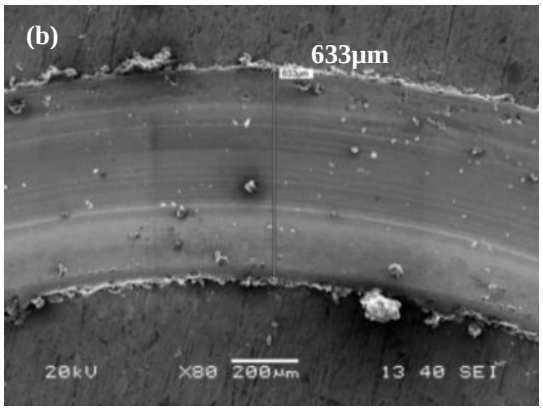

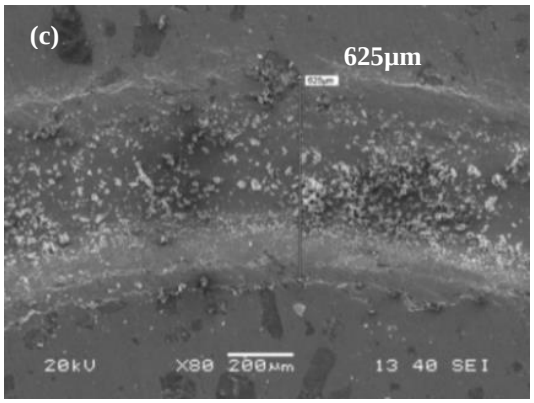

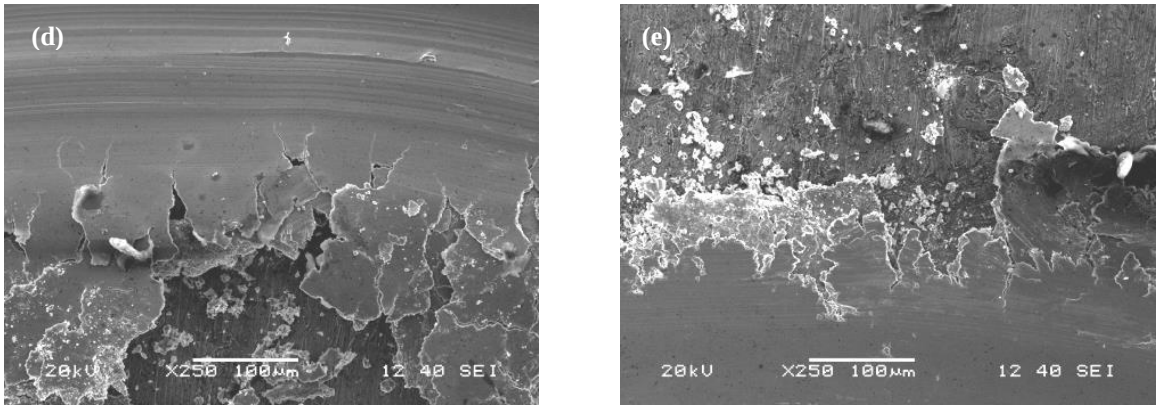

Fig.4.13 **(**a) Wear Characteristic of unmilled Cu- SiC composites. SEM images of the wear track of (b) unmilled Cu (c) unmilled Cu-40 vol. % SiCp composite. (d-e) High magnification SEM images of the wear track of unmilled Cu-40 vol. % SiCp composite

Fig. 4.13 (a) shows the wear characteristics of the various unmilled Cu-SiCp composites. The plot shows that the wear resistance of the Cu-SiCp composites are higher than that of the native Cu. It can be observed that with the increase in vol. % of SiCp in the Cu matrix the wear resistance of the composite increases significantly. Cu-40 vol. %SiCp shows the least wear depth (Fig. 4.13(a)).Fig. 4.13(b) and Fig. 4.13 (c) shows the SEM images of the wear track of unmilled Cu and unmilled Cu-40 vol. % SiCp composite respectively. Fig. 4.13 (d, e) are the high magnification SEM images of the wear track of unmilled Cu-40 vol. % SiCp composite. It was found that the hardness of Cu-SiCp composites increases with the addition of SiCp due to the presence of the harder ceramic particles of SiC. The hard SiC particles support the stresses between the contact surfaces preventing the large plastic deformations and abrasions. This reduces the amount of worn material. The Cu-SiCp composites containing the hard SiC particles show better wear resistance due to the formation of a tribolayer at the interface. During wear rapid removal and regeneration of the tribolayer at the interface takes place. The interface temperature also increases during the wear test and this causes oxidation of the sample. The increase of interface temperature during the wear test significantly enhances the loss of mass by oxidation, matrix softening, cracking and delamination wear. In the initial stages of wear, fine particles are generated from the two surfaces in contact by the micro-cutting and rubbing effects. Sharp SiC particle edges

protrude out of the Cu-SiCp composite surface. The wear particles entrapped by the contacting surfaces undergo a mechanical mixing process, which is very similar to the mechanical alloying (MA) process. During milling some original particles fracture further and expose atomically clean surfaces that come in contact with each other. With further mixing, cold welding and particle fracturing takes place which leads to a steady state particle size distribution in the mixture. Few fine particles are dislodged from the interface whereas some agglomerate and pile up. Due to the pressing and flattening effect of the normal load and frictional forces a compact mechanically mixed layer on the stationary and relatively soft composite surface is formed. This layer acts as a protective layer for the composite. It should be noted that due to the fine size of the debris particles and high temperature at the contact the metal components like Cu can be oxidized very rapidly. The drastic reduction in wear rate may be attributed to the enhancement in hardness of the composite reinforced by SiC particles and greater reduction of direct load contact between the Cu-SiCp composite surface and ball due to load bearing component action of the hard SiC particles. Fig. 4.13 (b,c) shows the SEM images of wear track of unmilled Cu and unmilled Cu-40 vol. % SiCp composite respectively. From the images it is evident that Cu-40 vol. % SiCp composites show less width of wear track as compared to pure Cu [80-85].

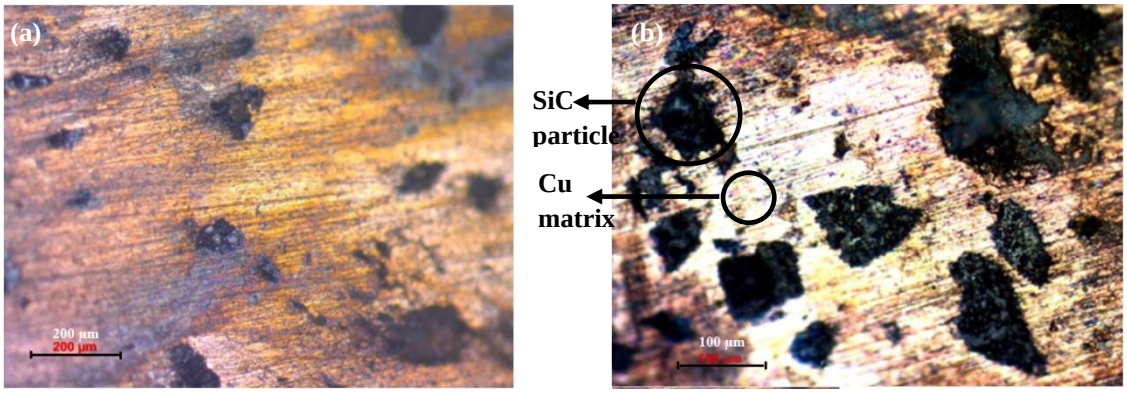

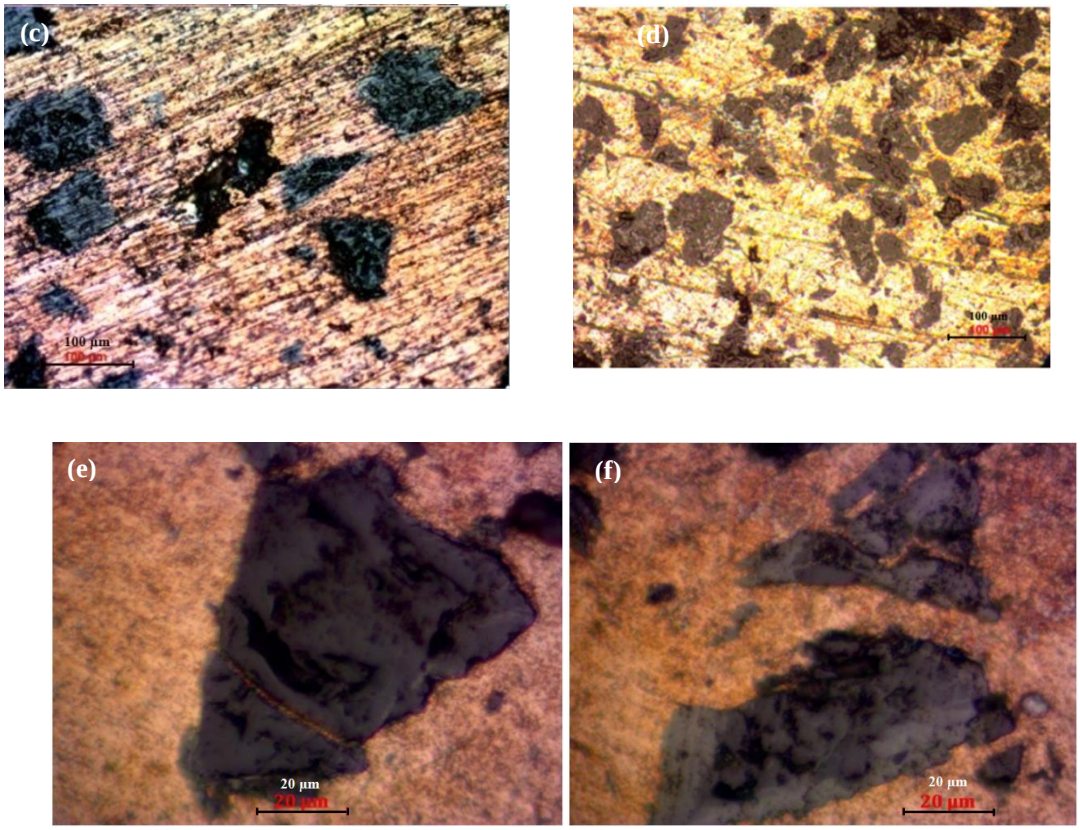

Fig.4.14 (a-d) Optical micrographs of as- milled Cu-SiCp composites (10,20, 30 and 40 vol% of SiCp) (e, f) High magnification optical micrographs of as-milled Cu-40 vol. % SiCp composite

Fig.4.14 shows optical micrographs of as-milled Cu-SiCp composites for different vol. % of SiCp. From the micrographs it is evident that SiC particles are homogenously distributed all over the Cu matrix. The high magnification optical micrographs of as-milled Cu-40 vol. % SiCp composites in Fig. 4.14 (e, f) show the interface between the SiC particle and the Cu matrix. Good interfacial bonding can be observed between Cu and SiCp.

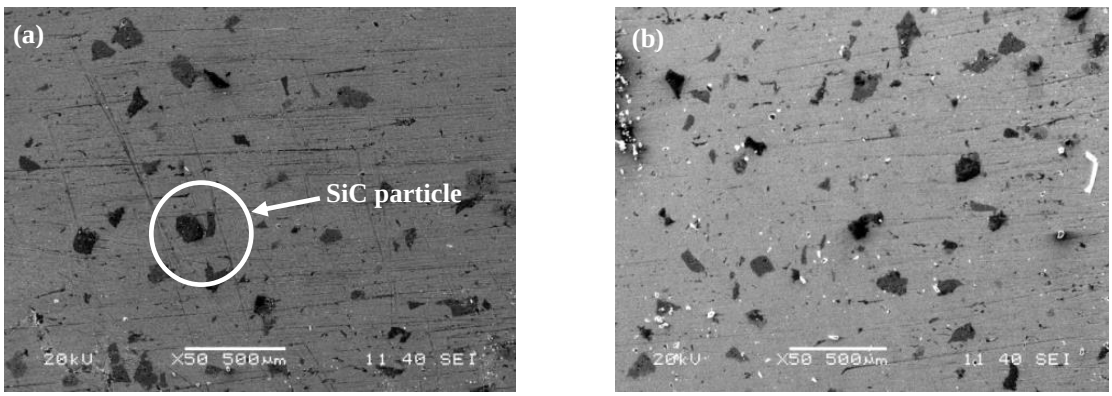

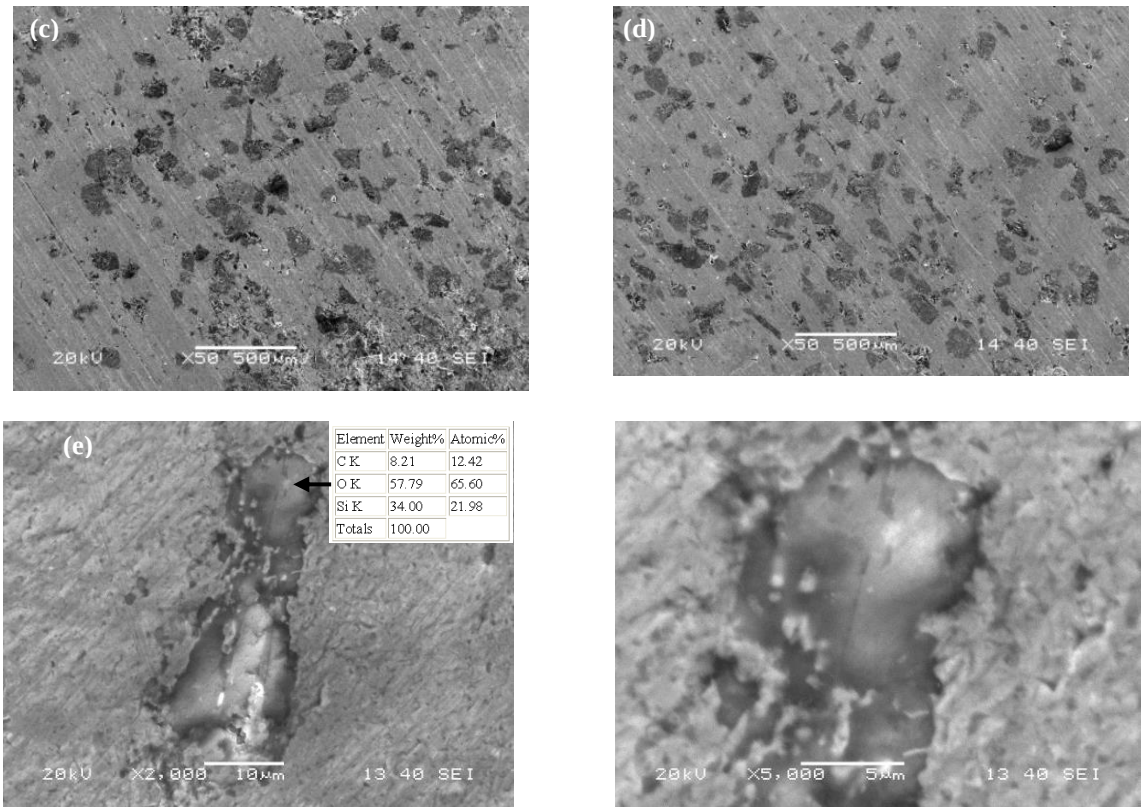

Fig.4.15 SEM image of (a) as-milled Cu-10 vol. %SiCp composite (b) as-milled Cu-20 vol. %SiCp composite(c) as-milled Cu-30 vol. % SiCp composite and (d) as-milled Cu-40 vol. %SiCpcomposite(e, f) High magnification SEM images of as-milled Cu-40 vol.% SiCp composite. The inset image in (e) shows the EDX analysis of SiC particle

Figs. 4.15 (a-d) are the SEM images of as-milled Cu-SiCp composites for different vol. % of reinforcement. The SEM images of the composites also show homogeneous dispersion of reinforcement in the Cu matrix. The scanning electron micrographs given in Fig. 4.15show the typical microstructural features of a composite. In the micrographs of the various Cu-SiCp composites a range of SiC particulate sizes could be seen. Good interfacial integrity between the SiCp and the Cu matrix could also be observed. High magnification SEM images of as-milled Cu-40 vol. % SiCp composites in Figs.4.15 (e, f) show the interface between the SiC particle and the Cu matrix. EDX analysis inset in Fig.4.15 (e) confirms that the dark particles are SiC. The SiC particles are embedded in the Cu matrix. The interface between the reinforcement and the matrix plays a crucial role in determining the mechanical properties of

the composites. The SEM images the Cu-SiCp interface suggests that the bonding between the Cu matrix and the SiC particles is very strong.

Fig. 4.16shows the XRD plots of as-milled Cu-SiCp composites for different vol. % of SiC particles. Peak corresponding to Cu_2O could be detected in the x-ray diffraction plots of all the sintered as-milled Cu-SiCp composites. This is because of the oxidation of Cu due to the residual oxygen present in the sintering atmosphere.

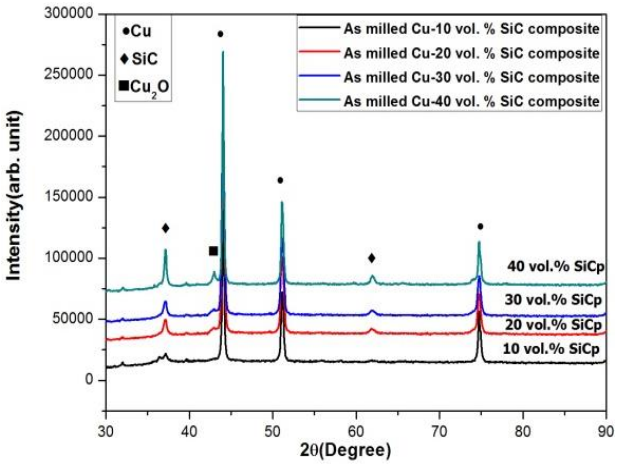

Fig. 4.16 XRD plot of various as-milled sintered Cu-SiCp composite

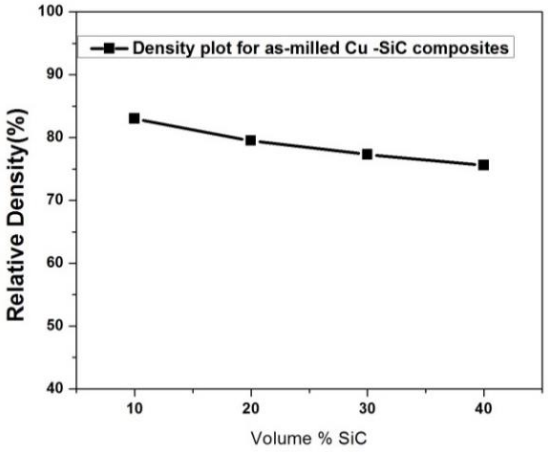

Fig. 4.17 Variation of Relative Density plots of sintered as-milled Cu- SiCp composite

Fig.4.17 shows the variation of relative density of as-milled Cu-SiCp composite for different vol. % of reinforcement. The relative density gradually decreases with the increase in the content of SiCp as the incorporation of hard and brittle material in the soft Cu matrix leads to presence of voids in the composites. Fine particles of 20 h milled Cu produces finer pores which diminishes earlier as compared to coarser pores formed by large sized Cu particles. This is why composites developed from finer 20 h milled Cu powder leads to better densification and hardness as compared to the composites developed from coarser unmilled Cu powder.

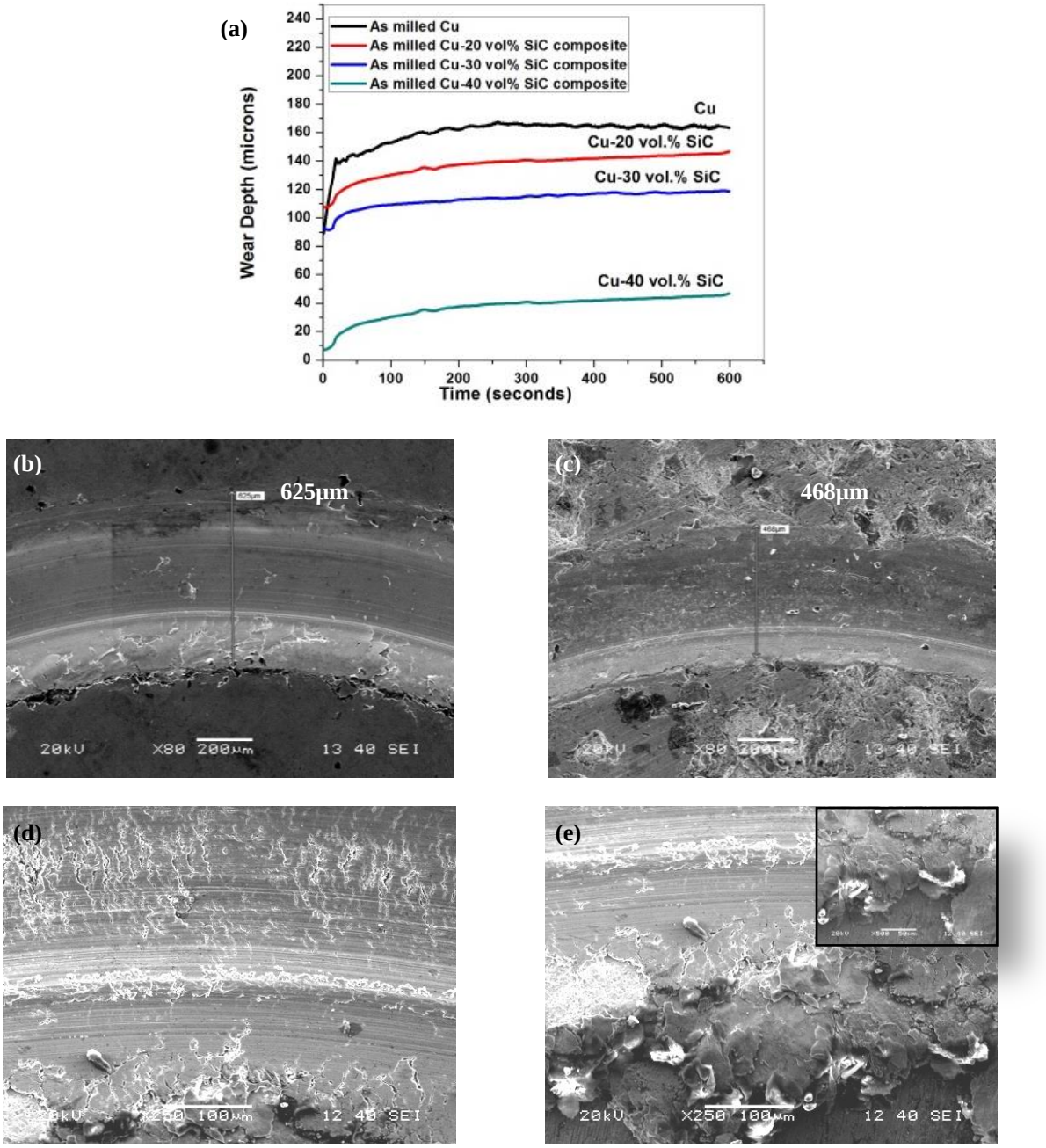

Fig.4.18 (a) Wear Characteristic of various as-milled Cu- SiCp composites. SEM images of the wear track of (b) as-milled Cu (c) as-milled Cu-40 vol. %SiCp composite (d, e) High magnification SEM images of the wear track of as-milled Cu-40 vol. %SiCp composite. Inset image in (e) shows the edge of the wear track of as-milled Cu-40 vol. %SiCp composite

The wear resistance of the pure as-milled Cu and the various as-milled Cu-SiCp sintered composites were determined using a ball-on-plate tribometer. Fig. 4.18 shows the variation of wear depth of the various as-milled Cu-SiCp composites. It has been found that the as-milled Cu-SiCp composites exhibits better wear in comparison to pure Cu. As-milled Cu- 40 vol. % SiCp composite shows highest wear resistance. The enhancement of wear resistance is

possibly due to the strengthening of the composites because of the fine dispersion of the SiC particles in the Cu matrix. The dispersion of the SiC particles, as a hard ceramic phase in the Cu matrix, improves the wear resistance significantly. From Fig. 4.12(b) it is evident that there is an enhancement of microhardness due to the dispersed SiC particles in the Cu matrix and this consequently improves the wear resistance of the composite. The enhancement in the wear resistance of the composites can also be attributed to the good bonding between the Cu and the SiC particles. Bonding between the matrix and the reinforcement is known to play an important role in the wear resistance. Reduction of direct load at the contact between the Cu-SiCp composite surface and the ball due to load bearing component action of the hard SiC particles as compared to that of pure Cu also enhances the wear resistance of the Cu-SiCp composites. The wear mechanism was found to involve a combination of abrasion and delamination. Figs. 4.18 (b,c) are the SEM images of wear tracks of as-milled Cu and as-milled Cu- 40 vol.% SiCp composite.The width of the wear track in case of as-milled Cu- 40 vol.% SiCp composite was found to be much lower as compared to that of as-milled pure Cu [86-88].

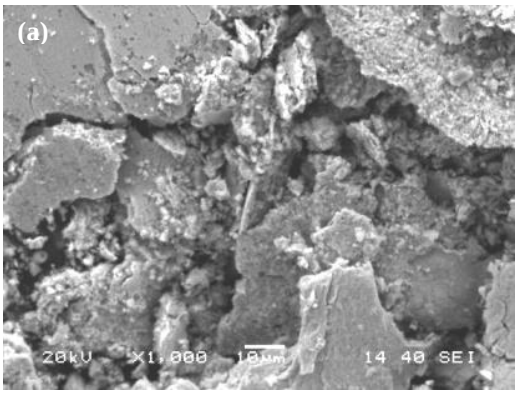

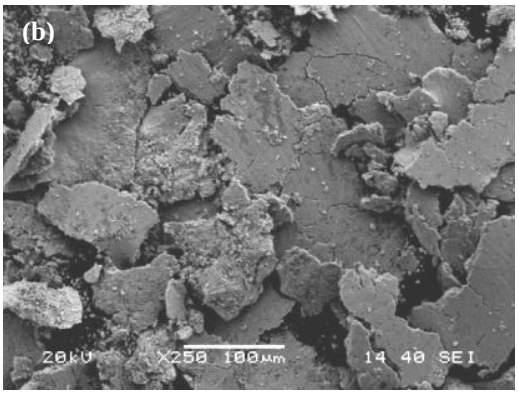

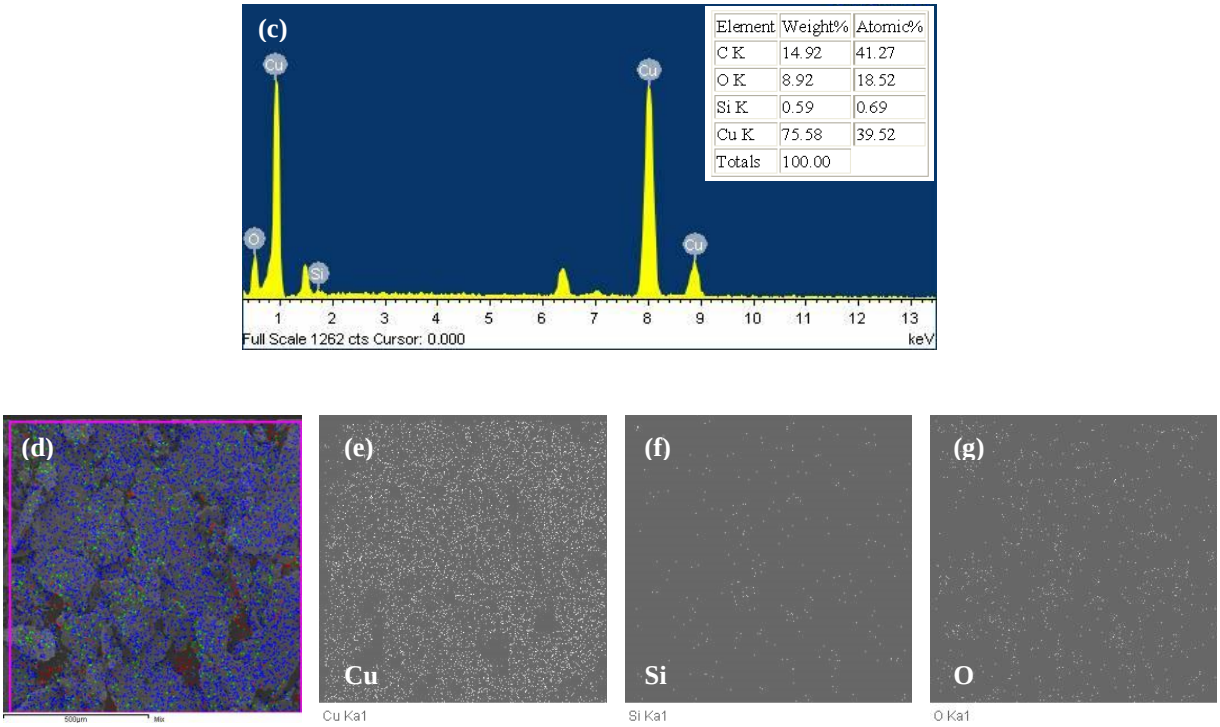

Fig. 4.19 (a, b) SEM images of wear debris from as-milled Cu-40 vol. %SiCp composite (c) EDX analysis of the wear debris(d) SEM image of the wear debris selected for elemental mapping. Elemental map of (e) Cu (f) Si (g)O

Figs.4.19 (a, b) are the SEM images of the wear debris from as-milled Cu-40 vol. % SiCp composite. The EDX analysis of the wear debris in Fig. 4.19 (c)shows mainly the presence of Cu and very small amount of Si. This suggests that the wear debris consists mainly of Cu and has a very small amount of SiC in it. The elemental map of Cu and Si in the selected area shown in the SEM image in Fig.4.19 (d) also suggests that the wear debris mainly consists of Cu and there is only a very small amount of SiC in it. The oxygen in the wear debris is possibly due to the oxidation of the sample by the unavoidable oxygen present during sintering. Oxidation of the wear debris could also take place during the wear test [89, 90].

4.3 Cu-E-Glass Fiber Composites

E-Glass fibers are the most widely used glass fibers as reinforcement in the composites. E-glass fibers are alumina-borosilicate glass with less than 1% w/w alkali oxides and are mainly used for glass-reinforced plastics. E-glass or electrical grade glass was originally developed

for use as an insulators for electrical wiring which was later found to have excellent fiber forming capabilities and is now widely used as the reinforcing phase in composites and is commonly known as fiber glass. E-glass fibers exhibit useful bulk properties such as hardness (6000 MPa), dimensional stability, resistance to chemical attack and high strength. It has a tensile strength of 3500MPa and its Young's modulus is 85 GPa. The compressive strength of E-glass fiber is 5000 MPa. The maximum hardness of E-glass fibers is around 6000 MPa and its density is 2.58 gm/cc.

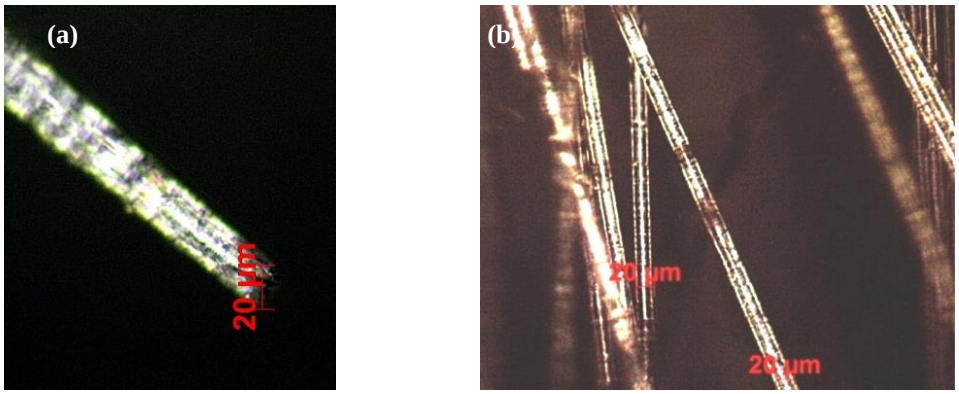

Fig. 4.20 (a, b) Optical images of E-glass fiber used in composite

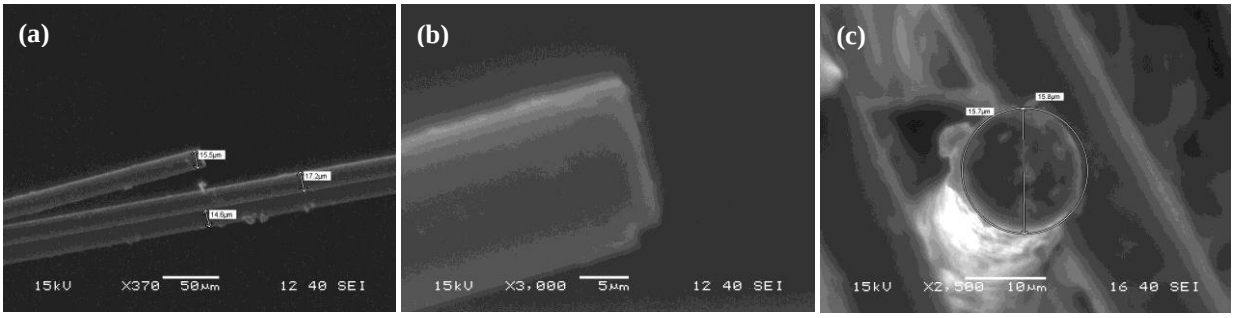

Fig. 4.21 (a-c) SEM image of E-glass fiber used in composite

Fig 4.20 and Fig 4.21 shows the optical and SEM images of the E-glass fiber used as the reinforcement for development of Cu-E-glass fiber composites respectively. The fibers have diameter ranging from 14.6 µm to 17.2 µm. The tensile test of the fiber was carried out in Instron 1195. The fiber shows brittle fracture with elongation to failure of 4.134 %.Table 4.2 shows the results of the tensile test. The elongation to fracture for the E-glass fiber is very low as compared to that of ductile metals.

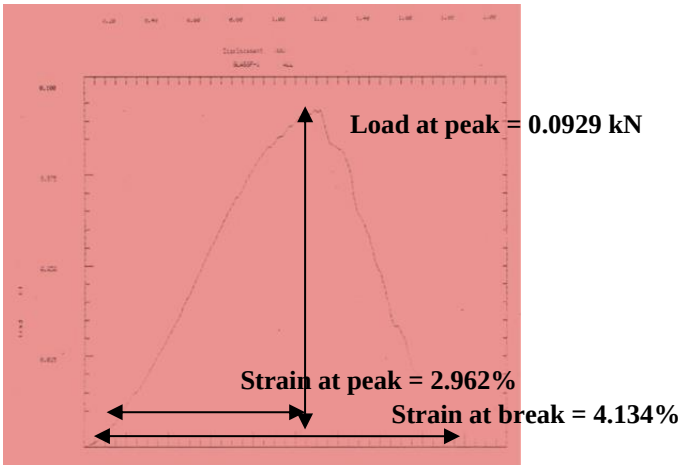

Fig.4.22 Load vs Displacement plot of E-glass fiber

Table 4.2 Results obtained from the tensile test of E-glass fiber
(The tensile test was performed for a bunch of 15 E-glass fibers)

Strain at peak (%)	Strain at Break (%)	Load at Peak (kN)
2.962	4.134	0.0929

E-glass fiber is highly brittle and shows almost flat fracture surface. The maximum elongation to fracture for E-glass fiber has been reported as 4.8 % and it has 100 % recovery when stressed below the point of rupture. The tensile test for the E-glass fiber used in the Cu-E-glass fiber composites has also shown a similar strain to failure value of 4.134 %. The tensile strength of a single E-glass fiber was found to be ~2336 MPa [25].

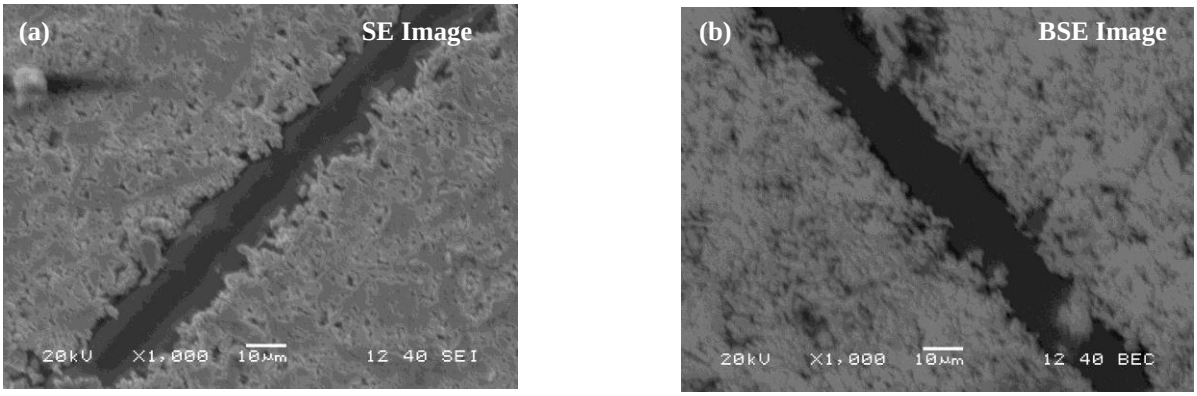

Fig. 4.23.1 (a) Secondary Electron SEM image (b) Backscattered Electron SEM image of unmilled Cu-10 vol. % E-glass fiber composite sample sintered at 900^{o}C for 1h

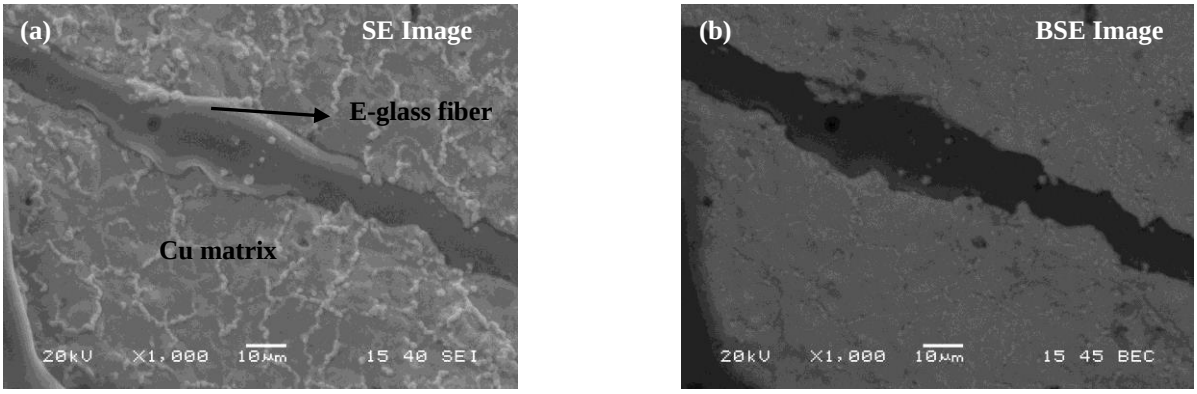

Fig. 4.23.2 (a) Secondary Electron SEM image (b) Backscattered Electron SEM image of unmilled Cu-20 vol. % E-glass fiber composite sample sintered at 900^{o}C for 1h

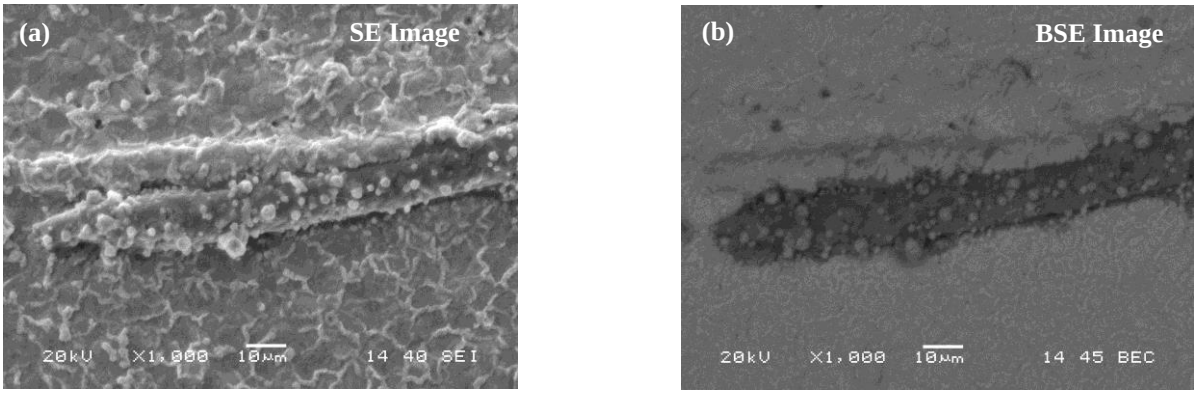

Fig. 4.23.3 (a) Secondary Electron SEM image (b) Backscattered Electron SEM image of unmilled Cu-30 vol. % E-glass fiber composite sample sintered at 900^{o}C for 1h

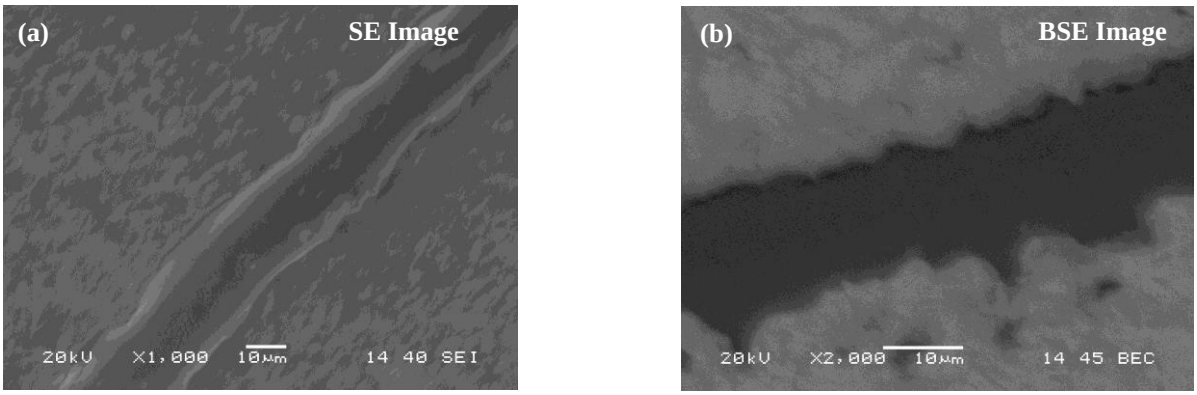

Fig. 4.23.4 (a) Secondary Electron SEM image (b) Backscattered Electron SEM image of unmilled Cu-40 vol. % E-glass fiber composite sample sintered at 900^{o}C for 1h

Fig. 4.23 shows the microstructure of various sintered unmilled Cu-E-glass fiber composites developed containing different vol. % of E-glass fiber. Sintering was done at 900^{o}C for 1 h in Ar atmosphere. From the microstructural analysis it is evident that the composites fabricated have random distribution of the reinforcement in the Cu matrix and shows very good bonding

with the matrix. The fibers show good wettability with Cu and shows good bonding with the Cu matrix. Back scattered electron SEM image shows very good wettability of Cu with E-glass fiber. Relative density of 85.8 % could be achieved from 10 vol. % Cu - E-glass fiber composite [91,92].

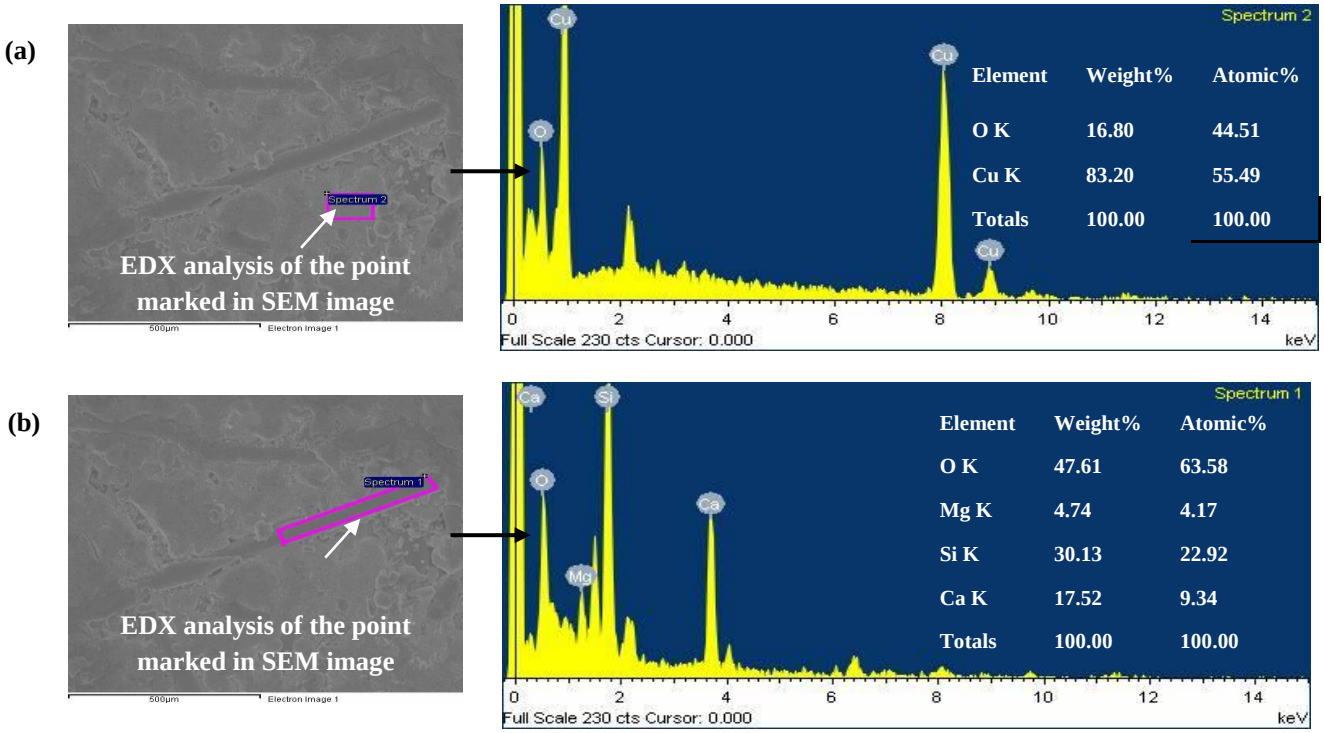

Fig. 4.24 (a, b) EDX analyses of unmilled Cu-40vol. % composite sintered at 900^{o}C for 1h

Fig. 4.24(a) shows the EDX analysis of the matrix phase in the unmilled Cu-40 vol. % composite. Fig. 4.24 (b) shows the EDX analysis of the E-glass fiber reinforcement. The EDX analysis of the Cu matrix in Fig 4.24 (a) shows a small amount of oxygen in the matrix. This is possibly due to the unavoidable oxygen present in the furnace during sintering. Spectrums have been taken at different places to show the various phases in the composite. The EDX analysis of the E-glass fiber in Fig. 4.24 (b) shows presence of elements like Mg (4.17 at. %), Ca (9.34 at. %), Si (22.92 at. %) and O (63.58 at. %).

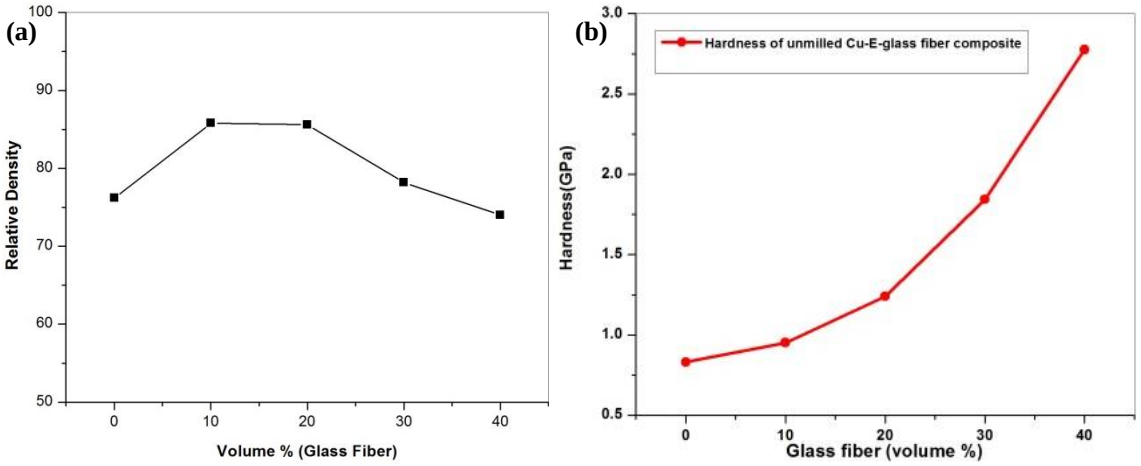

Fig. 4.25 (a) Relative Density plot of various sintered unmilled Cu-E-glass fiber composite (b) Vickers hardness plot of various unmilled Cu-E-glass fiber composite

Fig. 4.25 (a) shows the variation of relative density of unmilled Cu-E-glass fiber composite containing different vol. % reinforcement. The densities of all the specimens have been found out using the Archimedes' principle. The relative density increases initially with the increase in the content of E-glass fiber in the unmilled Cu-E-glass fiber composite but it shows slight decreases when higher vol. % of glass fiber was added. It should be noted that a high vol. % of glass fiber could lead to a lower theoretical density of the unmilled Cu-E-glass fiber composite. Fig. 4.25 (b) shows the variation of Vickers hardness test for unmilled Cu-E-glass fiber composites containing different vol. % of E-glass fiber. The hardness of the Cu-E-glass fiber composite increased with increase in vol. % of glass fiber in the composite. This is due to the strengthening of Cu matrix by the glass fiber. The fracture surface of the various samples was analysed using a SEM. Fractographs of unmilled Cu-E-glass fiber composites are shown in Fig.4.26. It can be observed that the Cu matrix undergoes ductile fracture showing the presence of dimples in the fractured surface as shown in Fig.4.26.1 (a). E-glass fibers could be seen embedded in the Cu matrix.

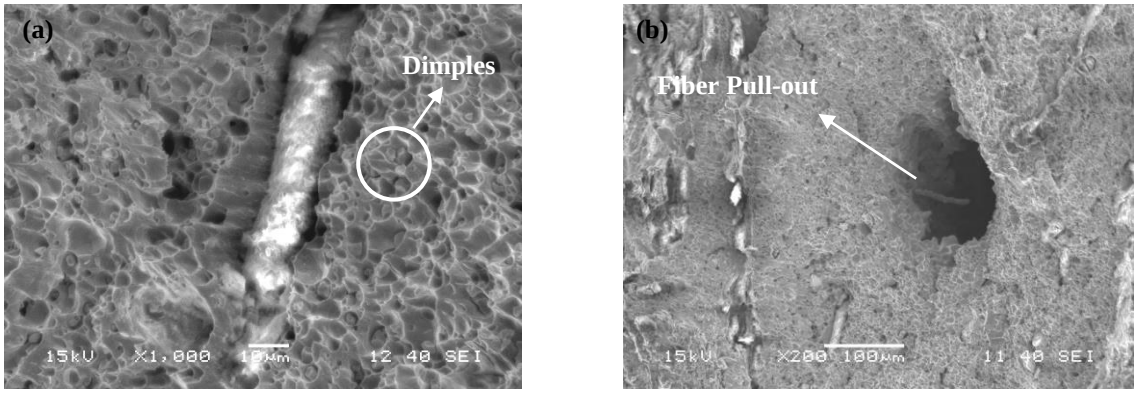

Fig.4.26.1 (a, b) SEM images of fracture samples of unmilled Cu- 10 vol. % E-glass fiber composite

Fiber pull out could be seen in the unmilled Cu-10 vol. % E-glass fiber composite sample in Fig.4.26.1(b).This is possibly due to the low load bearing capacity when the vol. % of glass fiber is lower. Higher stress on each fiber leads to pull-out of the fiber. The stress on the fiber also leads to plastic deformation of the Cu matrix around the fiber which is evident in the SEM image in Fig.4.26.1(a).The fiber tries to restrict the plastic deformation in the Cu matrix.

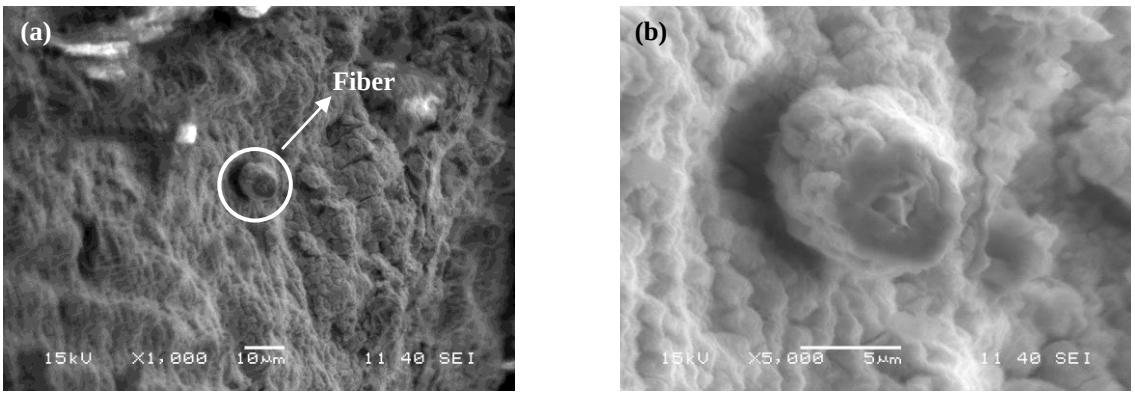

Fig. 4.26.2(a, b) SEM images of fracture samples of unmilled Cu- 20 vol. % E-glass fiber composite

Fig. 4.26.2 (a, b) are the SEM images of the fracture surfaces of unmilled Cu-20 vol. % E-glass fiber composite. From the SEM images it is clear that the nature of fracture in the Cu matrix is ductile whereas the E-glass fiber undergoes brittle fracture. The fractured E-glass fibers have Cu adhered to its surface indicating good wettability and bonding between the Cu

matrix and the glass fiber. Figs.4.26.3 (a,b) are the SEM images of the fracture surfaces of unmilled Cu-30 vol.% of E-glass fiber composite. Here also we seeductile nature of fratcure in the Cu matrix and brittle fracture in the E-glass fibers. The SEM image in Fig.4.26.3 (a) show pull-out of the E-glass fiber. The SEM images also show the presence of higher amount of pores in the sample. It was also found out earlier (Fig. 4.25(a)) that the relative density of the unmilled Cu- 30 vol. % E-glass fiber composite (78.2 %) is less than the relative density of unmilled Cu- 20 vol. % E-glass fiber composite (85.6%). Addition of E-glass fiber beyond 20 vol. % has led to a decrease in the relative density of the composite.

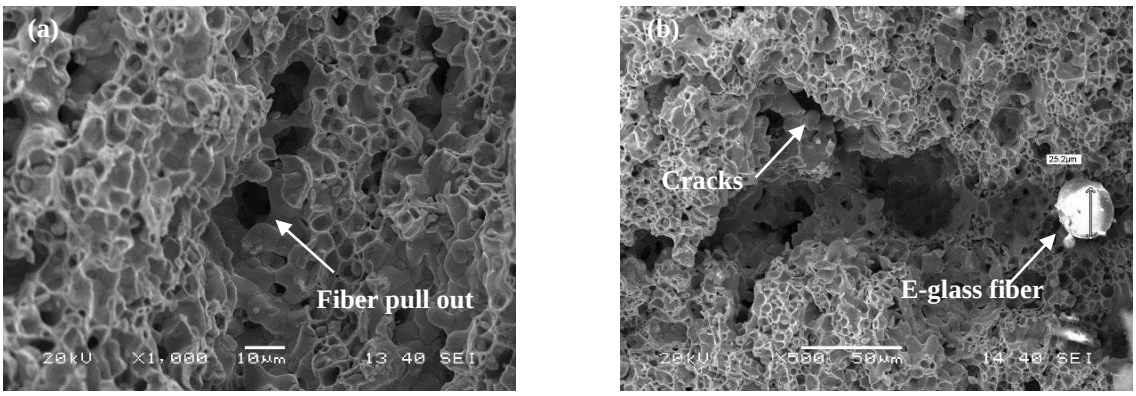

Fig. 4.26.3 (a, b) SEM images of the fracture surface of unmilled Cu- 30 vol. % E-glass fiber composite

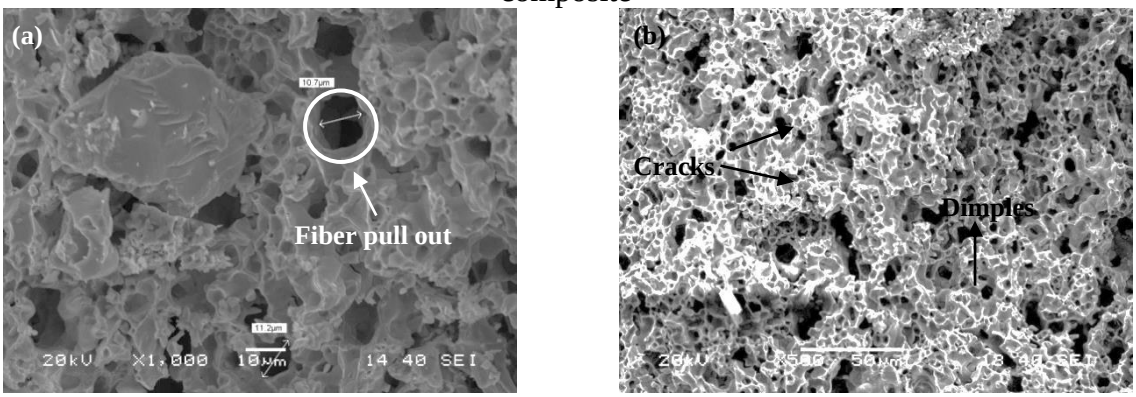

Fig. 4.26.4 (a, b) SEM images of the fracture surface of unmilled Cu- 40 vol. % E-glass fiber composite

Figs.4.26.4 (a,b) showthe fracture surface of unmilled Cu-40 vol.% of E-glass fiber composite. The Cu matrix shows dimples on its fracture surface which suggests the ductile nature of fracture in Cu matrix.Several cracks can be clearly seen in the Cu matrix. As can be

seen from the Fig. 4.25(a) the relative density of the unmilled Cu-40 vol. % E-glass fiber composite is even lower than that of the unmilled Cu-30 vol. % E-glass fiber composite. Addition of glass fiber beyond 20 vol. % deteriorates the relative density even further. Addition of glass fiber beyond 20 vol. % leads to poor sinterability and densification of the composites. This is the reason why we see a large number of pores in the Cu matrix.

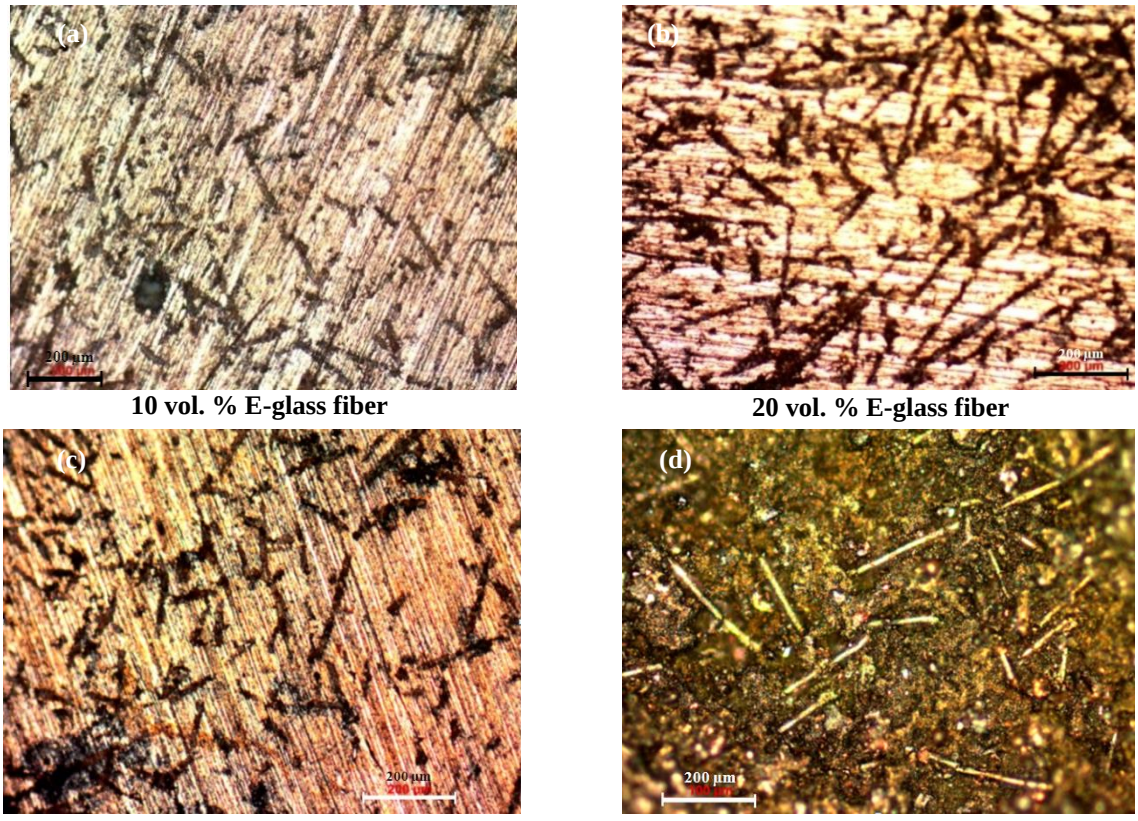

10 vol. % E-glass fiber **20 vol. % E-glass fiber**

30 vol. % E-glass fiber **40 vol. % E-glass fiber**

Fig.4.27 (a-d) Optical micrographs of as-milled Cu-E-glass fiber composites for different vol. % of fiber used as reinforcement (10, 20, 30 and 40 vol. %).

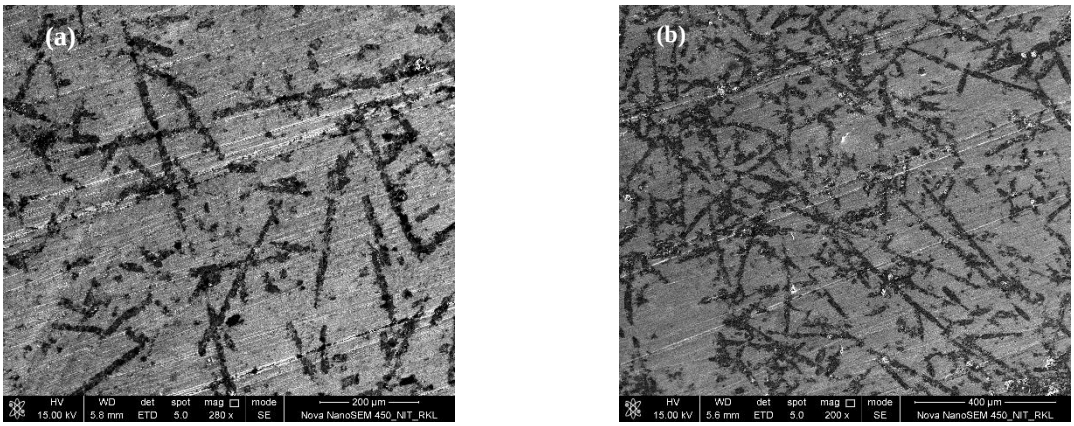

10 vol. % E-glass fiber **20 vol. % E-glass fiber**

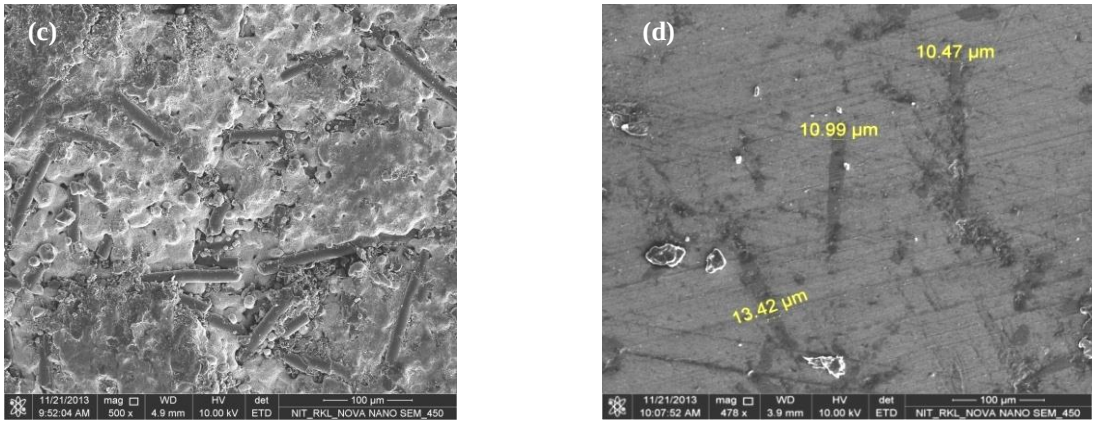

30 vol. % E-glass fiber **40 vol. % E-glass fiber**

Fig.4.28 (a-d) FESEM images of as- milled Cu-E-glass fiber composites for different vol. % of fiber used as reinforcement (10, 20, 30 and 40 vol. %)

From the Figs.4.27 (a-d) it is clearly evident that there is a homogenous dispersion of fibers throughout the Cu matrix. The diameters of fibers are approximately 20µm or lower. It is clearly evident from the FESEM images that the fibers are embedded in the Cu matrix. FESEM images of as-milled Cu-E-glass fiber composites in Fig. 4.28 (a-d) also show the random distribution of reinforcements throughout the Cu matrix.

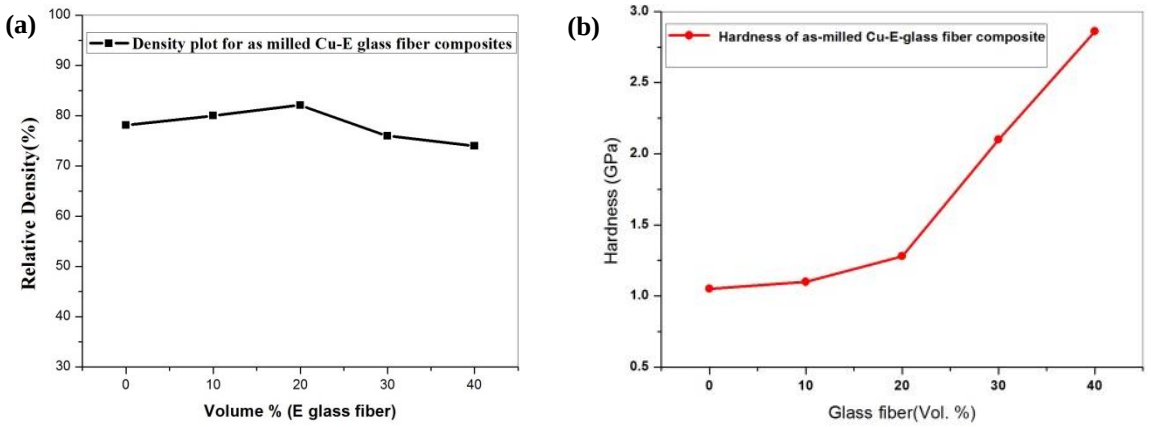

Fig 4.29 (a) Variation of relative density of various sintered as-milled Cu-E-glass fiber composites (b) Variation of Vickers hardness of various as-milled Cu-E-glass fiber composites

Comparison of the plots in Fig. 4.29 (a) and Fig. 4.25 (a) it is evident that the relative density of the various sintered as-milled Cu-E-glass fiber composites is higher than that of the various sintered unmilled Cu-E-glass fiber composites. In the case of as-milled Cu-E-glass fiber composites 20 h milled nanocrystalline Cu is used as the matrix which results in better

sinterability and densification. Cu has a melting temperature of 1083^{o}C. Nanocrystalline nature of Cu could reduce the melting point of Cu. This is why as-milled Cu possibly softens at the sintering temperature of 900^{o}C and results in better sinterability and densification compared to the unmilled Cu-E-glass fiber composites. Nanocrystalline Cu has higher surface area per unit volume and this could reduce its melting point. The hardness of the composites shown in Fig.4.29 (b) also shows a gradual rise with the rise in vol. % of E-glass fiber in the composites.Fig.4.29 (b) shows the variation of Vickers microhardness of as-milled Cu-E-glass fiber composites. As-milled Cu-E-glass fiber composites possess better hardness because of better densification during sintering at 900^{o}C for 1 h. The fractured surfaces of the samples were analyzed under SEM. Fractographs of as-milled Cu-E-glass fiber composites are shown in Fig.4.30. The dimples on the matrix shown in Figs.4.30.1 (a, b) suggest the ductile fracture of the Cu matrix. It can also be seen that fibers are embedded inside the Cu matrix and has good binding with the matrix. The SEM image in Fig.4.30.1 (b) clearly shows the brittle fracture of E-glass fiber.

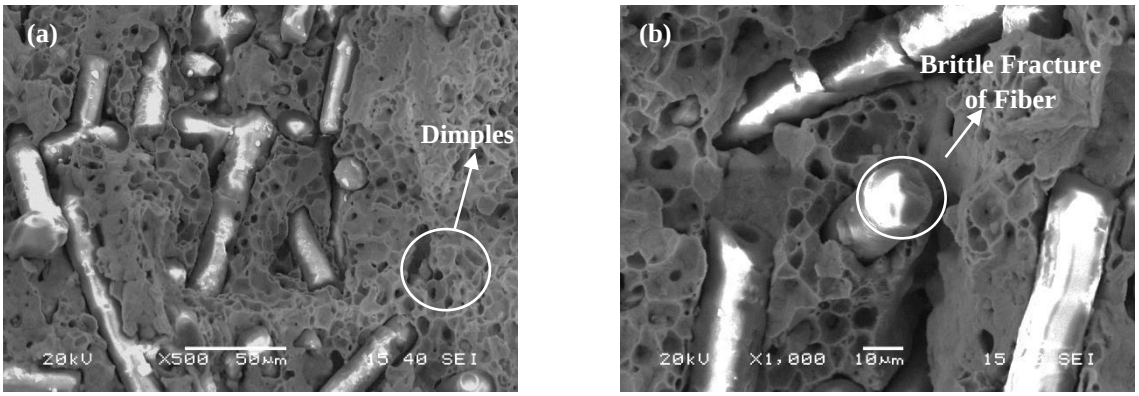

Fig.4.30.1 (a, b) SEM image of fracture surface of as-milled Cu- 10 vol. % E-glass fiber composite

Figs. 4.30.2 (a, b) show the SEM images of as-milled Cu-20 vol.% E-glass fiber composites. The fibers are deeply penetrated insided the Cu matrix. There is a random distribution of fibers inside the Cu matrix. Fiber pull-out can easily be seen in Fig.4.30.2 (b).

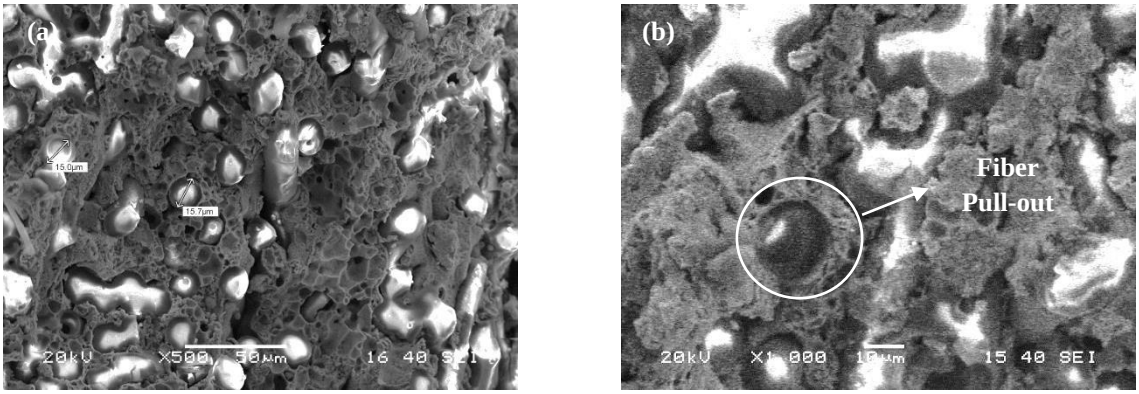

Fig.4.30.2 (a,b) SEM images of the fracture surface of as-milled Cu- 20 vol. % E- glass fiber composite

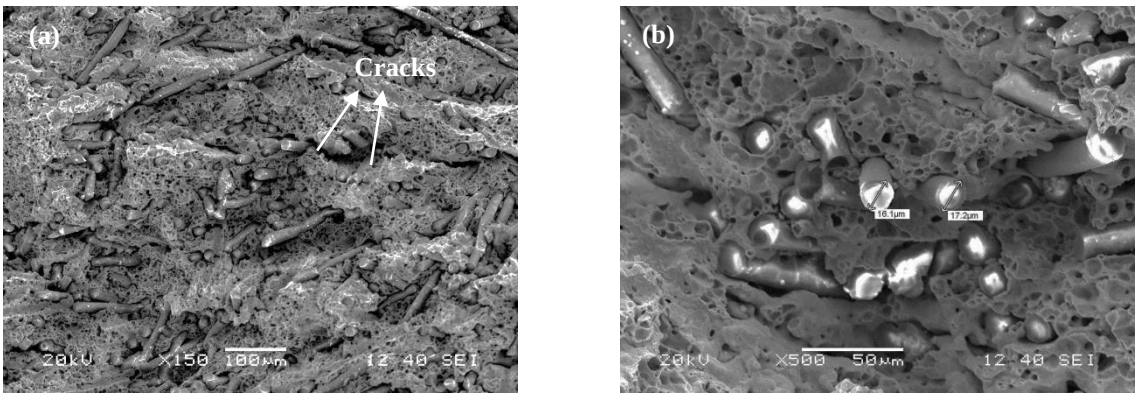

Fig.4.30.3 (a, b) SEM images of the fracture surface of as-milled Cu- 30 vol. % E glass fiber composite

Figs.4.30.3 (a,b) show the SEM images of the fracture surface of as-milled Cu-30 vol.% E-glass fiber composite. The fibers show good interfacial integrity with the Cu matrix. Cracks could be seen in the Cu matrix. However, in the case of as-milled Cu-30 vol. % E-glass fiber composite fewer numbers of pores and cracks could be seen in the Cu matrix as compared to the unmilled Cu-30 vol. % E-glass fiber composite. This can be seen by comparing the fractographs of the two composites in Figs.4.26.3 (a, b) and Figs.4.30.3 (a, b).This is possibly due to better sinterability and densification in the case of as-milled Cu composite as compared to the unmilled Cu composite. It should be noted that the Cu-E-glass fiber composites developed by using as-milled Cu have higher relative density values as compared to the Cu-E-glass fiber composites developed by using unmilled Cu.

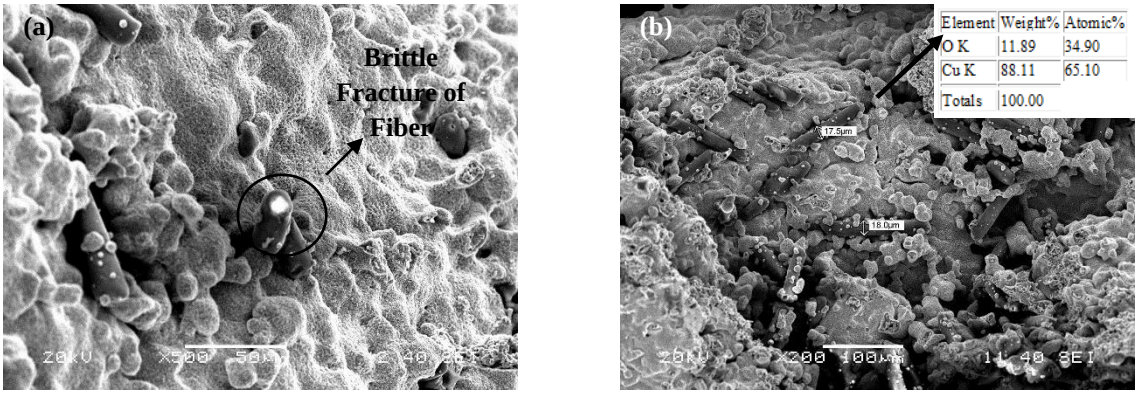

Fig.4.30.4 (a, b) SEM image of fracture surface of as-milled Cu- 40 vol. % E- glass fiber composite. Inset in Fig (b) shows the EDX of agglomerated finer Cu particle

Fig.4.30.4 shows the SEM image of the fracture surface of as-milled Cu-40 vol.% E-glass fiber composite. The SEM images clearly show Cu adhered to the E-glass fiber surface. The brittle fracture of the glass fiber could be clearly seen in Fig.4.30.4(a). In the case of as-milled Cu-40 vol. % E-glass fiber composite a large number of Cu rich spherical particles could be seen. This is possibly due to the agglomeration of fine Cu particles which tend to come together to form larger particles thereby reducing the surface area per unit volume.The surafce area per unit volume (1/r) varies inversely with the radius of the particle (r). This is due to the Gibb-Thomson effect whichpredicts that nanoparticles dissolve at a lower electrochemical potential as compared to the bulk materials. The Gibbs-Thomson effect is due to the reduction of local chemical potential caused by nanoscale curvature. This was not seen in thecase of unmilled Cu composites due to the coarse nature of the Cu particles in the matrix [93-97].

4.4 Cu-Multi Walled Carbon Nanotubes Composites

Carbon nanotubes are very unique material found till date. The small dimension, strength and other remarkable properties make them a promising candidate for potential applications. CNTs are tube shaped material and can be synthesized with high purity and yield. CNTs are made of carbon having diameter measuring on nanometer scale. Carbon nanotubes typically

have diameters ranging from <1 nm to 50 nm. CNTs show a unique combination of properties like strength, stiffness and tenacity compared to other fibers and materials. They show high thermal and electrical conductivity values comparable to other conducting materials. CNTs possess extraordinary mechanical properties compared to carbon fibers. Their elastic modulus value is in the range of 0.3-1 TPa, tensile strength is of the order of 10-60 GPa, thermal conductivity is 3000 W/mK and electrical conductivity is 10^6-10^7 S/m. Carbon nanotubes have strength approximately 100 times greater than that of steel of the same diameter. The density of multiwalled CNTs is 2.6 gm/cc and their specific surface area is about 200-400 m^2/gm. CNTs do not show any environmental or physical degradation like thermal expansion, corrosion and sensitivity to radiation. In order to optimize carbon nanotubes yield and quality, three main synthesis processes have been used, namely, arc discharge, laser ablation and chemical vapour deposition (CVD). Amongst the above three mentioned processes, CVD is the most promising route for bulk production of high purity nanotubes. The CVD method involves the catalytic decomposition of the hydrocarbon with the aid of supported transition metal catalysts (Fe, Co, Ni, etc.). It is a versatile process in which the gas phases are decomposed to form reactive species. These species lead to particle or film growth. A conventional horizontal quartz tube having dimensions approximately 1 m long and 50 mm diameter was used. The temperature was maintained at 900^{o}C with holding time of 40 minutes. Subsequently, the synthesis was initiated by introducing a flow of 20 sccm acetylene (C_2H_2), 50 sccm ammonia (NH_3) and 40 sccm hydrogen (H_2) for 40 minutes. Acetylene (C_2H_2) was used as the carbon source and was fed into the tube furnace at a controlled rate. To prevent oxidation and removal of gaseous by products argon (Ar) gas was fed at a controlled rate of 600 sccm during the whole heating-up, growth and cooling down periods [98-101].The improvement of mechanical properties of Cu is important for its use in many applications. Carbon nanotubes (CNTs), since their discovery, have been used as a

reinforcement material for the fabrication of a variety of composites. CNTs provide a new avenue for the reinforcement of copper based materials. Carbon nanotubes not only help in retaining the properties of the Cu matrix, but also enhance the mechanical, electrical and thermal properties of Cu. Cu-MWCNT composites would give significantly improved mechanical as well as electrical properties.

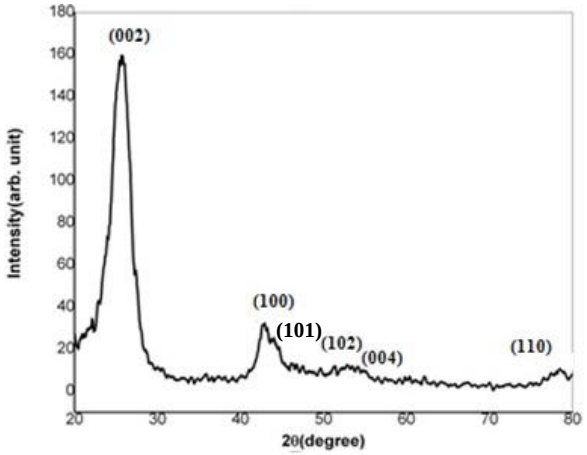

Fig.4.31 XRD of the MWCNTs synthesized by LPCVD process

Fig. 4.31 shows the x-ray diffraction plot of MWCNTs synthesized by low pressure chemical vapour deposition (LPCVD) process. The x-ray diffraction plot confirms the peaks corresponding to MWCNTs. The x-ray diffraction plot confirms the crystalline nature of the carbon nanotubes. Peaks indexed to (002), (100) and (101) planes reflects the hexagonal structure of the carbon nanotubes. The presence of (002) peak in the x-ray diffraction plot, suggests multiwalled nature of carbon nanotubes [102 ,103].

Figs. 4.32 (a-c) are the FESEM images of the carbon nanotubes prepared by the LPCVD process. The average diameter of the MWCNTs is found to be in the range of 10-30 nm with length of several micrometers. From the SEM images it can be seen that carbon nanotubes are agglomerated. The agglomerated lumps of carbon nanotubes were dispersed by ultrasonication.

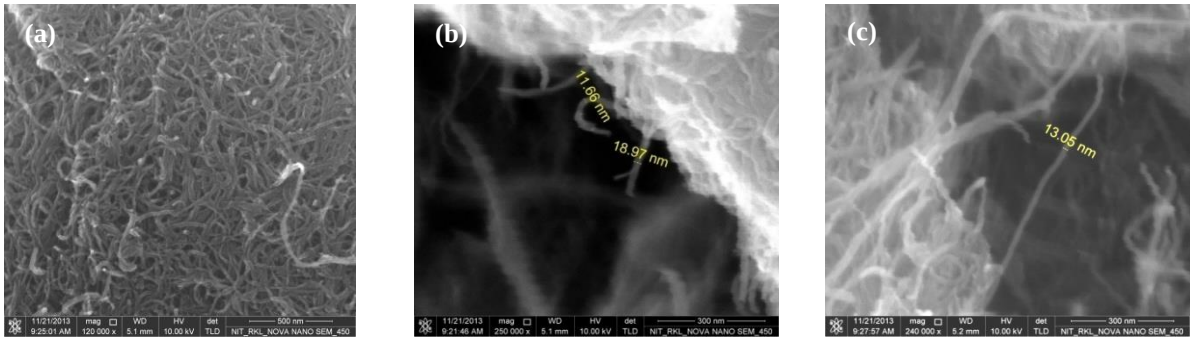

Fig.4.32 (a-c) FESEM images of MWCNTs synthesized by LPCVD process

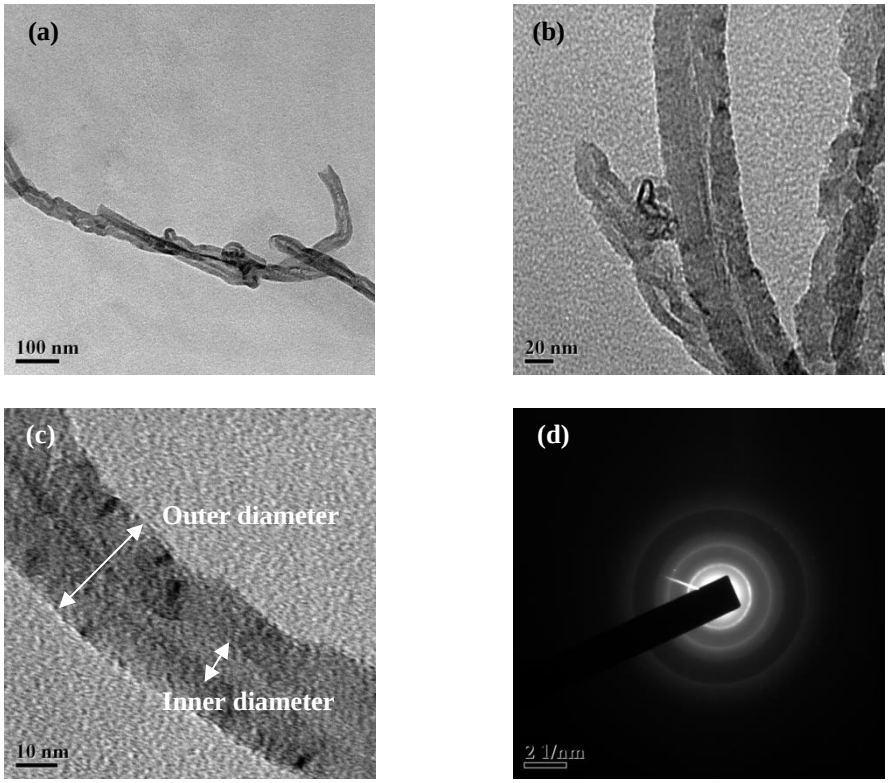

Fig.4.33 (a-c) HRTEM images and (d) SAD pattern of MWCNTs synthesized by LPCVD process

Figs. 4.33 (a-c) are the HRTEM images of the MWCNTs synthesized by LPCVD process. From the HRTEM images it is evident that the carbon nanotubes synthesized are multiwalled in nature. The average length of the nanotubes is approximately 2 μm. The SAD image in Fig. 4.33 (d) shows complete ring pattern which indicates the nanometric dimension of the MWCNTs.

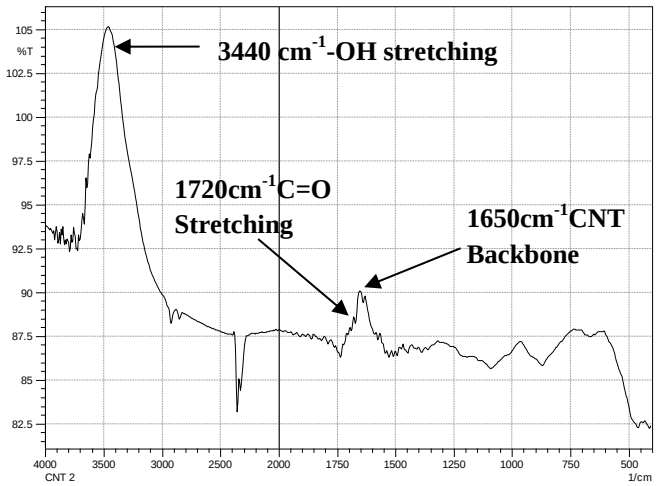

Fig. 4.34 FTIR analysis of CNTs after acidic functionalization

Functionalization of MWCNTs is an essential part for the formation of the Cu-MWCNT composites. The functional groups provide a point of bonding between the metal surface and the MWCNTs. Fig. 4.34 shows the FTIR spectrum for the acid treated MWCNTs in range of wave numbers (400-4000 cm^{-1}). Stretching vibrations from carboxyl groups (C=O) could be seen at around 1720 cm^{-1}.The bands of the hydroxyl group (-OH) stretching vibrations are seen at 3440 cm^{-1} in the FTIR plot. At 1650 cm^{-1} skeletal vibration from unoxidized graphitic domains of the carbon nanotube backbone were observed. These results suggest that the MWCNTs were successfully acid-modified [104].

The Cu-MWCNT composites were prepared by powder metallurgy route. Cu powder with different volume fractions of MWCNTs (1, 2 and 5 vol. %) were developed by blending the constituents followed by cold compaction of the samples in a uniaxial compaction machine under a load of 665 MPa. Sintering of the samples was done at 900^{o}C for 1 h in Ar atmosphere. Microstructure analysis and the dispersion of acid functionalized MWCNTs in Cu matrix were studied using both optical microscope and SEM. The optical micrographs in Figs. 4.35 (a-c) show the homogeneous dispersion of MWCNTs in the Cu matrix. The SEM images in Figs.4.36 (a-c) show the surface of the sintered samples. MWCNTs are clearly visible on the surface of the Cu-MWCNT composites. The SEM images show the

homogeneous distribution of MWCNTs in the Cu matrix and very less agglomeration of MWCNTs is noted.

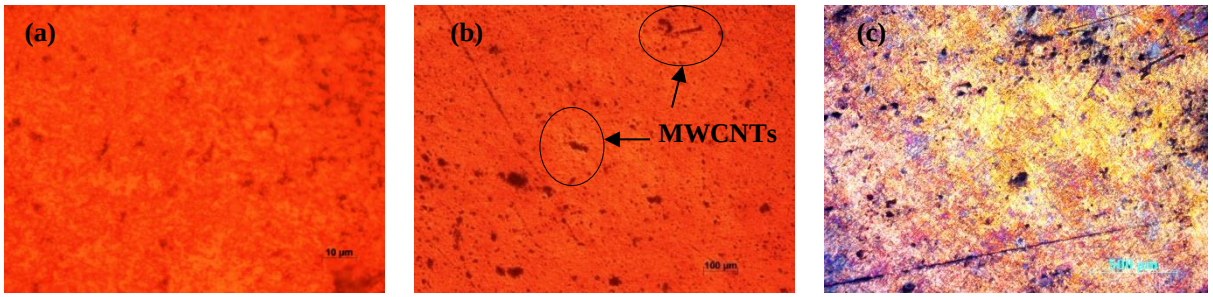

Fig.4.35 Optical micrographs of (a) Cu-1 vol. % MWCNT (b) Cu-2 vol. % MWCNT and (c) Cu-5 vol. % MWCNT composite

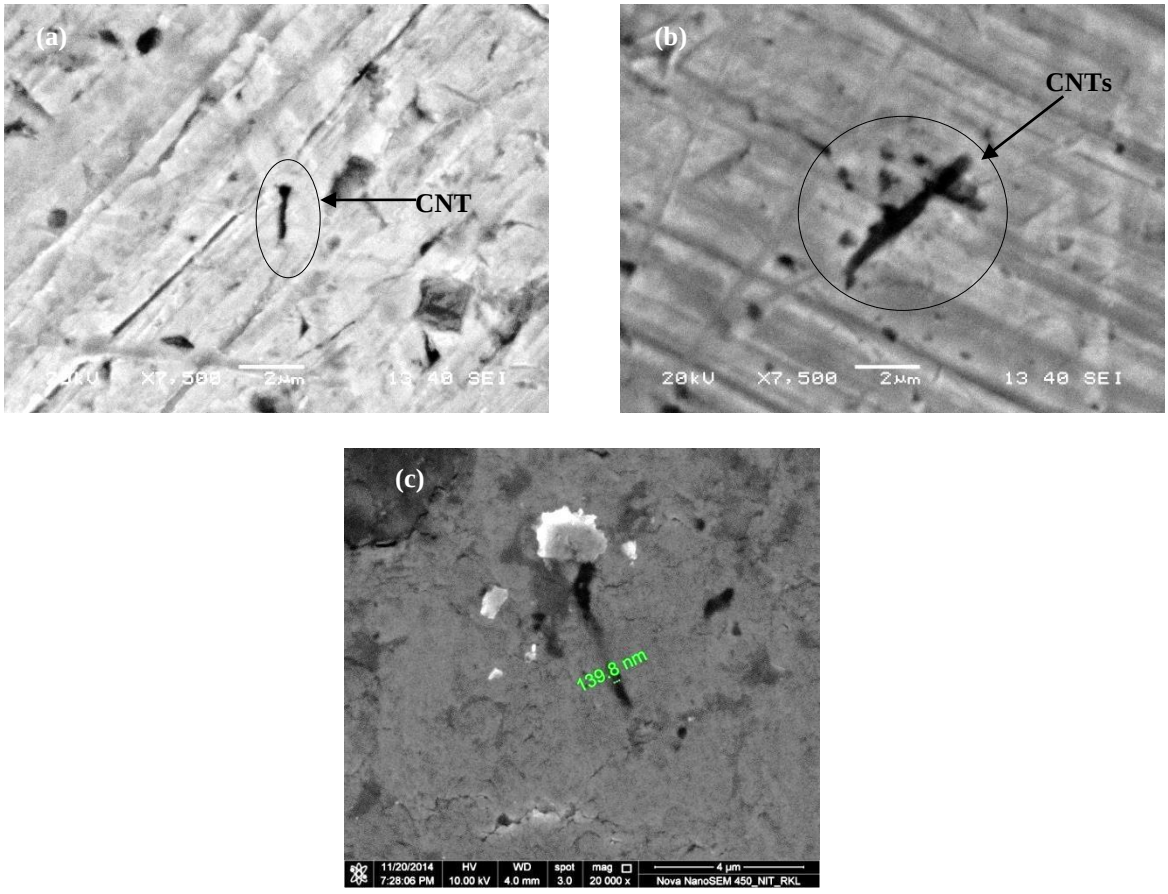

Fig.4.36 SEM image of (a) Cu- 1 vol. % MWCNTs (b) Cu- 2 vol. % MWCNTs and (c) Cu- 5 vol. % MWCNTs composite

Fig. 4.37 shows the EDX analysis for Cu-1 vol. % MWCNT composite. The EDX analysis was done at the dark region marked in the SEM image in Fig. 4.37. The EDX analysis shows the

presence of some percentage of Cu (22.90 at. %) as carbon nanotubes (77.10 at. %) are surrounded by the Cu matrix.

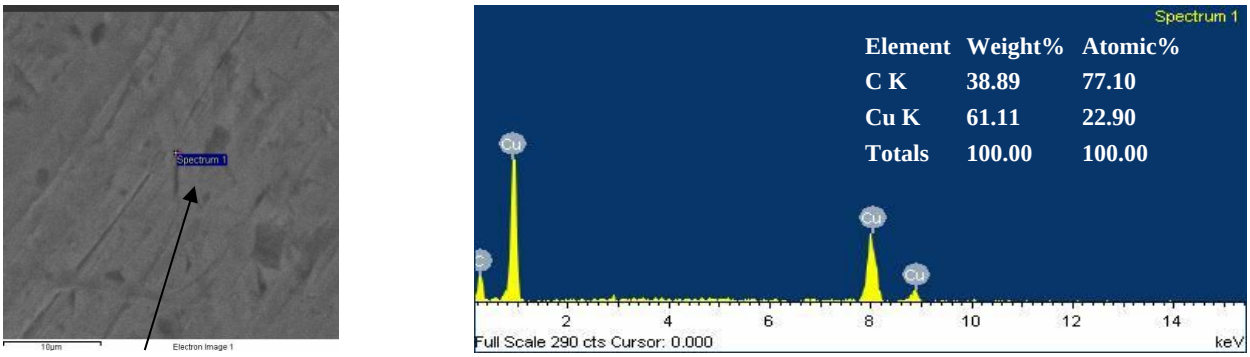

EDX analysis of the point marked in SEM image

Fig.4.37 EDX analysis of Cu- 1 vol. % MWCNT composite

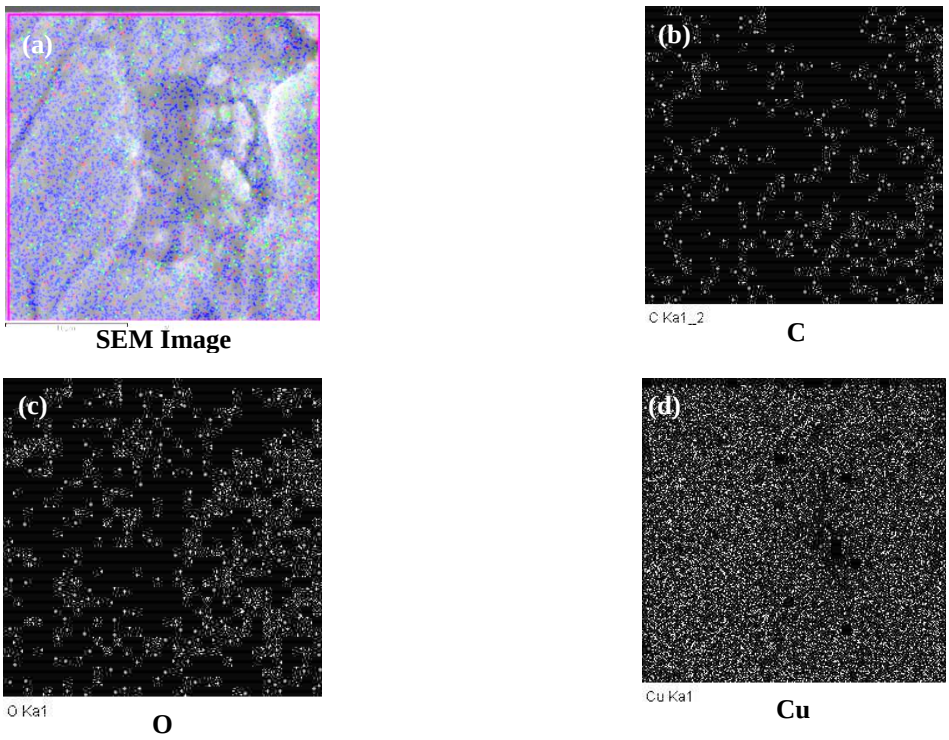

SEM Image

C

O

Cu

Fig.4.38 (a) SEM image. Elemental map of (b) C (c) O (d) Cu in Cu-5 vol. % MWCNT composite

Fig. 4.38 shows the elemental maps of C, O and Cu in Cu- 5 vol. % MWCNTs composite. The elemental map of C in Fig.4.37 (b) shows the distribution of the MWCNTs in the Cu matrix. The elemental map of O in Fig.4.38 (c) shows the distribution of oxygen in the Cu rich matrix. Fig. 4.39shows the x-ray diffraction plots of the various Cu-MWCNT composites

containing different vol. % of MWCNTs. The most intense (002) peak of carbon nanotubes at $2\theta = 26.4^{o}$ is not visible as the concentration of the MWCNTs in the Cu-MWCNT composites is very small. Peak corresponding to Cu_2Ocould be seen at $2\theta = 37.2^{o}$. This is due to the possible oxidation of Cu by the residual oxygen present during the sintering.

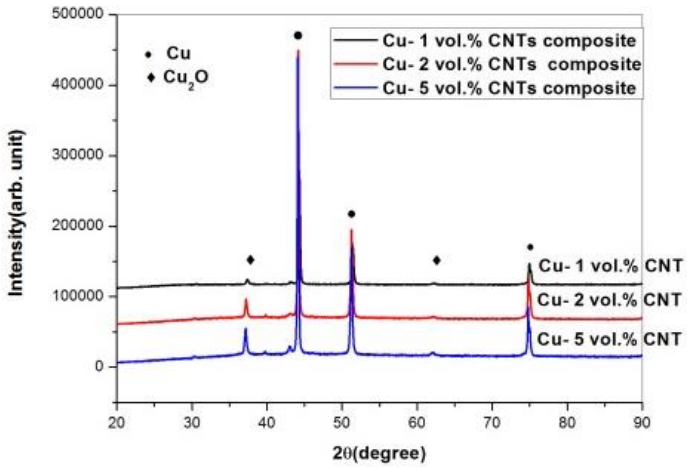

Fig.4.39X-ray diffraction plots of various Cu-MWCNT composites

Fig. 4.40 shows the relative density of Cu-MWCNT composites for different vol. % of MWCNT reinforcement. It can be observed that the relative density increases with the increase in volume fraction of carbon nanotubes in the Cu matrix. This is possibly due to filling of the micro-voids in the Cu matrix by the nanometric MWCNTs. However, it does not show significant increase in densification after addition of 2 vol. % of MWCNTs in the Cu matrix. The chemical bonding formed between the MWCNTs and the Cu matrix provides homogeneous distribution of CNTs as well as high interfacial strength. It should be noted that there is a good bonding between the Cu matrix and the MWCNTs due to the acidic treatment of the MWCNTs during functionalization which produces active sites providing better wettability.

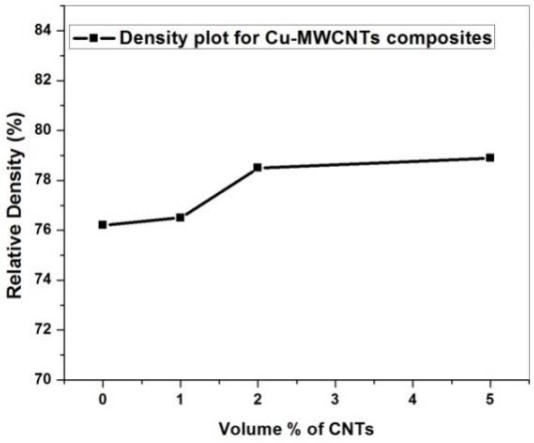

Fig.4.40Relative density plot of various Cu-MWCNT composites

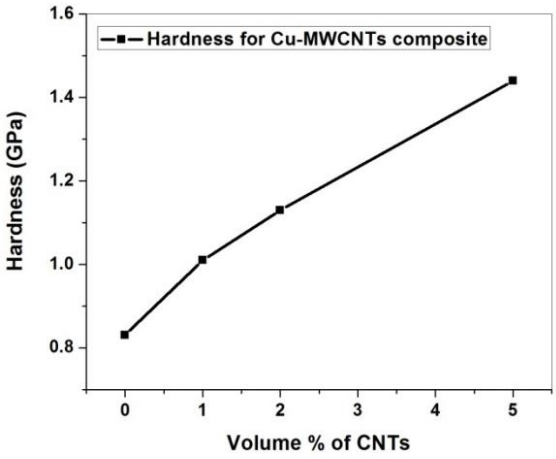

Fig.4.41 Variation of microhardness of various Cu- MWCNT composites

Fig.4.41 shows the Vickers microhardness of various Cu-MWCNT composites. The hardness values of Cu-MWCNT composites increase gradually with the increase in the amount of carbon nanotubes in the Cu-MWCNT composites. Carbon nanotubes can withstand much higher loads than the Cu matrix and hence there is a substantial increase in the hardness values. Another important factor is the interfacial bonding between the MWCNTs and the Cu matrix, which is aided by the functionalization of MWCNTs. Introduction of carboxyl and hydroxyl groups on the surface of the carbon nanotubes during functionalization provides binding sites for the Cu matrix to the MWCNTs [105,106].

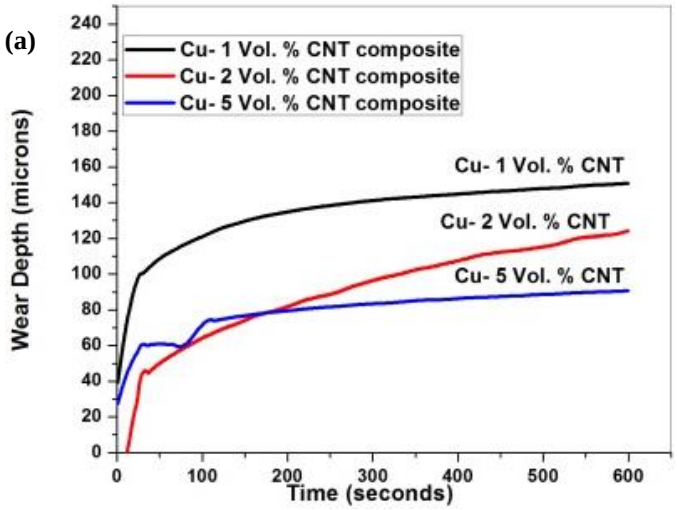

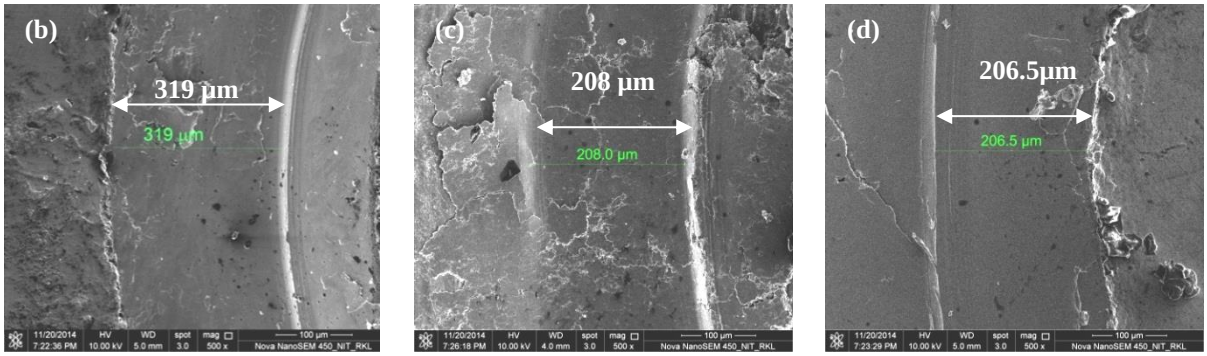

Fig. 4.42 (a) Wear Characteristic of Cu- MWCNT composites and FESEM images of the wear track of (b) Cu- 1 vol.% MWCNT (c) Cu- 2 vol.% MWCNT and (d) Cu- 5 vol.% MWCNTs composite

MWCNT reinforced Cu-based metal matrix composites were fabricated by powder metallurgy method. The dispersion of CNTs in the Cu matrix plays important role in enhancing the wear resistance of the Cu-MWCNTs composites. The wear characteristics for Cu-MWCNTs composites shown in Fig. 4.42 (a) indicate that the wear resistance of the Cu-MWCNTs composites increases with increasing volume fraction of the MWCNTs in the composite. The MWCNTs act as a lubricating carbon film. The low coefficient of friction of the MWCNTs leads to higher wear resistance of the Cu-MWCNTs composite. With the addition of MWCNTs there is reduction in direct contact between the Cu matrix and the indenter. Figs. 4.42 (b-d) show the FESEM images of the wear tracks of Cu-1, 2 and 5 vol. % MWCNTs composites. It can be seen that the width of the wear track reduces with the increase in volume fraction of MWCNTs in the Cu-MWCNTs composite [107-110].

……

Chapter 5
Conclusions

Conclusions

This thesis reports the results of a systematic study of development and characterization of Cu-based metal matrix composites using SiCp, E-glass fiber and multiwalled carbon nanotubes (MWCNTs) as reinforcements. The conclusions drawn from the present investigation are as follows:

1. Milling of elemental Cu powder for 20 h led to the formation of nanostructured Cu. The crystallite size of Cu after 20 h of milling was found to be around 18 nm. This was confirmed by both x-ray diffraction analysis and high resolution transmission electron microscopy images.There is a gradual increase in the lattice strain with milling time due to the severe deformation of the milled powder and the strain reaches a maximum value of around 0.383 % after 20 h of milling when the crystallite size was smallest.
2. X-ray diffraction analysis of 20 h milled Cu powder reveals that there has been no trace of contamination from the milling media.
3. Heat treatment of the 20 h milled Cu powder showed growth in crystallite size of Cu with the increase in the heat treating temperature. There was a gradual rise in the crystallite size of 20 h milled Cu with the increase in the heat treatment temperature and beyond the heat treating temperature of 400^{o}C the crystallite size of Cu was found to be above 100 nm.
4. The hardness of the Cu-SiCp composite increases with the increase in the content of SiCp. As-milled Cu-SiCp composites showed higher hardness as compared to the unmilled Cu-SiCp composites due to the better sinterability when milled Cu was used as the matrix. The highest value of hardness was found to be 3.24 GPa for the as-milled Cu- 40 vol. % SiCp composites.

5. Cu-based MMCs reinforced by SiCp have significantly enhanced the wear resistance of the Cu-SiCp composites both in the case of unmilled and as-milled Cu-SiCp composites. The rise in SiCp reinforcement content imparts higher wear resistance values as compared to native Cu.
6. The hardness values of Cu-E-glass fibre composite increases with the increase in vol. % of E-glass fiber in the composite both in the case of unmilled and as-milled Cu-E-glass fiber composites.
7. As-milled Cu-E-glass fiber composites shows better densification and sinterability compared to the unmilled Cu-E-glass fiber composites due to the finer size of Cu particles in the milled Cu powder. Better densification and sinterability has led to higher hardness. The maximum hardness of 2.86 GPa was found in the case of as-milled Cu-40 vol. % E-glass fiber composite.
8. The relative density of the Cu-MWCNTs composites increase with the increase in the volume fraction of carbon nanotubes in the Cu matrix. However, the Cu-MWCNTs composites do not show significant increase in densification after addition of 2 vol. % of MWCNTs in the Cu matrix.
9. The hardness of Cu-MWCNTs composites increases gradually with the increase in the amount of carbon nanotubes in the Cu-MWCNTs composites. Cu-5 vol. % MWCNTs composite showed highest hardness of 1.44 GPa.
10. Addition of MWCNTs to the Cu matrix improved the wear resistance of the Cu-MWCNTs composites. An increase in wear resistance of the Cu-MWCNTs composites was seen with the addition of upto 5 vol. % of MWCNTs.

……..

References

[1] B. Harris, *Engineering Composite Materials*. IOM, 1999.

[2] D. Hull and T. W. Clyne, *An Introduction to Composite Materials*. Cambridge University Press, 1996.

[3] F. L. Matthews and R. D. Rawlings, *Composite Materials: Engineering and Science*. Elsevier, 1999.

[4] S.-M. Choi and H. Awaji, "Nanocomposites—a new material design concept," *Sci. Technol. Adv. Mater.*, vol. 6, no. 1, pp. 2–10, Jan. 2005.

[5] S. C. Tjong and Z. Y. Ma, "Microstructural and mechanical characteristics of in situ metal matrix composites," *Mater. Sci. Eng. R Rep.*, vol. 29, no. 3, pp. 49–113, Aug. 2000.

[6] L. E. Asp and E. S. Greenhalgh, "Structural power composites," *Compos. Sci. Technol.*, vol. 101, pp. 41–61, Sep. 2014.

[7] R. Everett, *Metal matrix composites: Processing and Interfaces*. Academic Press, 2012.

[8] M. Murphy, "Copper," *Met. Finish.*, vol. 95, no. 2, p. 36, Feb. 1997.

[9] T. Schubert, B. Trindade, T. Weißgärber, and B. Kieback, "Interfacial design of Cu-based composites prepared by powder metallurgy for heat sink applications," *Mater. Sci. Eng. A*, vol. 475, no. 1–2, pp. 39–44, Feb. 2008.

[10] L. J. Broutman, *Composite Materials*. Academic Press, 1974.

[11] K. K. Chawla, *Composite Materials: Science and Engineering*. Springer Science & Business Media.

[12] K. U. Kainer, "Basics of Metal Matrix Composites," in *Metal Matrix Composites*, K. U. Kainer, Ed. Wiley-VCH Verlag GmbH & Co. KGaA, pp. 1–54,2006.

[13] D. B. Miracle, "Metal matrix composites – From science to technological significance," *Compos. Sci. Technol.*, vol. 65, no. 15–16, pp. 2526–2540, Dec. 2005.

[14] K. U. Kainer, *Metal Matrix Composites: Custom-made Materials for Automotive and Aerospace Engineering*. John Wiley & Sons, 2006.

[15] K. Prakasan and S. Seshan, "Microstructure and properties of squeeze cast Cu-carbon fibre metal matrix composite," *J. Mater. Sci.*, vol. 34, no. 20, pp. 5045–5049, Oct. 1999.

[16] H. Fu, H. Zhang, H. Wang, Q. Zhang, and Z. Hu, "Synthesis and mechanical properties of Cu-based bulk metallic glass composites containing in-situ TiC particles," *Scr. Mater.*, vol. 52, no. 7, pp. 669–673, Apr. 2005.

[17] R. Thiraviam, T. Sornakumar, and A. Senthil Kumar, “Development of copper:alumina Metal Matrix Composite by Powder Metallurgy method,” *Int. J. Mater. Prod. Technol.*, vol. 31, no. 2, pp. 305–313, Jan. 2008.

[18] G. Sundberg, P. Paul, C. Sung, and T. Vasilos, “Fabrication of CuSiC metal matrix composites,” *J. Mater. Sci.*, vol. 41, no. 2, pp. 485–504, Jan. 2006.

[19] D. D. L. C. Pay Yih, “Silicon carbide whisker copper-matrix composites fabricated by hot pressing copper coated whiskers,” vol. 31, no. 2, pp. 399–406, 1995.

[20] S. C. Tjong and K. C. Lau, “Tribological behaviour of SiC particle-reinforced copper matrix composites,” *Mater. Lett.*, vol. 43, no. 5–6, pp. 274–280, May 2000.

[21] T. Schubert, A. Brendel, K. Schmid, T. Koeck, Ł. Ciupiński, W. Zieliński, T. Weißgärber, and B. Kieback, “Interfacial design of Cu/SiC composites prepared by powder metallurgy for heat sink applications,” *Compos. Part Appl. Sci. Manuf.*, vol. 38, no. 12, pp. 2398–2403, Dec. 2007.

[22] N. B. Dhokey and R. K. Paretkar, “Study of wear mechanisms in copper-based SiCp (20% by volume) reinforced composite,” *Wear*, vol. 265, no. 1–2, pp. 117–133, Jun. 2008.

[23] G. Celebi Efe, T. Yener, I. Altinsoy, M. Ipek, S. Zeytin, and C. Bindal, “The effect of sintering temperature on some properties of Cu–SiC composite,” *J. Alloys Compd.*, vol. 509, no. 20, pp. 6036–6042, May 2011.

[24] H. R. Akramifard, M. Shamanian, M. Sabbaghian, and M. Esmailzadeh, “Microstructure and mechanical properties of Cu/SiC metal matrix composite fabricated via friction stir processing,” *Mater. Des.*, vol. 54, pp. 838–844, Feb. 2014.

[25] F. T. Wallenberger, “Commercial and Experimental Glass Fibers,” in *Fiberglass and Glass Technology*, F. T. Wallenberger and P. A. Bingham, Eds. Springer US, pp. 3–90,2010.

[26] G. Zak, M. N. Sela, V. Yevko, C. B. Park, and B. Benhabib, “Layered-Manufacturing of Fiber-Reinforced Composites,” *J. Manuf. Sci. Eng.*, vol. 121, no. 3, pp. 448–456, Aug. 1999.

[27] C. L. Schutte, “Environmental durability of glass-fiber composites,” *Mater. Sci. Eng. R Rep.*, vol. 13, no. 7, pp. 265–323, Nov. 1994.

[28] S. Iijima, P. M. Ajayan, and T. Ichihashi, “Growth model for carbon nanotubes,” *Phys. Rev. Lett.*, vol. 69, no. 21, pp. 3100–3103, Nov. 1992.

[29] D. N. Futaba, K. Hata, T. Yamada, T. Hiraoka, Y. Hayamizu, Y. Kakudate, O. Tanaike, H. Hatori, M. Yumura, and S. Iijima, “Shape-engineerable and highly densely packed single-walled carbon nanotubes and their application as super-capacitor electrodes,” *Nat. Mater.*, vol. 5, no. 12, pp. 987–994, Dec. 2006.

[30] A. Agarwal, S. R. Bakshi, and D. Lahiri, *Carbon Nanotubes: Reinforced Metal Matrix Composites*. CRC Press, 2010.

[31] H. Li, A. Misra, Z. Horita, C. C. Koch, N. A. Mara, P. O. Dickerson, and Y. Zhu, “Strong and ductile nanostructured Cu-carbon nanotube composite,” *Appl. Phys. Lett.*, vol. 95, no. 7, p. 071907, Aug. 2009.

[32] P. V. Trinh, T. B. Trung, N. B. Thang, B. H. Thang, T. X. Tinh, L. D. Quang, D. D. Phuong, and P. N. Minh, “Calculation of the friction coefficient of Cu matrix composite reinforced by carbon nanotubes,” *Comput. Mater. Sci.*, vol. 49, no. 4, Supplement, pp. S239–S241, Oct. 2010.

[33] M. Lal, S. K. Singhal, I. Sharma, and R. B. Mathur, “An alternative improved method for the homogeneous dispersion of CNTs in Cu matrix for the fabrication of Cu/CNTs composites,” *Appl. Nanosci.*, vol. 3, no. 1, pp. 29–35, Feb. 2013.

[34] S. Suresh, A. Mortensen, and A. Needleman, *Fundamentals of Metal-matrix Composites*. Butterworth-Heinemann, 1993.

[35] R. M. German, *Powder Metallurgy Science*, 2 Sub edition. Princeton, N.J.: Metal Powder Industry, 1994.

[36] P. Ramakrishanan, *Powder Metallurgy*. New Age International, 2007.

[37] K. K. Gan, N. Chen, Y. Wang, and M. Y. Gu, “SiC/Cu composites with tungsten coating prepared by powder metallurgy,” *Mater. Sci. Technol.*, vol. 23, no. 1, pp. 119–122, Jan. 2007.

[38] G. S. Upadhyaya, *Powder Metallurgy Technology*. Cambridge Int Science Publishing, 1997.

[39] J. S. Benjamin, “Dispersion strengthened superalloys by mechanical alloying,” *Metall. Trans.*, vol. 1, no. 10, pp. 2943–2951, Oct. 1970.

[40] J. S. Benjamin and T. E. Volin, “The mechanism of mechanical alloying,” *Metall. Trans.*, vol. 5, no. 8, pp. 1929–1934, Aug. 1974.

[41] C. C. Koch, “Materials Synthesis by Mechanical Alloying,” *Annu. Rev. Mater. Sci.*, vol. 19, no. 1, pp. 121–143, 1989.

[42] B. S. Murty, M. Mohan Rao, and S. Ranganathan, “Milling maps and amorphization during mechanical alloying,” *Acta Metall. Mater.*, vol. 43, no. 6, pp. 2443–2450, Jun. 1995.

[43] S. K. Pabi, J. Joardar, and B. S. Murty, “Formation of nanocrystalline phases in the Cu-Zn system during mechanical alloying,” *J. Mater. Sci.*, vol. 31, no. 12, pp. 3207–3211, Jan. 1996.

[44] S. K. Pabi and B. S. Murty, “Mechanism of mechanical alloying in NiAl and CuZn systems,” *Mater. Sci. Eng. A*, vol. 214, no. 1–2, pp. 146–152, Aug. 1996.

[45] B. S. Murty and S. Ranganathan, “Novel materials synthesis by mechanical alloying/milling,” *Int. Mater. Rev.*, vol. 43, no. 3, pp. 101–141, Jan. 1998.

[46] C. Suryanarayana, E. Ivanov, and V. V. Boldyrev, “The science and technology of mechanical alloying,” *Mater. Sci. Eng. A*, vol. 304–306, pp. 151–158, May 2001.

[47] C. Suryanarayana, “Mechanical alloying and milling,” *Prog. Mater. Sci.*, vol. 46, no. 1–2, pp. 1–184, Jan. 2001.

[48] I. Manna, P. P. Chattopadhyay, F. Banhart, and H. J. Fecht, “Development of amorphous and nanocrystalline Al65Cu35−xZrx alloys by mechanical alloying,” *Mater. Sci. Eng. A*, vol. 379, no. 1–2, pp. 360–365, Aug. 2004.

[49] I. Manna †, P. Nandi, and P. M. G. Nambissan, “Mechanism and kinetics of solid-state amorphization by mechanical alloying of Al65Cu 35−x Nb x,” *Philos. Mag.*, vol. 84, no. 33, pp. 3585–3598, Nov. 2004.

[50] R. M. Davis, B. McDermott, and C. C. Koch, “Mechanical alloying of brittle materials,” *Metall. Trans. A*, vol. 19, no. 12, pp. 2867–2874, Dec. 1988.

[51] K. L. Choy, “Chemical vapour deposition of coatings,” *Prog. Mater. Sci.*, vol. 48, no. 2, pp. 57–170, 2003.

[52] S. Iijima and T. Ichihashi, “Single-shell carbon nanotubes of 1-nm diameter,” *Nature*, vol. 363, no. 6430, pp. 603–605, Jun. 1993.

[53] S. Iijima, C. Brabec, A. Maiti, and J. Bernholc, “Structural flexibility of carbon nanotubes,” *J. Chem. Phys.*, vol. 104, no. 5, pp. 2089–2092, Feb. 1996.

[54] L.-C. Qin, X. Zhao, K. Hirahara, Y. Miyamoto, Y. Ando, and S. Iijima, “Materials science: The smallest carbon nanotube,” *Nature*, vol. 408, no. 6808, pp. 50–50, Nov. 2000.

[55] S. Iijima, “Carbon nanotubes: past, present, and future,” *Phys. B Condens. Matter*, vol. 323, no. 1–4, pp. 1–5, Oct. 2002.

[56] V. Datsyuk, M. Kalyva, K. Papagelis, J. Parthenios, D. Tasis, A. Siokou, I. Kallitsis, and C. Galiotis, “Chemical oxidation of multiwalled carbon nanotubes,” *Carbon*, vol. 46, no. 6, pp. 833–840, May 2008.

[57] S. Campidelli, C. Klumpp, A. Bianco, D. M. Guldi, and M. Prato, “Functionalization of CNT: synthesis and applications in photovoltaics and biology,” *J. Phys. Org. Chem.*, vol. 19, no. 8–9, pp. 531–539, 2006.

[58] D. Balzar and H. Ledbetter, “Voigt-function modeling in Fourier analysis of size- and strain-broadened X-ray diffraction peaks,” *J. Appl. Crystallogr.*, vol. 26, no. 1, pp. 97–103, Feb. 1993.

[59] D. Balzar, N. Audebrand, M. R. Daymond, A. Fitch, A. Hewat, J. I. Langford, A. Le Bail, D. Louër, O. Masson, C. N. McCowan, N. C. Popa, P. W. Stephens, and B. H. Toby, “Size–strain line-broadening analysis of the ceria round-robin sample,” *J. Appl. Crystallogr.*, vol. 37, no. 6, pp. 911–924, Dec. 2004.

[60] T. Raghu, R. Sundaresan, P. Ramakrishnan, and T. R. Rama Mohan, “Synthesis of nanocrystalline copper–tungsten alloys by mechanical alloying,” *Mater. Sci. Eng. A*, vol. 304–306, pp. 438–441, May 2001.

[61] T. Venugopal, K. P. Rao, and B. S. Murty, “Synthesis of copper–alumina nanocomposite by reactive milling,” *Mater. Sci. Eng. A*, vol. 393, no. 1–2, pp. 382–386, Feb. 2005.

[62] K. A. Padmanabhan, “Mechanical properties of nanostructured materials,” *Mater. Sci. Eng. A*, vol. 304–306, pp. 200–205, May 2001.

[63] K. Ďurišinová, J. Ďurišin, M. Orolínová, M. Ďurišin, and J. Szabó, “Effect of mechanical milling on nanocrystalline grain stability and properties of Cu–Al2O3 composite prepared by thermo-chemical technique and hot extrusion,” *J. Alloys Compd.*, vol. 618, pp. 204–209, Jan. 2015.

[64] T. H. de Keijser, J. I. Langford, E. J. Mittemeijer, and A. B. P. Vogels, “Use of the Voigt function in a single-line method for the analysis of X-ray diffraction line broadening,” *J. Appl. Crystallogr.*, vol. 15, no. 3, pp. 308–314, Jun. 1982.

[65] C. C. Koch, “The synthesis and structure of nanocrystalline materials produced by mechanical attrition: A review,” *Nanostructured Mater.*, vol. 2, no. 2, pp. 109–129, Mar. 1993.

[66] C. C. Koch, “Synthesis of nanostructured materials by mechanical milling: problems and opportunities,” *Nanostructured Mater.*, vol. 9, no. 1–8, pp. 13–22, 1997.

[67] J. Eckert, J. c. Holzer, C. e. Krill, and W. l. Johnson, “Structural and thermodynamic properties of nanocrystalline fcc metals prepared by mechanical attrition,” *J. Mater. Res.*, vol. 7, no. 07, pp. 1751–1761, 1992.

[68] C. C. Koch and Y. S. Cho, “Nanocrystals by high energy ball milling,” *Nanostructured Mater.*, vol. 1, no. 3, pp. 207–212, May 1992.

[69] J. Eckert, J. C. Holzer, C. E. K. Iii, and W. L. Johnson, “Mechanically driven alloying and grain size changes in nanocrystalline Fe- Cu powders,” *J. Appl. Phys.*, vol. 73, no. 6, pp. 2794–2802, Mar. 1993.

[70] H.-J. Fecht, “Nanostructure formation by mechanical attrition,” *Nanostructured Mater.*, vol. 6, no. 1–4, pp. 33–42, 1995.

[71] R. Daly, M. Khitouni, and N. Njeh, “Effect of high energy mechanical milling on the properties of CuA1 copper,” *Phys. Procedia*, vol. 2, no. 3, pp. 685–691, Nov. 2009.

[72] K. Zhang, I. V. Alexandrov, and K. Lu, “The X-ray diffraction study on a nanocrystalline CU processed by equal-channel angular pressing,” *Nanostructured Mater.*, vol. 9, no. 1–8, pp. 347–350, 1997.

[73] D. L. Zhang, “Processing of advanced materials using high-energy mechanical milling,” *Prog. Mater. Sci.*, vol. 49, no. 3–4, pp. 537–560, 2004.

[74] S. Patra, Gouthama, and K. Mondal, “Densification behavior of mechanically milled Cu–8 at% Cr alloy and its mechanical and electrical properties,” *Prog. Nat. Sci. Mater. Int.*, vol. 24, no. 6, pp. 608–622, Dec. 2014.

[75] Y. Ogino, S. Murayama, and T. Yamasaki, “Influence of milling atmosphere on amorphization of chromium and Cr-Cu powders by ball milling,” *J. Common Met.*, vol. 168, no. 2, pp. 221–235, Mar. 1991.

[76] P. S. Gilman and J. S. Benjamin, “Mechanical Alloying,” *Annu. Rev. Mater. Sci.*, vol. 13, no. 1, pp. 279–300, 1983.

[77] K. M. Shu and G. C. Tu, “Fabrication and characterization of Cu-SiCp composites for electrical discharge machining applications,” Jan. 2001.

[78] A. R. F. Azreen, A. G. E. Sutjipto, and E. Y. T. Adesta, “Fabrication of CuSiC Composite by Powder Metallurgy Route,” *Adv. Mater. Res.*, vol. 264–265, pp. 748–753, Jun. 2011.

[79] D. Zhu, G. Wu, G. Chen, and Q. Zhang, “Fabrication and properties of SiC/Cu composites for electronic packaging,” in *2005 6th International Conference on Electronic Packaging Technology*, pp. 191–194, 2005.

[80] A. C. Balbahdur, F. E. Kennedy, “The friction and wear of Cu-based silicon carbide particulate metaal matrix composites for brake applications,” *Wear*, pp. 715–721, 1997.

[81] R. Dasgupta and H. Meenai, “Sliding wear properties of Al-Cu based alloys with SiC particle reinforced composites under varying experimental conditions,” *J. Mater. Sci. Lett.*, vol. 22, no. 22, pp. 1573–1576, Nov. 2003.

[82] Y. S. Zhang, Z. Han, K. Wang, and K. Lu, “Friction and wear behaviors of nanocrystalline surface layer of pure copper,” *Wear*, vol. 260, no. 9–10, pp. 942–948, May 2006.

[83] A. K. Pradhan and S. Das, “Dry Sliding Wear and Friction Behavior of Cu-SiC Nanocomposite Coating Prepared by Pulse Reverse Electrodeposition,” *Tribol. Trans.*, vol. 57, no. 1, pp. 46–56, Jan. 2014.

[84] M. Barmouz, M. K. Besharati Givi, and J. Seyfi, “On the role of processing parameters in producing Cu/SiC metal matrix composites via friction stir processing: Investigating microstructure, microhardness, wear and tensile behavior,” *Mater. Charact.*, vol. 62, no. 1, pp. 108–117, Jan. 2011.

[85] M. Barmouz and M. K. B. Givi, “Fabrication of in situ Cu/SiC composites using multi-pass friction stir processing: Evaluation of microstructural, porosity, mechanical and electrical behavior,” *Compos. Part Appl. Sci. Manuf.*, vol. 42, no. 10, pp. 1445–1453, Oct. 2011.

[86] P. A. M Barmouz, “Investigation of mechanical properties of Cu/SiC composite fabricated by FSP: Effect of SiC particles' size and volume fraction,” *Mater. Sci. Eng. A*, vol. 528, pp. 1740–1749, 2011.

[87] C. S. Ramesh, R. Noor Ahmed, M. A. Mujeebu, and M. Z. Abdullah, “Development and performance analysis of novel cast copper–SiC–Gr hybrid composites,” *Mater. Des.*, vol. 30, no. 6, pp. 1957–1965, Jun. 2009.

[88] J. Zhu, L. Liu, B. Shen, and W. Hu, “Mechanical properties of Cu/SiCp composites fabricated by composite electroforming,” *Mater. Lett.*, vol. 61, no. 13, pp. 2804–2809, May 2007.

[89] Y. Zhan and G. Zhang, “The effect of interfacial modifying on the mechanical and wear properties of SiCp/Cu composites,” *Mater. Lett.*, vol. 57, no. 29, pp. 4583–4591, Nov. 2003.

[90] T. Ram Prabhu, V. K. Varma, and S. Vedantam, “Tribological and mechanical behavior of multilayer Cu/SiC + Gr hybrid composites for brake friction material applications,” *Wear*, vol. 317, no. 1–2, pp. 201–212, Sep. 2014.

[91] T. W. Chou, A. Kelly, and A. Okura, “Fibre-reinforced metal-matrix composites,” *Composites*, vol. 16, no. 3, pp. 187–206, Jul. 1985.

[92] J. R. Brockenbrough, S. Suresh, and H. A. Wienecke, “Deformation of metal-matrix composites with continuous fibers: geometrical effects of fiber distribution and shape,” *Acta Metall. Mater.*, vol. 39, no. 5, pp. 735–752, May 1991.

[93] B. Budiansky, J. W. Hutchinson, and A. G. Evans, “Matrix fracture in fiber-reinforced ceramics,” *J. Mech. Phys. Solids*, vol. 34, no. 2, pp. 167–189, 1986.

[94] J. E. Bolander, S. Choi, and S. R. Duddukuri, “Fracture of fiber-reinforced cement composites: effects of fiber dispersion,” *Int. J. Fract.*, vol. 154, no. 1–2, pp. 73–86, Nov. 2008.

[95] V. Srinivasa, V. Shivakumar, V. Nayaka, S. Jagadeeshaiaih, M. Seethram, R. Shenoy, and A. Nafidi, “Fracture morphology of carbon fiber reinforced plastic composite laminates,” *Mater. Res.*, vol. 13, no. 3, pp. 417–424, Sep. 2010.

[96] Q. Du, M. Perez, W. J. Poole, and M. Wells, “Numerical integration of the Gibbs–Thomson equation for multicomponent systems,” *Scr. Mater.*, vol. 66, no. 7, pp. 419–422, Apr. 2012.

[97] I. McCue, J. Snyder, X. Li, Q. Chen, K. Sieradzki, and J. Erlebacher, “Apparent Inverse Gibbs-Thomson Effect in Dealloyed Nanoporous Nanoparticles,” *Phys. Rev. Lett.*, vol. 108, no. 22, p. 225503, May 2012.

[98] G. Che, B. B. Lakshmi, C. R. Martin, E. R. Fisher, and R. S. Ruoff, “Chemical Vapor Deposition Based Synthesis of Carbon Nanotubes and Nanofibers Using a Template Method,” *Chem. Mater.*, vol. 10, no. 1, pp. 260–267, 1998.

[99] J. Kong, A. M. Cassell, and H. Dai, “Chemical vapor deposition of methane for single-walled carbon nanotubes,” *Chem. Phys. Lett.*, vol. 292, no. 4–6, pp. 567–574, Aug. 1998.

[100] W. Yang, Y. Feng, and W. Chu, “Catalytic Chemical Vapor Deposition of Methane to Carbon Nanotubes: Copper Promoted Effect of Ni/MgO Catalysts,” *J. Nanotechnol.*, vol. 2014, p. e547030, Jun. 2014.

[101] M. Inagaki, F. Kang, M. Toyoda, and H. Konno, “Chapter 2 - Carbon Nanotubes: Synthesis and Formation,” in *Advanced Materials Science and Engineering of Carbon*, M. I. K. T. Konno, Ed. Boston: Butterworth-Heinemann, pp. 15–40, 2014.

[102] H. Li, A. Misra, Y. Zhu, Z. Horita, C. C. Koch, and T. G. Holesinger, “Processing and characterization of nanostructured Cu-carbon nanotube composites,” *Mater. Sci. Eng. A*, vol. 523, no. 1–2, pp. 60–64, Oct. 2009.

[103] K. T. Kim, J. Eckert, S. B. Menzel, T. Gemming, and S. H. Hong, “Grain refinement assisted strengthening of carbon nanotube reinforced copper matrix nanocomposites,” *Appl. Phys. Lett.*, vol. 92, no. 12, p. 121901, Mar. 2008.

[104] L. Stobinski, B. Lesiak, L. Kövér, J. Tóth, S. Biniak, G. Trykowski, and J. Judek, “Multiwall carbon nanotubes purification and oxidation by nitric acid studied by the FTIR and electron spectroscopy methods,” *J. Alloys Compd.*, vol. 501, no. 1, pp. 77–84, Jul. 2010.

[105] K. T. Kim, S. I. Cha, and S. H. Hong, “Hardness and wear resistance of carbon nanotube reinforced Cu matrix nanocomposites,” *Mater. Sci. Eng. A*, vol. 449–451, pp. 46–50, Mar. 2007.

[106] D. H. Nam, J. H. Kim, S. I. Cha, S. I. Jung, J. K. Lee, H. M. Park, H. D. Park, and S. H. Hong, “Hardness and Wear Resistance of Carbon Nanotube Reinforced Aluminum-Copper Matrix Composites,” *J. Nanosci. Nanotechnol.*, vol. 14, no. 12, pp. 9134–9138, Dec. 2014.

[107] S. R. Dong, J. P. Tu, and X. B. Zhang, “An investigation of the sliding wear behavior of Cu-matrix composite reinforced by carbon nanotubes,” *Mater. Sci. Eng. A*, vol. 313, no. 1–2, pp. 83–87, Aug. 2001.

[108] T. Suzuki, M. Kato, H. Saito, and H. Iizuka, “Effect of Carbon Nanotube (CNT) Size on Wear Properties of Cu-Based CNT Composite Electrodes in Electrical Discharge Machining,” *J. Solid Mech. Mater. Eng.*, vol. 5, no. 7, pp. 348–359, 2011.

[109] R. Patil, V. Chatpalli, and R. C, “Wear Properties of Cu-CNT Nanocomposites,” in *Carbon Nanotubes - From Research to Applications*, S. Bianco, Ed. InTech, 2011.

[110] G. M. Liu, B. Li, J. H. Du, and X. H. Zheng, “Effect of CNTs on Properties of Cu-Based Composites and Mechanism,” *Adv. Mater. Res.*, vol. 557–559, pp. 262–266, Jul. 2012.

……

Publications/Conferences

- S.N.Alam, Harshpreet Singh, Development of copper-based metal matrix composites: An analysis by SEM, EDS and XRD, Microscopy and Analysis, 28(4) (2014) 8-13.
- Harshpreet Singh, Lailesh Kumar, Syed Nasimul Alam, Development of Cu reinforced SiC particulate Composite, IOP Conference Series: Materials Science and Engineering 75 (1) (2015) 012007.
- Oral Presentation at IUMRS-ICA-2013 held at IISc Bangalore, Title "Development of Cu based metal matrix composites by mechanical alloying route".
- Poster Presentation at 5th National Symposium for Research Scholars at IIT Bombay, Title "Synthesis of Cu-E glass fibre Metal matrix Composites".
- Oral Presentation at NCPCM-2013 held at NIT Rourkela, Title "Synthesis and Characterization of SiC particle reinforced Cu Matrix Composites".
- Oral Presentation at NCPCM-2014 held at NIT Rourkela, Title "Development of Cu reinforced SiC particulate Composite".

……

Bio Data

Name Harshpreet Singh

Date of Birth 22.02.1990

Permanent Address 4M/2 Dabouli
Ratan lal Nagar
Kanpur
Uttar Pradesh
India
Pin: 208022

E-mail ID harshpreet00@gmail.com

Languages Known English, Hindi, Punjabi

Educational Qualifications:

Year	Degree/Certificate	Institution	Marks obtained
2012	Bachelor of Technology (Mechanical Engineering)	Sunderdeep Engg. College	78.9% 1st Div. Honours
2008	S.S.C (CBSE Board)	Harmilap Mission School, Kanpur	76% 1stDiv.
2006	H.S.C (ICSE Board)	U P Kirana Public School, Kanpur	72.5% 1stDiv.